NASA Contractor Report 4493

Control Design Variable Linking for Optimization of Structural/Control Systems

Min Jin and Lucien A. Schmit

GRANT NSG-1490
FEBRUARY 1993

NASA

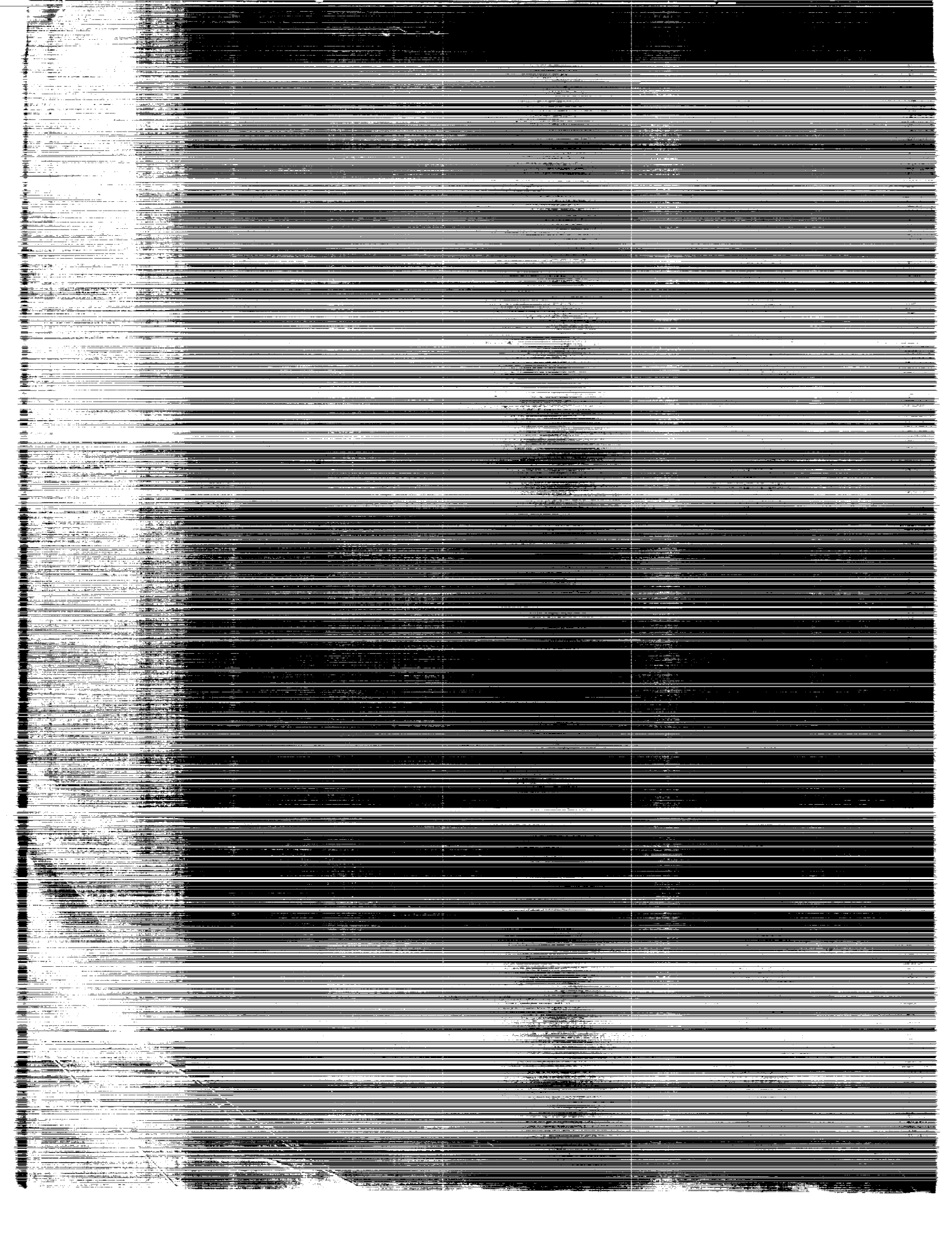

NASA Contractor Report 4493

Control Design Variable Linking for Optimization of Structural/Control Systems

Ik Min Jin and Lucien A. Schmit
University of California, Los Angeles
Los Angeles, California

Prepared for
Langley Research Center
under Grant NSG-1490

National Aeronautics and
Space Administration
Office of Management
Scientific and Technical
Information Program
1993

TABLE OF CONTENTS

LIST OF TABLES

LIST OF FIGURES

LIST OF SYMBOLS

A	Area
$[A_o]$	Open-loop system matrix ($2N \times 2N$)
$[A]$	Closed-loop system matrix ($2N \times 2N$)
B	Width of the cross section
$[b]$	Control input coefficient matrix ($N \times M$)
$[B]$	System control input coefficient matrix ($2N \times M$)
CE	Control effort
c_K	Coefficient of stiffness matrix for proportional damping matrix
c_M	Coefficient of mass matrix for proportional damping matrix
$[C]$	Viscous damping matrix ($N \times N$)
E	Young's modulus
$[e]$	External disturbance coefficient matrix ($N \times L$)
$[E]$	System external disturbance coefficient matrix ($2N \times L$)
$\{f\}$	Disturbance vector ($L \times 1$)
$\{F\}$	Load vector in 2nd order dynamic equation ($N \times 1$)
$\{FC\}_k$	*k-th* cosine component of disturbance vector ($L \times 1$)
$\{FP\}_p$	*p-th* polynomial component of disturbance vector ($L \times 1$)
$\{FS\}_k$	*k-th* sine component of disturbance vector ($L \times 1$)
$F(\mathbf{Y})$	Objective function
G	Shear modulus
$G_j(\mathbf{Y})$	*j-th* constraint function
H	Depth of the cross section

$[H]$	Feedback gain matrix $(M \times 2N)$
$\lfloor H \rfloor_j$	j-th row of $[H]$ $(1 \times 2N)$
$[H_p],[H_v]$	Position and velocity parts of $[H]$ $(M \times N)$
$\lfloor H_p \rfloor_j, \lfloor H_v \rfloor_j$	j-th rows of $[H_p]$, $[H_v]$ $(1 \times N)$
$\{H_p\}^i,\{H_v\}^i$	i-th columns of $[H_p]$, $[H_v]$ $(M \times 1)$
$[I]$	Identity matrix
$I_y,\ I_z$	Section bending inertia
j	Equal to $\sqrt{-1}$
J	Torsional stiffness constant
$[K]$	Stiffness matrix $(N \times N)$
L	Number of different disturbances
l	Length of frame element
M	Number of actuators
$[M]$	Mass matrix $(N \times N)$
N	Number of total degrees of freedom
$NCON$	Number of constraints
NDV	Number of design variables
$NIDV$	Number of intermediate design variables
N_p	Number of highest polynomial in disturbance
N_Ω	Number of different driving frequencies
PI	Performance index of full order LQR
PI_i	Performance index of i-th mode
$[P]$	Riccati solution matrix $(2N \times 2N)$
$\{q\}$	Vector of nodal degrees of freedom $(N \times 1)$

$[Q]$	State weighting matrix $(2N \times 2N)$
$[Q_i]$	State weighting matrix of *i-th* mode (2×2)
r	Number of retained modes in 2×2 Riccati equations
R	Number of retained modes in transient response calculation
$[R]$	Control weighting matrix $(M \times M)$
$[R_i]$	*i-th* control weighting matrix $(M \times M)$
$[R_{CE}]$	Control effort weighting matrix $(M \times M)$
T	Thickness of box beam cross section
T2,T3	Flange and web thicknesses
t	Time
t_f	Time interval during which external force is applied
$\{ u \}$	Control force vector $(M \times 1)$
$\{ v_i \}$, $[V]$	*i-th* Normal eigenvector, eigenmatrix $(N \times 1,\ N \times r)$
$\{ w_i \}$	State vector of *i-th* modal equation (2×1)
X, Y, Z	Global coordinate axes
$\{ x \}$	State vector $(2N \times 1)$
X(Y)	Intermediate design variable vector $(NIDV \times 1)$
Y	Design variable vector $(NDV \times 1)$
$\{ z \}$	Normal coordinate vector $(r \times 1)$

GREEK

α	Design variable
γ_i	Weighting coefficient of *i-th* control force $([R_i] = \gamma_i [I])$
δ_{ij}	Kronecker delta

$\{\eta\}$	Complex modal coordinate vector ($2R \times 1$)
λ_i	*i-th* complex eigenvalue ($=\sigma_i + j\omega_{di}$)
$[\Lambda]$	Diagonal matrix of complex eigenvalues ($2R \times 2R$)
ν	Poisson's ratio
ξ_i	*i-th* modal damping factor
ρ	Mass density
σ_i	Real part of *i-th* complex eigenvalue
$\{\phi_i\}$	*i-th* complex right hand eigenvector ($2N \times 1$)
$[\Phi]$	Right hand eigenmatrix ($2N \times 2R$)
$\{\psi_i\}$	*i-th* complex left hand eigenvector ($2N \times 1$)
$[\Psi]$	Left hand eigenmatrix ($2N \times 2R$)
ω_i	*i-th* natural frequency
ω_{di}	Imaginary part of *i-th* complex eigenvalue
Ω_k	*k-th* driving frequency

SUBSCRIPTS

a	Denotes allowable value
I	Denotes imaginary part
i	Denotes *i-th* component, or *i-th* equation
ij	Denotes (i,j)-*th* element of a matrix
o	Denotes initial value
R	Denotes real part

SUPERSCRIPTS

e	Denotes element matrix
L	Denotes lower bound
T	Denotes matrix transpose
U	Denotes upper bound
-1	Denotes matrix inverse

SPECIAL SYMBOLS

$\cdot$	Denotes partial differentiation with respect to time
$\sim$	Denotes explicit approximation of function
$\lvert \cdot \rvert$	Denotes absolute value
∂	Denotes partial differential operator

ACKNOWLEDGEMENT

This report presents some results of a research program entitled "Fundamental Studies of Methods for Structural Synthesis" sponsored by NASA Research Grant No. NSG-1490. The work reported herein was carried out in the School of Engineering and Applied Science at UCLA during the period from August 1988 to June 1992.

ABSTRACT

A method is presented to integrate the design space of structural/control system optimization problems in the case of linear state feedback control. Conventional structural sizing variables and elements of the feedback gain matrix are both treated as strictly independent design variables in optimization by extending design variable linking concepts to the control gains. Several approximation concepts including new control design variable linking schemes are used to formulate the integrated structural/control optimization problem as a sequence of explicit nonlinear mathematical programming problems. Examples which involve a variety of behavior constraints, including constraints on dynamic stability, damped frequencies, control effort, peak transient displacement, acceleration and control force limits, are effectively solved by using the method presented.

Chapter I

INTRODUCTION

1.1 INTRODUCTION

Large space structures usually have low stiffness and low damping characteristics due to their light weight requirements. In order to suppress the vibration and maintain the strict shape specifications, it is necessary to enhance stiffness and/or damping of the structures through some type of active controls (Ref. 1).

Conventionally structural and controller design is performed separately (namely, the structure is designed first to minimize the weight satisfying structural constraints and then a control law is found for the fixed structure minimizing some kind of control performance index), and as a result the final design cannot ensure the best performance of the overall system since the dynamic interaction between the two systems is not directly considered in the design process. In Ref. 2 it was shown that slight structural modification can lead to considerable improvement in the control system performance, and there has been a growing effort to integrate the design optimization of structures and control systems in order to achieve a better performance and directly handle cross coupling effects and dynamic interactions between the two systems.

Most of this research has focused on linear control laws based on output feedback or state feedback. In the case of output feedback several studies have been made where the structural dimensions and the control gains are treated as strictly independent design variables in optimization (Refs. 2-10). On the other hand, in the case of full state feedback control a sequential approach is usually adopted in which the control gains are determined by solving Riccati equations corresponding to the changing structural system during design iterations (Refs. 11-17). When the gain variables are determined by solving Riccati equations for a fixed plant, they implicitly become dependent design variables and the resulting design optimization is constrained to a subspace where the optimality conditions of a control subproblem are satisfied. The tendency to subordinate gains to a dependent variable status can be attributed to the fact that for system models with a large number of degrees of freedom, the gain matrix $[H]$ contains prohibitively large numbers of independent design variables (i.e. $M \times 2N$ control design variables, where M is the number of actuators and N is the number of degrees of freedom in the structural model).

The main purpose of this study is to suggest a new simultaneous optimization method where both structural and control system variables are treated as strictly independent design variables in the case of state feedback control. This is accomplished via an adaptation of the design variable linking idea to the control system design variables (see Refs. 26 and 27). This innovation makes it possible to simultaneously optimize the structure/control sys-

tem, while avoiding a prohibitively large increase in the total number of independent design variables.

1.2 BACKGROUND

In Refs. 2-10 both structural and control variables are treated as independent in optimization. Output feedback is adopted as a control law so the number of elements in the feedback gain matrix is relatively small. As a result the gain elements along with structural design variables can be directly treated as independent design variables.

In Ref. 2 collocated direct velocity output feedback, which is similar to a viscous dashpot, is used as a controller. The viscous damping coefficient is minimized, with constraints on the closed-loop eigenvalues, by allowing small changes of the structural dimensions.

In Refs. 3-5 in addition to structural dimensions and control gains, sensor/actuator locations are also used as design variables. Homotopy and sequential linear programming algorithms are used to optimize either structural mass, robustness or eigenvalue sensitivity. Also in Ref. 3 the state feedback control case is cast into a similar simultaneous optimization form by using elements of weighting matrices of the LQR (linear quadratic regulator) as independent design variables, but only the output feedback case is illustrated by giving a numerical example.

In Refs. 6 and 7 collocated output feedback is chosen as a controller to optimize a control augmented structure. In addition to the structural sizing variables and control feedback gains, lumped nonstructural masses are treated simultaneously as independent design variables. Harmonic dynamic loadings are applied and a variety of constraints are considered including natural frequencies, static displacement and stress, dynamic displacements and actuator forces. Due to the characteristics of the collocated sensor/actuator pairs, system stability can be ensured by imposing side constraints on the control gains.

In Refs. 8 and 9 noncollocated output feedback is chosen instead of collocated sensor/actuator pairs, and constraints on the stability (real parts of closed-loop eigenvalues) are included.

In Ref. 10 several output feedback control laws are used in the case of stochastic disturbances with constraints on the allowable mean square deflection or control effort.

In Refs. 11-25 LQR theory is used for the case of state feedback control. In the LQR problem once the weighting matrices in the quadratic performance index are chosen, the control law (or all the closed-loop characteristics) is determined by solving a nonlinear matrix Riccati equation. So the choice of weighting matrices in the LQR problem is very important and two problems arise. One is how to select meaningful weighting matrices, and the other is the solution of the Riccati equation for problems involving a large number of degrees of freedom.

In Ref. 12 structural mass is minimized using structural design variables while satisfying open-loop frequency constraints and then the LQR problem is solved for the fixed structure with given weighting matrices. Here weighting matrices are chosen such that the quadratic performance index represents the absolute weighted sum of kinetic, strain and potential energies, and the effect of relative weighting of these energy terms is discussed. In Refs. 11 and 13 structural variables are optimized with constraints on the closed-loop eigenvalue and modal damping ratios, then the LQR problem is solved for the fixed structure with given weighting matrices (identity matrices in this case). In Refs. 14-17 the Frobenious norm of the gain matrix is introduced as either an objective or a constraint.

Refence 20 points out the difficulties of simultaneous structural/control design and suggests optimization of the closed-loop system using only structural tailoring. In this case the objective of structural tailoring is to maximize modal stiffness in order to minimize control effort. The control law is determined by solving the Riccati equation and the weighting matrices for the LQR problem are similar to those in Ref. 12 except that only two independent weighting coefficients are used instead of three.

In Ref. 21 the weighted sum of the structural mass and control system performance index is minimized.

Reference 22 treats structural variables as well as coefficients of the weighting matrices and orientation of an actuator as design variables. Numerical results are shown for a two bar truss example.

In Ref. 23 a nested optimization method is presented for the state feedback control which minimizes the total equivalent mass of the system (structural mass plus the mass effect of the control effort). Structural dimensions and the coefficient of the control effort are optimized simultaneously to minimized the objective with a constraint on the mean square of the response. Then the control law is determined by solving the Riccati equation with a new set of weighting matrices (since the coefficient of the control effort is optimized, the performance index is updated for each iteration).

In Refs. 24 and 25 locations of actuators and sensors are treated in terms of (0,1) discrete variables. A utopian multiobjective function containing structural mass, control effort and number of actuators is minimized by treating structural variables, (0,1) actuator/sensor location variables and open-loop gains as independent design variables in optimization.

1.3 SCOPE OF THE WORK

In this study the finite element method and linear state feedback are combined to formulate the control augmented structural optimization problem. A truly simultaneous structural/control optimization scheme is presented in the sense that it uses only one set of constraints and one set of design variables

(which includes structural sizing, control gain and actuator mass variables). As mentioned earlier, this scheme was usually adopted for the output feedback control case where the number of gains is relatively small, but by extending design variable linking concepts to the control system gains, design space integration is achieved for the case of full state feedback control while using a relatively small number of control system design variables. Several control design variable linking schemes are presented and their feasibility and effectiveness are shown by solving several examples.

Chapter II

PROBLEM STATEMENTS

2.1 INTRODUCTION

In this study a new simultaneous approach to the design of both the structural and the control system is presented. The finite element method is used to model the structure and linear full state feedback control is chosen as the control law. Dynamic analysis equations from the finite element model and the equations of the control system are combined and the design problem is formulated as a general nonlinear inequality constrained mathematical programming problem.

2.2 PROBLEM FORMULATION

The total mass of the systems has been chosen as the objective function and constraints on: (1) dynamic stability (real parts of complex eigenvalues or modal damping ratios); (2) damped frequencies (imaginary parts of complex eigenvalues); (3) peak transient responses; (4) peak transient control forces; (5) control effort; and (6) actutor mass constraints are included in this study. The optimization problem treated here can be stated as follows:

Design a control augmented structural system which minimizes the total mass and satisfies various behavior constraints as well as side constraints on

the design variables, while treating both structural and control design variables simultaneously and independently in the optimization loop.

In this problem there are three types of design variables. First group contains the usual structural design variables (SDV's) such as the cross sectional dimensions (CSD's). The second group includes nonstructural lumped mass design variables such as actuator masses. And finally the third group contains the control design variables (CDV's). Since linear state feedback is chosen, the elements of the feedback gain matrix constitute a possible set of control design variables. However, this approach is limited because the number of control design variables grows very rapidly as the size of the model becomes larger. In order to overcome this limitation several control design variable linking schemes are introduced (see Chapter IV).

The foregoing problem statement can be cast in mathematical form as follows:

Find $\mathbf{Y}$ to minimize

$$F(\mathbf{Y}) \tag{2.1}$$

subject to

$$G_j(\mathbf{Y}) \leq 0\,, \qquad j = 1, \ldots, NCON \tag{2.2}$$

with bounds

$$\mathbf{Y}_i^L \leq \mathbf{Y}_i \leq \mathbf{Y}_i^U \qquad i = 1, \ldots, NDV \tag{2.3}$$

where NDV is the total number of design variables, $\mathbf{Y} = [\mathbf{Y}_1, \mathbf{Y}_2, \ldots, \mathbf{Y}_{NDV}]^T$ is an $NDV \times 1$ design variable vector, F is a scalar objective function, $NCON$ is the total number of constraints, G_j is the *j-th* behavior constraint, and $\mathbf{Y}_i^L$, $\mathbf{Y}_i^U$ are lower and upper bounds of the *i-th* design variable, respectively.

Chapter III

MODELLING

3.1 FINITE ELEMENT MODEL

The equations of motion are based on a finite element formulation. The element stiffness and mass matrices for a general frame finite element in local coordinates are given in Appendix A. By assembling the element matrices in the global coordinates the equations of motion can be written as follows:

$$[M]\{\ddot{q}\} + [C]\{\dot{q}\} + [K]\{q\} = \{F\} \tag{3.1}$$

where $\{q\}$ is an $N \times 1$ vector of nodal degrees of freedom (DOF), $\{\dot{q}\}$ and $\{\ddot{q}\}$ are first and second time derivatives of $\{q\}$ respectively, $[M]$ is an $N \times N$ mass matrix, $[K]$ is an $N \times N$ stiffness matrix, $[C]$ is an $N \times N$ viscous damping matrix, and $\{F\}$ is an $N \times 1$ load vector.

It is assumed that the preassigned damping inherent to the structure can be represented by a proportional damping matrix which is a linear combination of the structural mass and stiffness matrices, i.e.,

$$[C] = c_M[M] + c_K[K], \quad c_M, c_K \text{ constants} \tag{3.2}$$

There are two kinds of load in the vector $\{F\}$ of Eq. (3.1): control (actuator) forces and external disturbances. With the assumption that the

actuator forces and the disturbances act at nodes of the finite element model, $\{F\}$ can be written as

$$\{F\} = [b]\{u\} + [e]\{f\} \tag{3.3}$$

where $\{u\}$ is an $M \times 1$ actuator force vector, M is the number of actuators, $\{f\}$ is an $L \times 1$ vector of external disturbances, L is the number of different external disturbances making up a single load condition, and $[b]$ and $[e]$ are $N \times M$ and $N \times L$ coefficient matrices consisting of the directional cosines which respectively relate actuator and disturbance forces to the global coordinates.

Now Eq. (3.1) can be written as

$$[M]\{\ddot{q}\} + [C]\{\dot{q}\} + [K]\{q\} = [b]\{u\} + [e]\{f\} \tag{3.4}$$

3.2 CONTROL MODEL

Equation (3.4) can be transformed into the first order state space equation

$$\{\dot{x}\} = [A_o]\{x\} + [B]\{u\} + [E]\{f\} \tag{3.5}$$

where $\{x\}$ is a $2N \times 1$ state vector which is the concatenation of the vector of nodal DOF's and its time derivative ($\{q\}$and $\{\dot{q}\}$), $[A_o]$ is the $2N \times 2N$ system open-loop matrix, $[B]$ is the $2N \times M$ system control input matrix, and $[E]$ is the $2N \times L$ system disturbance matrix. The foregoing transformation is accomplished by combining the identity $\{\dot{q}\} = [I]\{\dot{q}\}$ with the result

obtained by solving Eq. (3.4) for $\{ \ddot{q} \}$ and then introducing the following notation: $\{ x \}^T = \lfloor \{ q \}^T \{ \dot{q} \}^T \rfloor$,

$$[A_o] = \begin{bmatrix} [0] & [I] \\ -[M]^{-1}[K] & -[M]^{-1}[C] \end{bmatrix} \tag{3.6}$$

$$[B] = \begin{bmatrix} [0] \\ [M]^{-1}[b] \end{bmatrix} \tag{3.7}$$

$$[E] = \begin{bmatrix} [0] \\ [M]^{-1}[e] \end{bmatrix} \tag{3.8}$$

where $[\ ]^{-1}$ denotes a matrix inverse, and $[0]$ and $[I]$ are zero and identity matrices of appropriate dimensions respectively.

In control design problems the control law is to be determined. In this study linear full state feedback is chosen for the control $\{ u \}$ under the assumption that all the states (components of $\{ x \}$) are available, that is

$$\{ u \} = -[H]\{ x \} = -\left[[H_p] [H_v] \right] \begin{Bmatrix} q \\ \dot{q} \end{Bmatrix} \tag{3.9}$$

where $[H]$ is the $M \times 2N$ feedback gain matrix, and $[H_p]$ and $[H_v]$ are the $M \times N$ sub matrices containing position and velocity components of $[H]$ respectively.

Once $\{ u \}$ and/or $[H]$ are determined, the closed-loop state equation can be written as

$$\{\dot{x}\} = [A]\{x\} + [E]\{f\} \tag{3.10}$$

where the closed-loop system matrix $[A]$ is

$$[A] = [A_o] - [B][H]$$

$$= \begin{bmatrix} [0] & [I] \\ -[M]^{-1}([K] + [b][H_p]) & -[M]^{-1}([C] + [b][H_v]) \end{bmatrix} \tag{3.11}$$

Chapter IV

DESIGN VARIABLE LINKING AND INITIAL CONTROLLER DESIGN

4.1 STRUCTURAL DESIGN VARIABLE LINKING

In the structural optimization problem some kind of linking scheme is commonly used in order to reduce the number of independent design variables. In this study two kinds of cross sections are used for the frame finite elements, namely box beam and solid rectangular beam cross sections (see Figure 1). For box beam type elements there are 4 cross sectional dimensions which can be chosen as design variables, i.e., width (B), depth (H), flange and web thicknesses (T2 and T3). For the rectangular beam element there are two candidates for design variables: width (B) and depth (H). These cross sectional dimensions can be linked in different configurations. In Table 1 possible choices for design variables of an element are shown along with the linking options within the element. Once design variables for a particular master finite element are chosen, it is rather straightforward to link the design variables of any other element to those of the master element.

4.2 INITIAL STARTUP FEEDBACK GAIN MATRIX

The purpose of control design variable linking is to keep the number of independent control design variables within a tractable range for design optimization. When any kind of linking scheme is imposed on the feedback gain matrix, some design space freedom will be sacrificed and this will usually lead to final objective function values that are inferior to those that could theoretically be achieved using a full set of control gain variables with no linking. However, the performance of the overall design process will depend not only on what kind of linking schemes are used but also on what kind of startup gain matrices are used. Three different methods for generating initial startup gain matrices, before imposing any kind of control variable linking, are suggested here.

The first initializing method sets the feedback gains arbitrarily (e.g. $[H] = [0]$) and then carries out a few design iterations without any control design variable linking (i.e., all the elements of the feedback gain matrix are independent design variables). This allows all the gains as well as the structural design variables to change freely for a few iterations in order to find a reasonable initial design prior to imposing some linking on the set of $M \times 2N$ control design variables. Even though the unlinked option is used for only a few iterations, this can still be a serious restriction, limiting the application of the method to small problems. In Chapter VIII this method is only applied to small example problems.

The second initializing method is to solve the $2N \times 2N$ nonlinear matrix Riccati equation once in order to find the linear optimal control law corresponding to the initial structural design. The initial gain values obtained from the matrix Riccati equation solution are then used to establish fixed ratios between the gains that are assumed to hold throughout the design optimization process.

The third approach is the decoupled Riccati equation method, which gives an approximate solution to the conventional full order Riccati equation. This method uses normal modes to replace the full order Riccati equation by several sets of 2×2 Riccati equations that have explicit closed form solutions. By neglecting the coupling effect in the feedback loop, the gain matrix in the modal coordinates can be assembled (with feedback gain vectors corresponding to each 2×2 decoupled Riccati equation solution) and transformed to the physical coordinates using the normal mode information.

The second and third initializing methods are described further in the following subsections.

4.2.1 *Full Order Riccati Equation*

Consider Eqs. (3.4) and (3.5) with the external disturbance terms set to zero (i.e. $\{f\} = \{0\}$):

$$[M]\{\ddot{q}\} + [C]\{\dot{q}\} + [K]\{q\} = [b]\{u\} \tag{4.1}$$

$$\{\dot{x}\} = [A_o]\{x\} + [B]\{u\} \tag{4.2}$$

The optimal control law to minimize a given performance index

$$\text{PI} = \int_0^\infty \left(\{x\}^T [Q] \{x\} + \{u\}^T [R] \{u\} \right) dt \tag{4.3}$$

where $[Q]$ and $[R]$ are $2N \times 2N$ positive semi definite and $M \times M$ positive definite weighting matrices for states and control forces respectively, can be determined from (see Ref. 28)

$$\begin{aligned} \{u\} &= -[H^o]\{x\} \\ &= -\left[[H_p^o] \quad [H_v^o] \right] \begin{Bmatrix} q \\ \dot{q} \end{Bmatrix} \\ &= -[R]^{-1}[B]^T[P]\{x\} \end{aligned} \tag{4.4}$$

where superscript o denotes the initial startup matrix, and the $2N \times 2N$ positive definite symmetric matrix $[P]$ satisfies the following $2N \times 2N$ nonlinear matrix Riccati equation:

$$[P][A_o] + [A_o]^T[P] + [Q] - [P][B][R]^{-1}[B]^T[P] = [0] \tag{4.5}$$

Here $\{\ \}^T$ and $[\ ]^T$ represent transposed vectors and matrices, respectively.

4.2.2 *Decoupled Riccati Equation Solution*

In this subsection an alternative method which bypasses solution of the full order Riccati equation (Eq. (4.5)) is presented. First find the natural frequencies and normal modes of

$$[M]\{\ddot{q}\} + [K]\{q\} = \{0\} \tag{4.6}$$

that is solve the standard eigenproblem

$$\omega_i^2 [M]\{v_i\} = [K]\{v_i\} \qquad i = 1,2,\ldots,r \tag{4.7}$$

and normalize the modes $\{v_i\}$ so that

$$\{v_i\}^T [M]\{v_j\} = \delta_{ij}, \qquad i,j = 1,2,\ldots,r \tag{4.8}$$

where r is the number of normal modes retained ($r \leq N$) and δ_{ij} is the Kronecker delta. Let

$$\{q\} = [V]\{z\} \tag{4.9}$$

where the *i-th* column of the $N \times r$ normal mode matrix $[V]$ is the *i-th* normal mode $\{v_i\}$ and $\{z\} = \lfloor z_1, z_2, \ldots, z_r \rfloor^T$ is an $r \times 1$ normal coordinate vector. Substituting Eq. (4.9) into Eq. (4.1) and premultiplying $[V]^T$ results in

$$\{\ddot{z}\} + \text{Diag}\,[c_i]\{\dot{z}\} + \text{Diag}\,[\omega_i^2]\{z\} = [V]^T [b]\{u\} \tag{4.10}$$

where Diag $[c_i]$ and Diag $[\omega_i^2]$ are diagonal $r \times r$ matrices whose components are $c_i's$ and $\omega_i^2's$. It is noted that $c_i = c_M + c_K \omega_i^2$, in view of the proportional damping assumption embodied in Eq. (3.2). Equation (4.10) can be written in scalar form as follows:

$$\ddot{z}_i + c_i \dot{z}_i + \omega_i^2 z_i = \{v_i\}^T [b]\{u\}, \quad i = 1,2,\ldots,r \tag{4.11}$$

Now assume that the part of the control vector $\{u\}$ which is related to the *i-th* normal coordinate (z_i and $\dot{z}_i$) can be calculated independently and

that the resulting $\{ u \}$ is the sum of all the parts corresponding to each scalar equation Eq. (4.11).

The foregoing assumption can be stated as follows:

$$\ddot{z}_i + c_i \dot{z}_i + \omega_i^2 z_i = \{ v_i \}^T [b] \left(\{ u \}^{(i)} + \sum_{k \neq i}^{r} \{ u \}^{(k)} \right) \tag{4.12}$$

where

$$\{ u \}^{(i)} = - \left[\{ \tilde{H}_p \}^{(i)} \{ \tilde{H}_v \}^{(i)} \right] \begin{Bmatrix} z_i \\ \dot{z}_i \end{Bmatrix}, \qquad i = 1,2, \ldots ,r \tag{4.13}$$

and

$$\begin{aligned} \{ u \} &= \sum_{i=1}^{r} \{ u \}^{(i)} \\ &= - \left[\{ \tilde{H}_p \}^{(1)} \{ \tilde{H}_v \}^{(1)} \{ \tilde{H}_p \}^{(2)} \{ \tilde{H}_v \}^{(2)} \ldots \{ \tilde{H}_p \}^{(r)} \{ \tilde{H}_v \}^{(r)} \right] \\ &\quad \times \left[z_1 \ \dot{z}_1 \ z_2 \ \dot{z}_2 \ \ldots \ z_r \ \dot{z}_r \right]^T \\ &= - \left[\{ \tilde{H}_p \}^{(1)} \{ \tilde{H}_p \}^{(2)} \ldots \{ \tilde{H}_p \}^{(r)} \{ \tilde{H}_v \}^{(1)} \{ \tilde{H}_v \}^{(2)} \ldots \{ \tilde{H}_v \}^{(r)} \right] \\ &\quad \times \left[z_1 \ z_2 \ \ldots \ z_r \ \dot{z}_1 \ \dot{z}_2 \ \ldots \ \dot{z}_r \right]^T \\ &= - \left[\ [\tilde{H}_p] \quad [\tilde{H}_v] \ \right] \begin{Bmatrix} z \\ \dot{z} \end{Bmatrix} \end{aligned} \tag{4.14}$$

The vector $\{ u \}^{(i)}$ defined by Eq. (4.13) is an $M \times 1$ control vector which contains only *i-th* normal mode information $(z_i, \dot{z}_i)$. Furthermore, $\{ \tilde{H}_p \}^{(i)}$, $\{ \tilde{H}_v \}^{(i)}$ are $M \times 1$ feedback gain vectors which relate $\{ u \}^{(i)}$ with $z_i, \dot{z}_i$ respec-

tively, while $[\tilde{H}_p]$ and $[\tilde{H}_v]$ denote $M \times r$ position and velocity gain matrices the columns of which are $\{ \tilde{H}_p \}^{(i)}$ and $\{ \tilde{H}_v \}^{(i)}$, respectively.

In order to recover the initial feedback gain matrix ($[H^o]$) in the original coordinates from $[\tilde{H}_p]$ and $[\tilde{H}_v]$ in the normal coordinates, premultiply Eq. (4.9) by $[V]^T [M]$ and note that $[V]^T [M] [V] = [I]$, in view of the normalization imposed by Eq. (4.8), so that

$$\{ z \} = [V]^T [M] \{ q \} \tag{4.15}$$

Then substitute the above equation into the final form of Eq. (4.14)

$$\begin{aligned} \{ u \} &= - [\tilde{H}_p] \{ z \} - [\tilde{H}_v] \{ \dot{z} \} \\ &= - [\tilde{H}_p] [V]^T [M] \{ q \} - [\tilde{H}_v] [V]^T [M] \{ \dot{q} \} \\ &= - [H_p^o] \{ q \} - [H_v^o] \{ \dot{q} \} \end{aligned} \tag{4.16}$$

from which it follows that

$$[H^o] = \left[[H_p^o] \; [H_v^o] \right] \tag{4.17}$$

$$[H_p^o] = [\tilde{H}_p][V]^T[M] \tag{4.18}$$

$$[H_v^o] = [\tilde{H}_v][V]^T[M] \tag{4.19}$$

Now the remaining problem consists of finding solutions for the r sets of modal gain vectors $\{ \tilde{H}_p \}^{(i)}$ and $\{ \tilde{H}_v \}^{(i)}$. Eq. (4.12) can be transformed into the standard first order state space form as

$$
\begin{aligned}
\{ \dot{w}_i \} &= [A_i] \{ w_i \} + [B_i] \left(\{ u \}^{(i)} + \sum_{k \neq i}^{r} \{ u \}^{(k)} \right) \\
&= \begin{bmatrix} 0 & 1 \\ -\omega_i^2 & -c_i \end{bmatrix} \{ w_i \} + \begin{bmatrix} [0] \\ \{ v_i \}^T [b] \end{bmatrix} \left(\{ u \}^{(i)} + \sum_{k \neq i}^{r} \{ u \}^{(k)} \right)
\end{aligned} \tag{4.20}
$$

where $\{ w_i \} = \lfloor z_i \;\; \dot{z}_i \rfloor^T$ is the 2×1 state vector, $[A_i]$ is the 2×2 system open-loop matrix and $[B_i]$ is the $2 \times M$ system input matrix for the *i-th* modal equation.

The performance index for the *i-th* mode (PI_i) has the form

$$
\mathrm{PI}_i = \int_0^{\infty} \left(\{ w_i \}^T [Q_i] \{ w_i \} + \{ u \}^{(i)T} [R_i] \{ u \}^{(i)} \right) dt \tag{4.21}
$$

where $[Q_i] = \mathrm{Diag}\,(Q_{11}^i, Q_{22}^i)$ $(Q_{11}^i, Q_{22}^i \geq 0)$ is a 2×2 weighting matrix for the *i-th* state vector and $[R_i] = \gamma_i [I]$ ($[I]$ is an $M \times M$ identity matrix, $\gamma_i > 0$) is a weighting matrix for the *i-th* modal control force vector. Then the *i-th* component of the control $\{ u \}^{(i)}$ can be determined by

$$
\begin{aligned}
\{ u \}^{(i)} &= -[R_i]^{-1} [B_i]^T [P_i] \{ w_i \} \\
&= -\frac{1}{\gamma_i} \begin{bmatrix} [0] & [b]^T \{ v_i \} \end{bmatrix} \begin{bmatrix} p_{11}^i & p_{12}^i \\ p_{12}^i & p_{22}^i \end{bmatrix} \begin{Bmatrix} z_i \\ \dot{z}_i \end{Bmatrix} \\
&= -\frac{1}{\gamma_i} \begin{bmatrix} [b]^T \{ v_i \} p_{12}^i & [b]^T \{ v_i \} p_{22}^i \end{bmatrix} \begin{Bmatrix} z_i \\ \dot{z}_i \end{Bmatrix} \\
&= -\frac{1}{\gamma_i} [b]^T \{ v_i \} p_{12}^i z_i - \frac{1}{\gamma_i} [b]^T \{ v_i \} p_{22}^i \dot{z}_i
\end{aligned} \tag{4.22}
$$

where the 2×2 positive definite symmetric matrix $[P_i] = \begin{bmatrix} p^i_{11} & p^i_{12} \\ p^i_{12} & p^i_{22} \end{bmatrix}$ satisfies the 2×2 Riccati equation

$$[P_i][A_i] + [A_i]^T[P_i] + [Q_i] - [P_i][B_i][R_i]^{-1}[B_i]^T[P_i] = [0] \qquad (4.23)$$

Equation (4.23) can be solved in closed form (see Appendix B) and the results are

$$p^i_{12} = \frac{-\omega_i^2 + \sqrt{\omega_i^4 + W_i Q^i_{11}}}{W_i}$$

$$p^i_{22} = \frac{-c_i + \sqrt{c_i^2 + W_i Q^i_{22} - 2\omega_i^2 + 2\sqrt{\omega_i^4 + W_i Q^i_{11}}}}{W_i} \qquad (4.24)$$

$$p^i_{11} = c_i p^i_{12} + \omega_i^2 p^i_{22} + p^i_{12} p^i_{22} W_i$$

where

$$W_i = \{v_i\}^T [b] [R_i]^{-1} [b]^T \{v_i\} = \frac{1}{\gamma_i} \{v_i\}^T [b] [b]^T \{v_i\} \qquad (4.25)$$

By comparing Eq. (4.13) and Eq. (4.22), the *i-th* feedback gain vectors in normal coordinates can be obtained as follows:

$$\{\tilde{H}_p\}^{(i)} = \frac{p^i_{12}}{\gamma_i} [b]^T \{v_i\}, \quad \{\tilde{H}_v\}^{(i)} = \frac{p^i_{22}}{\gamma_i} [b]^T \{v_i\} \qquad (4.26)$$

By substituting Eq. (4.22) into Eq. (4.12), the *i-th* closed-loop equation becomes

$$\ddot{z}_i + \left(c_i + \frac{1}{\gamma_i}\{v_i\}^T[b][b]^T\{v_i\}p_{22}^i\right)\dot{z}_i + \left(\omega_i^2 + \frac{1}{\gamma_i}\{v_i\}^T[b][b]^T\{v_i\}p_{12}^i\right)z_i = -\sum_{k\neq i}^{r}\left(\frac{1}{\gamma_k}\{v_k\}^T[b][b]^T\{v_k\}\left(p_{12}^k z_k + p_{22}^k \dot{z}_k\right)\right) \tag{4.27}$$

To summarize, the original full order Riccati equation Eq. (4.5) is replaced by r sets of 2×2 Riccati equations (Eq. (4.23)) which have explicit closed form solutions Eq. (4.24). Then the feedback gain matrix $[\tilde{H}] = [[\tilde{H}_p]\ [\tilde{H}_v]]$ in normal coordinates is transformed to $[H]$ in the original coordinate system by using Eqs. (4.17)-(4.19).

The method presented in this subsection has a considerable advantage over the full order Riccati equation solution approach described in the previous subsection. This innovative method is in fact explicit and efficient so that this 2×2 Riccati solution procedure can be performed periodically to update the fixed ratios initially established by the startup gain matrix.

4.3 CONTROL DESIGN VARIABLE LINKING (I): ROW-WISE AND COLUMN-WISE CONTROL DESIGN VARIABLE LINKING

In this section various linking options for control design variables based on row-wise and column-wise linking schemes of the feedback gain matrix are presented (see Ref. 26). First the feedback gain matrix $[H]$ can be written in various ways as follows:

$$
\begin{aligned}
[H] &= \begin{bmatrix} [H_p] & [H_v] \end{bmatrix} \\
&= \begin{bmatrix} \lfloor H \rfloor_1 \\ \lfloor H \rfloor_2 \\ \vdots \\ \lfloor H \rfloor_M \end{bmatrix} \\
&= \begin{bmatrix} \lfloor H_p \rfloor_1 & \lfloor H_v \rfloor_1 \\ \lfloor H_p \rfloor_2 & \lfloor H_v \rfloor_2 \\ \vdots & \vdots \\ \lfloor H_p \rfloor_M & \lfloor H_v \rfloor_M \end{bmatrix} \\
&= \begin{bmatrix} \{ H_p \}^1 & \{ H_p \}^2 \cdots & \{ H_p \}^N & \{ H_v \}^1 & \{ H_v \}^2 \cdots & \{ H_v \}^N \end{bmatrix} \\
&= \begin{bmatrix} H(1,1) & H(1,2) & \cdots & H(1,2N) \\ H(2,1) & H(2,2) & \cdots & H(2,2N) \\ \vdots & \vdots & & \vdots \\ H(M,1) & H(M,2) & \cdots & H(M,2N) \end{bmatrix}
\end{aligned}
\tag{4.28}
$$

where $[H]$ is the $M \times 2N$ feedback gain matrix, $[H_p]$ and $[H_v]$ are $M \times N$ sub matrices of $[H]$ containing position and velocity parts respectively, $\lfloor H \rfloor_j$ is the *j-th* row $(1 \times 2N)$ of $[H]$, $\lfloor H_p \rfloor_j$ and $\lfloor H_v \rfloor_j$ are the *j-th* rows $(1 \times N)$ of $[H_p]$,$[H_v]$ respectively, $\{ H_p \}^i$ and $\{ H_v \}^i$ are the *i-th* columns $(M \times 1)$ of $[H_p]$ and $[H_v]$ respectively and $H(j,i)$ is the (j,i)-*th* component of $[H]$.

The main ideas underlying the creation of alternative row-wise and column-wise control design variable linking schemes are: (1) separation of ve-

locity and position parts of the gain matrix; (2) various row and column schemes corresponding to actuator and degree of freedom linking; and (3) linking schemes based on only allowing changes in various sets of velocity gains. Combining the foregoing ideas leads to numerous linking schemes with distinct sets and various numbers of independent control system design variables (CDV's), ranging from 1 to $M \times 2N$ (see Table 2).

For example consider option number 5 in Table 2. The feedback gain matrix can be written as follows:

$$[H] = \begin{bmatrix} \lfloor H_p \rfloor_1 & \lfloor H_v \rfloor_1 \\ \lfloor H_p \rfloor_2 & \lfloor H_v \rfloor_2 \\ \cdot & \cdot \\ \cdot & \cdot \\ \cdot & \cdot \\ \lfloor H_p \rfloor_M & \lfloor H_v \rfloor_M \end{bmatrix} = \begin{bmatrix} \alpha_1 \lfloor H_p^o \rfloor_1 & \alpha_{M+1} \lfloor H_v^o \rfloor_1 \\ \alpha_2 \lfloor H_p^o \rfloor_2 & \alpha_{M+2} \lfloor H_v^o \rfloor_2 \\ \cdot & \cdot \\ \cdot & \cdot \\ \cdot & \cdot \\ \alpha_M \lfloor H_p^o \rfloor_M & \alpha_{2M} \lfloor H_v^o \rfloor_M \end{bmatrix} \tag{4.29}$$

Left hand side represents the $M \times 2N$ feedback gain matrix in partitioned row-wise form ($\lfloor H_p \rfloor_j$, $\lfloor H_v \rfloor_j$ represent the *j-th* rows of $[H_p]$ and $[H_v]$, respectively), and the right hand side has scalar participation coefficients ($\alpha_i's$) placed in front of the partitioned rows of the initial startup gain matrix on which the linking scheme is imposed (superscript *o* denotes the initial startup matrix). During optimization the $\alpha_i's$ are treated as independent design variables (simultaneously with the CSD's) and as they are optimized, the feedback gain matrix $[H]$ is optimized in the constrained design space corresponding to the fixed ratios established by the rows of the initial startup matrix.

4.4 CONTROL DESIGN VARIABLE LINKING (II): BLOCK TYPE CONTROL DESIGN VARIABLE LINKING

In this section a different approach to linking of control design variables is introduced and assessed when the decoupled 2 × 2 Riccati equation solution method is used in finding the initial startup gain matrix (see Ref. 27). The initial feedback gain matrix obtained by solving r sets of 2 × 2 Riccati equations (Eqs. (4.17)-(4.19)) can be rewritten in the following form

$$[H^o] = \left[\, [H_p^o]\ [H_v^o] \,\right] = \sum_{i=1}^{r} \left[\, [H_p^o]^{(i)}\ [H_v^o]^{(i)} \,\right] = \sum_{i=1}^{r} [H^o]^{(i)} \tag{4.30}$$

$$[H_p^o] = \sum_{i=1}^{r} \{\, \tilde{H}_p \,\}^{(i)} \{\, v_i \,\}^T [M] = \sum_{i=1}^{r} [H_p^o]^{(i)} \tag{4.31}$$

$$[H_v^o] = \sum_{i=1}^{r} \{\, \tilde{H}_v \,\}^{(i)} \{\, v_i \,\}^T [M] = \sum_{i=1}^{r} [H_v^o]^{(i)} \tag{4.32}$$

where superscripts (i) indicate that these quantities correspond to the *i-th* Riccati equation. The foregoing equations imply that the $[H_p^o]^{(i)}$'s and $[H_v^o]^{(i)}$'s or the $[H^o]^{(i)}$'s may be interpreted as basis matrices which can be used to generate the initial gain matrix. This suggests that the actual feedback gain matrix can be well approximated as a linear combination of these basis matrices, namely

$$[H] = \sum_{i=1}^{r} \alpha_i [H^o]^{(i)} \tag{4.33}$$

or

$$[H] = \sum_{i=1}^{r} \left[\alpha_i [H_p^o]^{(i)} \quad \alpha_{i+r} [H_v^o]^{(i)} \right] \tag{4.34}$$

The whole feedback gain matrix can be linked (Eq. (4.33)), or the position and velocity parts of the gain matrix can be block linked separately (Eq. (4.34)). During optimization the participation coefficients $\alpha_i's$ are treated as independent design variables along with the structural sizing variables. It should also be noted that these participation coefficients can be further linked with each other.

4.5 PROBLEMS IN CONTROL DESIGN VARIABLE LINKING

In this section some special aspects of using control design variable linking schemes are discussed.

When a specific control design variable linking scheme is used, the relative values of certain elements in the feedback gain matrix $[H]$ remain frozen throughout the design process according to the linking scheme selected. For example, if the last option of Table 2 (which links all the elements of $[H]$ together) is used, all the ratios among the elements of $[H]$ are invariant.

But, as mentioned earlier, 2 × 2 Riccati equations can be re-solved to update the fixed ratios between the elements of the gain matrix. This is done by finding a new weighting coefficient (γ_i, see Eq. (4.21)) for each mode. A rational procedure for updating the weighting matrices is described in Appen-

dix C. When the new sets of weighting matrices are found, special attention is given to preserving continuity of the real part of the closed-loop eigenvalues, so that the dynamic behavior remains relatively smooth between the updating stages.

Another problem to be adressed in using control design variable linking schemes is that higher modes, which are not directly constrained in the optimization problem, may become unstable after several design cycles. This effect is explained in detail in Appendix D and a way of preventing instability of unconstrained higher modes without knowing higher mode information is also suggested.

Chapter V

DYNAMIC BEHAVIOR CONSTRAINTS

5.1 INTRODUCTION

For the dynamic problems with transient external disturbances the set of possible behavior constraints should include: (1) complex eigenvalue constraints; (2) transient response and control force constraints; and (3) control effort constraints.

Every inequality behavior constraint can be written in the form

$$g \leq g_a \tag{5.1}$$

where g is a measure of a certain behavior and g_a is its allowable value. The above relation is transformed into a normalized form with respect to its allowable value such that the constraint function (G) is always negative.

$$G \leq 0 \tag{5.2}$$

where

$$\begin{aligned} G &= \frac{g}{g_a} - 1, \quad \text{when } g_a > 0, \\ G &= 1 - \frac{g}{g_a}, \quad \text{when } g_a < 0 \end{aligned} \tag{5.3}$$

5.2 COMPLEX EIGENPROBLEM

Since the closed-loop $[A]$ matrix (Eq. (3.11)) is not symmetric, eigenvalues and eigenvectors are complex and two distinct sets of eigenvectors exist for each eigenvalue. For the *i-th* eigenvalue λ_i , the right eigenvector $\{\phi_i\}$ satisfies

$$[A]\{\phi_i\} = \lambda_i\{\phi_i\} \tag{5.4}$$

and the left hand eigenvector $\{\psi_i\}$ satisfies

$$\{\psi_i\}^T[A] = \lambda_i\{\psi_i\}^T \tag{5.5}$$

and

$$\lambda_i = \sigma_i + \omega_{di} \tag{5.6}$$

where σ_i and ω_{di} are real and imaginary parts of the *i-th* complex eigenvalue. Also the modal damping factor ξ_i of the *i-th* mode is defined as

$$\xi_i = -\frac{\sigma_i}{\sqrt{\sigma_i^2 + \omega_{di}^2}} \tag{5.7}$$

These two sets of right and left hand eigenvectors are normalized such that (see Ref. 29)

$$\{\phi_i\}^T\{\phi_i\} = d_i \tag{5.8}$$

and

$$\{\psi_j\}^T\{\phi_i\} = \delta_{ij} \tag{5.9}$$

where d_i is a normalizing scalar constant for the *i-th* right eigenvector and δ_{ij} is a Kronecker delta. After solving both right and left eigenproblem, and normalizing the eigenvectors, it can be shown that the following matrix relations represent valid identities:

$$\begin{aligned} [A]\,[\Phi] &= [\Phi]\,[\Lambda] \\ [\Psi]^T\,[A] &= [\Lambda]\,[\Psi]^T \\ [\Psi]^T\,[\Phi] &= [I] \\ [\Psi]^T\,[A]\,[\Phi] &= [\Lambda] \end{aligned} \tag{5.10}$$

where $[\Phi] = [\,\phi_1\,\phi_2\,\ldots\,\phi_{2R}\,]$ is a $2N \times 2R$ eigenmatrix in which the *i-th* column is the *i-th* right hand eigenvector, $[\Psi] = [\,\psi_1\,\psi_2\,\ldots\,\psi_{2R}\,]$ is a $2N \times 2R$ eigenmatrix in which the *i-th* column is the *i-th* left hand eigenvector, $[\Lambda]$ is a $2R \times 2R$ diagonal matrix which contains eigenvalues on its diagonal and $2R$ is the number of eigenvalues and eigenvectors considered ($R \leq N$).

5.3 DYNAMIC TRANSIENT RESPONSE ANALYSIS

Time dependent response and control force constraints are replaced with a finite number of peak constraints by first finding the corresponding peak times using the adaptive one dimensional search method described in Ref. 30.

In order to calculate the transient response of the given system Eq. (3.10) should be integrated in the time domain. Since Eq. (3.10) is coupled and usually large, a set of complex eigenvectors is chosen as a basis to diagonalize and reduce the dimensions of the original equation. Let

$$\{x\} = [\Phi]\{\eta\} \tag{5.11}$$

where $[\Phi]$ is a $2N \times 2R\,(R \leq N)$ right hand eigenmatrix and $\{\eta\}$ is a $2R \times 1$ complex normal coordinate vector. Substituting Eq. (5.11) into Eq. (3.10) and premultiplying by $[\Psi]^T$ ($2R \times 2N$ left hand eigenmatrix transposed) yields

$$[\Psi]^T[\Phi]\{\dot{\eta}\} = [\Psi]^T[A][\Phi]\{\eta\} + [\Psi]^T[E]\{f\} \tag{5.12}$$

and introducing the identities in Eq. (5.10) leads to

$$\{\dot{\eta}\} = [\Lambda]\{\eta\} + [\Psi]^T[E]\{f\} \tag{5.13}$$

Equation (5.13) is equivalent to the following sets of $2R$ first order scalar differential equations

$$\dot{\eta}_i = \lambda_i \eta_i + \{\psi_i\}^T[E]\{f\}, \quad i = 1,2, \ \ldots\ , 2R \tag{5.14}$$

Integrating Eq. (5.14) with respect to time gives

$$\eta_i(t) = e^{\lambda_i(t-t_o)}\eta_i(t_o) + \int_{t_o}^{t} e^{\lambda_i(t-\tau)}\{\psi_i\}^T[E]\{f(\tau)\}\,d\tau \tag{5.15}$$

where t_o is an initial time and t is a specific time of interest. Here $\{f(t)\}$ is assumed to be expressed in terms of a truncated Fourier series and polynomials over a specified period of time i.e.,

$$\{f(t)\} = \sum_{k=1}^{N_\Omega} \left(\{FC\}_k \cos \Omega_k t + \{FS\}_k \sin \Omega_k t\right) + \sum_{p=0}^{N_P} \{FP\}_p t^p, \quad \text{when } 0 \le t \le t_f$$

$$\{f(t)\} = 0, \quad \text{when } t > t_f \tag{5.16}$$

where t_f is the specified time interval during which disturbances are applied, N_Ω is the number of different driving frequencies, $\{FC\}_k$ and $\{FS\}_k$ are $L \times 1$ vectors which contain cosine and sine components corresponding to the $k\text{-}th$ driving frequency Ω_k and N_P denotes the highest order polynomial term considered and the $L \times 1$ vector $\{FP\}_p$ corresponds to the $p\text{-}th$ order polynomial. Then substituting Eq. (5.16) into Eq. (5.15) yields

$$\begin{aligned}
\eta_i(t) = \; & e^{\lambda_i t}\eta_i(0) \\
& + \{\psi_i\}^T[E] \int_0^t e^{\lambda_i(t-\tau)} \left(\sum_{k=1}^{N_\Omega} \left(\{FC\}_k \cos \Omega_k \tau + \{FS\}_k \sin \Omega_k \tau\right) \right) d\tau \\
& + \{\psi_i\}^T[E] \int_0^t e^{\lambda_i(t-\tau)} \left(\sum_{p=0}^{N_P} \{FP\}_p \tau^p \right) d\tau \quad \text{when } 0 \le t \le t_f \\
\eta_i(t) = \; & e^{\lambda_i(t-t_f)}\eta_i(t_f) \quad \text{when } t > t_f
\end{aligned} \tag{5.17}$$

More detailed expressions for the $\eta_i's$ are given in Appendix E. After calculating the $\eta_i's$, $i = 1, \ldots, 2R$ the state vector $\{x(t)\}$ can be recovered from Eq. (5.11)

$$\{x\} = [\Phi]\{\eta\} \tag{5.11}$$

and the control force vector $\{u(t)\}$ (see Eq. (3.9)) is given by

$$\{u\} = -[H]\{x\} = -[H][\Phi]\{\eta\} \tag{5.18}$$

Also the transient acceleration can be calculated by differentiating Eq. (5.11) with respect to time and using the relation Eq. (5.13) to give:

$$\{\dot{x}\} = [\Phi]\{\dot{\eta}\} = [\Phi]([\Lambda]\{\eta\} + [\Psi]^T[E]\{f\}) \tag{5.19}$$

5.4 CONTROL EFFORT

The control effort can be defined as

$$\begin{aligned} \text{Control Effort} &= \int_0^{\infty} \{u\}^T [R_{CE}] \{u\}\, dt \\ &= \int_0^{t_f} \{u\}^T [R_{CE}] \{u\}\, dt + \int_{t_f}^{\infty} \{u\}^T [R_{CE}] \{u\}\, dt \end{aligned} \tag{5.20}$$

where $[R_{CE}]$ is an $M \times M$ positive definite symmetric weighting matrix.

When the time t_f (during which the external disturbance force is applied) is small, the first term of the right hand side is negligible compared with the second term. So in this work the control effort (CE) is defined as

$$\begin{aligned} CE &= \int_{t_f}^{\infty} \{u\}^T [R_{CE}] \{u\}\, dt \\ &= \int_{t_f}^{\infty} \{x\}^T [H]^T [R_{CE}] [H] \{x\}\, dt \\ &= \int_{t_f}^{\infty} \{x\}^T [Q_{CE}] \{x\}\, dt \end{aligned} \tag{5.21}$$

where $[Q_{CE}] = [H]^T [R_{CE}] [H]$.

Consider the closed-loop equation (Eq. (3.10)) when $t \geq t_f$

$$\{ \dot{x} \} = [A] \{ x \}, \quad t \geq t_f \tag{5.22}$$

Substituting Eq. (5.11) into Eq. (5.22), premultiplying by $[\Psi]^T$, and using the identities in Eq. (5.10) leads to the following expression

$$\{ \dot{\eta} \} = [\Lambda] \{ \eta \}, \quad t \geq t_f \tag{5.23}$$

Substituting Eq. (5.11) into Eq. (5.21) above gives

$$\begin{aligned} \text{CE} &= \int_{t_f}^{\infty} \{ \eta \}^T [\Phi]^T [Q_{\text{CE}}] [\Phi] \{ \eta \} \, dt \\ &= \int_{t_f}^{\infty} \{ \eta \}^T [\tilde{Q}] \{ \eta \} \, dt \end{aligned} \tag{5.24}$$

where $[\tilde{Q}] = [\Phi]^T [Q_{\text{CE}}] [\Phi]$. From Eq. (5.23), the complex response $\{ \eta (t) \}$ can be written as

$$\{ \eta (t) \} = e^{[\Lambda](t - t_f)} \{ \eta (t_f) \}, \quad t \geq t_f \tag{5.25}$$

Substituting Eq. (5.25) into Eq. (5.24) yields

$$\text{CE} = \{ \eta (t_f) \}^T \int_{t_f}^{\infty} e^{[\Lambda]^T (t - t_f)} [\tilde{Q}] \, e^{[\Lambda](t - t_f)} \, dt \; \{ \eta (t_f) \} \tag{5.26}$$

Let

$$[\tilde{W}] = \int_{t_f}^{\infty} e^{[\Lambda]^T (t - t_f)} [\tilde{Q}] \, e^{[\Lambda](t - t_f)} \, dt \tag{5.27}$$

then

$$
\begin{aligned}
& [\Lambda]^T [\tilde{W}] + [\tilde{W}] [\Lambda] \\
= & \int_{t_f}^{\infty} [\Lambda]^T e^{[\Lambda]^T (t - t_f)} [\tilde{Q}] e^{[\Lambda](t - t_f)} dt \\
& + \int_{t_f}^{\infty} e^{[\Lambda]^T (t - t_f)} [\tilde{Q}] e^{[\Lambda](t - t_f)} [\Lambda] dt \\
= & \int_{t_f}^{\infty} \frac{d}{dt} \left(e^{[\Lambda]^T (t - t_f)} [\tilde{Q}] e^{[\Lambda](t - t_f)} \right) dt \qquad (5.28) \\
= & \left[e^{[\Lambda]^T (t - t_f)} [\tilde{Q}] e^{[\Lambda](t - t_f)} \right] \Big|_{t_f}^{\infty} \\
= & [0] - [\tilde{Q}] \\
= & - [\tilde{Q}]
\end{aligned}
$$

or

$$
[\Lambda] [\tilde{W}] + [\tilde{W}] [\Lambda] = - [\tilde{Q}] \qquad (5.29)
$$

which is a Lyapunov equation. Therefore the control effort of Eq. (5.26) is given by

$$
\mathrm{CE} = \{ \eta (t_f) \}^T [\tilde{W}] \{ \eta (t_f) \} \qquad (5.30)
$$

where $[\tilde{W}]$ satisfies Eq. (5.29). Equation (5.29) can be solved element by element since $[\Lambda]$ is a diagonal matrix and $[\tilde{Q}]$ is a symmetric matrix, i.e.,

$$
\tilde{W}_{ij} = - \frac{\tilde{Q}_{ij}}{\lambda_i + \lambda_j} \qquad (5.31)
$$

where $\tilde{W}_{ij}$ and $\tilde{Q}_{ij}$ are the (i,j)-th element of $[\tilde{W}]$ and $[\tilde{Q}]$ ($\tilde{Q}_{ij} = \{\phi_i\}^T [Q_{CE}] \{\phi_j\}$) and $\{\phi_i\}$ is the i-th complex right hand eigenvector.

5.5 ACTUATOR MASS CONSTRAINTS

The actuators, located at specified structural nodes, can be sized so that they produce control forces or torques required to suppress the vibration. In Ref. 31, it is assumed that actuator masses are fixed during one cycle of optimization, and they are updated after finding peak control force or torque values of the new design according to functional or empirical relations between the maximum peak control forces or torques and the required actuator mass.

When the closed form solution for the transient peak control forces or torques is available, the relation between the actuator mass and the control forces or torques can be mathematically stated in a constraint form as follows:

$$m_A \geq c_1 \mid u(t) \mid^{c_2}, \qquad 0 \leq t \leq t_{\max} \tag{5.32}$$

or

$$m_A \geq c_1 \mid u(t_j^*) \mid^{c_2}, \qquad j = 1, \ldots, NPEAK \tag{5.33}$$

where m_A is the mass of the actuator, $t_{\max}$ is the time interval of interest, t_j^* is the j-th peak time for control forces or torques, $NPEAK$ is the number of control force peak times, and c_1 , c_2 are constants relating the peak control forces and required actuator masses. Eq. (5.33) can be normalized such that

$$G = \frac{c_1 \mid u(t_j^*) \mid^{c_2}}{m_A} - 1 \leq 0, \qquad j = 1, \ldots, NPEAK \tag{5.34}$$

Chapter VI

SENSITIVITY ANALYSIS

6.1 INTRODUCTION

In order to generate approximate problems first order system sensitivity information with respect to both structural and control design variables is required. Since it is assumed that the external loads are expressed in terms of a truncated Fourier series and polynomials over a specified period of time, it is possible to calculate all of the (first order) behavior sensitivity derivatives analytically.

6.2 FUNDAMENTAL SYSTEM MATRIX DERIVATIVES

Derivatives of $[H]$ with respect to control design variables are obtained directly and derivatives of $[M]$, $[C]$ and $[K]$ with respect to structural variables are obtained analytically from the finite element formulation. From this information analytic sensitivities of the system $[A]$ and $[E]$ matrices (see Eq. (3.10)) can be obtained with respect to an arbitrary intermediate or direct design variable α , as follows:

$$\frac{\partial[A]}{\partial\alpha} = \begin{bmatrix} [0] & [0] \\ \dfrac{\partial[A_{21}]}{\partial\alpha} & \dfrac{\partial[A_{22}]}{\partial\alpha} \end{bmatrix} \tag{6.1}$$

and

$$\frac{\partial[E]}{\partial\alpha} = \begin{bmatrix} [0] \\ \dfrac{\partial[E_2]}{\partial\alpha} \end{bmatrix} \tag{6.2}$$

where in general

$$\frac{\partial[A_{21}]}{\partial\alpha} = -\frac{\partial[M]^{-1}}{\partial\alpha}([K]+[b][H_p]) - [M]^{-1}\left(\frac{\partial[K]}{\partial\alpha}+[b]\frac{\partial[H_p]}{\partial\alpha}\right) \tag{6.3}$$

$$\frac{\partial[A_{22}]}{\partial\alpha} = -\frac{\partial[M]^{-1}}{\partial\alpha}([C]+[b][H_v]) - [M]^{-1}\left(\frac{\partial[C]}{\partial\alpha}+[b]\frac{\partial[H_v]}{\partial\alpha}\right)$$

$$\frac{\partial[E_2]}{\partial\alpha} = \frac{\partial[M]^{-1}}{\partial\alpha}[e] \tag{6.4}$$

It should be noted that the matrices $[b]$ and $[e]$ are constant with respect to any design variable and that according to the type of the design variable α, structural or control, some matrices are independent of that kind of design variable. In other words, the derivatives of $[M]$, $[C]$ and $[K]$ with respect to the control design variables are zero and those of $[H_p]$ and $[H_v]$ with respect to the structural design variables are also zero. The derivative $\partial[M]^{-1}/\partial\alpha$ is calculated by differentiating $[M][M]^{-1} = [I] =$ constant, which results in

$$\frac{\partial[M]^{-1}}{\partial\alpha} = -[M]^{-1}\frac{\partial[M]}{\partial\alpha}[M]^{-1} \tag{6.5}$$

6.3 EIGENPROBLEM SENSITIVITIES

Eigenvalue sensitivities are needed not only because eigenvalues themselves can be behavior constraints but also because they are required to calculate other response sensitivities (see Eq. (6.18)). Furthermore, in order to obtain precise transient response sensitivities, eigenvector sensitivities are also calculated using an analytic method (Refs. 32 and 33).

Differentiate Eq. (5.4) and (5.5) with respect to α and rearrange terms

$$([A] - \lambda_i [I]) \frac{\partial \{\phi_i\}}{\partial \alpha} = - \left(\frac{\partial [A]}{\partial \alpha} \{\phi_i\} - \frac{\partial \lambda_i}{\partial \alpha} \{\phi_i\} \right) \tag{6.6.a}$$

$$\frac{\partial \{\psi_i\}^T}{\partial \alpha} ([A] - \lambda_i [I]) = - \left(\{\psi_i\}^T \frac{\partial [A]}{\partial \alpha} - \frac{\partial \lambda_i}{\partial \alpha} \{\psi_i\}^T \right) \tag{6.6.b}$$

or

$$[Z_i] \frac{\partial \{\phi_i\}}{\partial \alpha} = - \{F_i\} \tag{6.7.a}$$

$$\frac{\partial \{\psi_i\}^T}{\partial \alpha} [Z_i] = - \{G_i\}^T \tag{6.7.b}$$

where

$$[Z_i] = [A] - \lambda_i [I] \tag{6.8}$$

$$\{F_i\} = \frac{\partial [A]}{\partial \alpha} \{\phi_i\} - \frac{\partial \lambda_i}{\partial \alpha} \{\phi_i\} \tag{6.9.a}$$

$$\{G_i\}^T = \{\psi_i\}^T \frac{\partial [A]}{\partial \alpha} - \frac{\partial \lambda_i}{\partial \alpha} \{\psi_i\}^T \tag{6.9.b}$$

Premultiplying Eq. (6.6.a) by $\{\psi_i\}^T$ and using Eq. (5.5) and Eq. (5.9) leads to the following expression for eigenvalue derivatives

$$\frac{\partial \lambda_i}{\partial \alpha} = \frac{\partial \sigma_i}{\partial \alpha} + \frac{\partial \omega_{di}}{\partial \alpha} = \{\psi_i\}^T \frac{\partial [A]}{\partial \alpha} \{\phi_i\} \tag{6.10}$$

or

$$\frac{\partial \sigma_i}{\partial \alpha} = \{\psi_i\}_R^T \frac{\partial [A]}{\partial \alpha} \{\phi_i\}_R - \{\psi_i\}_I^T \frac{\partial [A]}{\partial \alpha} \{\phi_i\}_I \tag{6.11}$$

and

$$\frac{\partial \omega_{di}}{\partial \alpha} = \{\psi_i\}_R^T \frac{\partial [A]}{\partial \alpha} \{\phi_i\}_I + \{\psi_i\}_I^T \frac{\partial [A]}{\partial \alpha} \{\phi_i\}_R \tag{6.12}$$

where subscripts R and I represent real and imaginary parts. The sensitivity of the modal damping factor ξ_i is calculated by differentiating Eq. (5.7) with respect to α as follows:

$$\frac{\partial \xi_i}{\partial \alpha} = \frac{\omega_{di}\left(\sigma_i \frac{\partial \omega_{di}}{\partial \alpha} - \frac{\partial \sigma_i}{\partial \alpha} \omega_{di}\right)}{\left(\sigma_i^2 + \omega_{di}^2\right)^{3/2}} \tag{6.13}$$

The derivative of the *i-th* eigenvector can be expressed as the sum of homogeneous and particular parts, as follows:

$$\frac{\partial \{\phi_i\}}{\partial \alpha} = a_i \{\phi_i\} + \{V_i\} \tag{6.14.a}$$

$$\frac{\partial \{\psi_i\}^T}{\partial \alpha} = b_i \{\psi_i\}^T + \{U_i\}^T \tag{6.14.b}$$

The particular solutions $\{ V_i \}$ and $\{ U_i \}^T$ satisfy

$$[\overline{Z}_i] \{ V_i \} = - \{ \overline{F}_i \} \tag{6.15.a}$$

$$\{ U_i \}^T [\overline{Z}_i] = - \{ \overline{G}_i \}^T \tag{6.15.b}$$

where $[\overline{Z}_i]$ is matrix $[Z_i]$ with the *r-th* column and row replaced by $\{ e_r \}$ and $\{ e_r \}^T$ respectively, $\{ e_r \}$ is a vector containing 1 in the *r-th* element and 0's elsewhere, $\{ \overline{F}_i \}$ and $\{ \overline{G}_i \}$ are vectors $\{ F_i \}$ and $\{ G_i \}$ respectively with the *r-th* element replaced by zero, where *r* is the location of the maximum absolute element in $\{ \phi_i \}$. The coefficients of the homogeneous parts, a_i and b_i, can be calculated by differentiating the normalization conditions Eq. (5.8) and Eq. (5.9), noting that d_i is a constant and $i = j$ as follows:

$$\frac{\partial}{\partial \alpha} \left(\{ \phi_i \}^T \{ \phi_i \} \right) = 0, \quad \frac{\partial}{\partial \alpha} \left(\{ \psi_i \}^T \{ \phi_i \} \right) = 0$$

hence (in view of Eq. (6.14))

$$\{ \phi_i \}^T \left(a_i \{ \phi_i \} + \{ V_i \} \right) = 0 ,$$

$$\left(b_i \{ \psi_i \}^T + \{ U_i \}^T \right) \{ \phi_i \} + \{ \psi_i \}^T \left(a_i \{ \phi_i \} + \{ V_i \} \right) = 0$$

so that

$$a_i = - \frac{\{ \phi_i \}^T \{ V_i \}}{\{ \phi_i \}^T \{ \phi_i \}} = - \frac{\{ \phi_i \}^T \{ V_i \}}{d_i} \tag{6.16.a}$$

$$b_i = - a_i - \{ U_i \}^T \{ \phi_i \} - \{ \psi_i \}^T \{ V_i \} \tag{6.16.b}$$

6.4 TRANSIENT RESPONSE SENSITIVITIES

For an arbitrary peak time t, peak response sensitivities can be calculated by differentiating Eq. (5.11) as

$$\begin{aligned}\frac{\partial \{ x(t) \}}{\partial \alpha} &= \frac{\partial}{\partial \alpha} ([\Phi] \{ \eta(t) \}) \\ &= \frac{\partial [\Phi]}{\partial \alpha} \{ \eta(t) \} + [\Phi] \frac{\partial \{ \eta(t) \}}{\partial \alpha}\end{aligned} \tag{6.17}$$

In the above equation, the only term not previously derived is $\partial \{ \eta(t) \}/\partial \alpha$ and it can be obtained by differentiating Eq. (5.15) with respect to the design variable α, assuming that the external disturbances are independent of the design variables, i.e. Ω_k, $\{FC\}_k$, $\{FS\}_k$, $k = 1, N_\Omega$ and $\{FP\}_p$, $p = 1, N_P$ are constant as follows:

$$\begin{aligned}\frac{\partial \eta_i(t)}{\partial \alpha} &= \frac{\partial}{\partial \alpha} \left\{ e^{\lambda_i (t - t_o)} \eta_i(t_o) + \int_{t_o}^{t} e^{\lambda_i (t-\tau)} \{ \psi_i \}^T [E] \{ f(\tau) \} \, d\tau \right\} \\ &= \frac{\partial \lambda_i}{\partial \alpha} (t - t_o) e^{\lambda_i (t-t_o)} \eta_i(t_o) + e^{\lambda_i (t-t_o)} \frac{\partial \eta_i(t_o)}{\partial \alpha} \\ &\quad + \int_{t_o}^{t} \frac{\partial \lambda_i}{\partial \alpha} (t - \tau) e^{\lambda_i (t-\tau)} \{ \psi_i \}^T [E] \{ f(\tau) \} \, d\tau \\ &\quad + \int_{t_o}^{t} e^{\lambda_i (t-\tau)} \frac{\partial \{ \psi_i \}^T}{\partial \alpha} [E] \{ f(\tau) \} \, d\tau \\ &\quad + \int_{t_o}^{t} e^{\lambda_i (t-\tau)} \{ \psi_i \}^T \frac{\partial [E]}{\partial \alpha} \{ f(\tau) \} \, d\tau\end{aligned} \tag{6.18}$$

Once $\partial \{ \eta(t) \}/\partial \alpha$ is calculated, sensitivities of control force and acceleration can be obtained by differenting Eqs. (5.18) and (5.19), respectively.

A more detailed derivation of $\partial \eta_i(t)/\partial \alpha$ is given in Appendix E. It should be noted that the above calculation is carried out only at previously identified peak response or peak control force times.

6.5 CONTROL EFFORT DERIVATIVE

The sensitivity of the control effort with respect to the design variable α is obtained by differentiating Eq. (5.30),

$$\frac{\partial(\mathrm{CE})}{\partial \alpha} = \{\eta(t_f)\}^T \frac{\partial[\tilde{W}]}{\partial \alpha} \{\eta(t_f)\} + 2\{\eta(t_f)\}^T [\tilde{W}] \frac{\partial\{\eta(t_f)\}}{\partial \alpha} \tag{6.19}$$

In the above expression $\partial\{\eta(t_f)\}/\partial \alpha$ can be calculated according to the procedure presented in the previous section for $t = t_f$ and the only unknown term is $\partial[\tilde{W}]/\partial \alpha$ and it can be determined by differentiating Eq. (5.31) as follows:

$$\begin{aligned} \frac{\partial \tilde{W}_{ij}}{\partial \alpha} &= -\frac{\partial}{\partial \alpha}\left(\frac{1}{\lambda_i + \lambda_j}\right)\tilde{Q}_{ij} - \frac{1}{\lambda_i + \lambda_j}\frac{\partial \tilde{Q}_{ij}}{\partial \alpha} \\ &= \frac{1}{(\lambda_i + \lambda_j)^2}\left(\frac{\partial \lambda_i}{\partial \alpha} + \frac{\partial \lambda_j}{\partial \alpha}\right)\tilde{Q}_{ij} - \frac{1}{(\lambda_i + \lambda_j)}\frac{\partial \tilde{Q}_{ij}}{\partial \alpha} \end{aligned} \tag{6.20}$$

but

$$\tilde{Q}_{ij} = \{\phi_i\}^T [Q_{\mathrm{CE}}] \{\phi_j\} \tag{6.21}$$

so that

$$\frac{\partial \tilde{Q}_{ij}}{\partial \alpha} = \{\phi_i\}^T \frac{\partial [Q_{CE}]}{\partial \alpha} \{\phi_j\} + \frac{\partial \{\phi_i\}^T}{\partial \alpha} [Q_{CE}] \{\phi_j\} + \{\phi_i\}^T [Q_{CE}] \frac{\partial \{\phi_j\}}{\partial \alpha} \tag{6.22}$$

6.6 ACTUATOR MASS CONSTRAINT DERIVATIVE

The sensitivity of the actuator mass constraint with respect to an arbitrary design variable α is obtained by differentiating Eq. (5.34) so that

$$\frac{\partial G}{\partial \alpha} = c_1 \frac{\partial}{\partial \alpha} \left(\frac{|u(t_j^*)|^{c_2}}{m_A} \right) \tag{6.23}$$

which gives

$$\frac{\partial G}{\partial \alpha} = c_1 \left[\frac{1}{m_A} c_2 \left\{ u(t_j^*) \right\}^{c_2 - 1} \frac{\partial u(t_j^*)}{\partial \alpha} + \left\{ u(t_j^*) \right\}^{c_2} \frac{\partial}{\partial \alpha} \left(\frac{1}{m_A} \right) \right] \tag{6.24}$$

when $u(t_j^*) \geq 0$ and

$$\frac{\partial G}{\partial \alpha} = c_1 \left[-\frac{1}{m_A} c_2 \left\{ -u(t_j^*) \right\}^{c_2 - 1} \frac{\partial u(t_j^*)}{\partial \alpha} + \left\{ -u(t_j^*) \right\}^{c_2} \frac{\partial}{\partial \alpha} \left(\frac{1}{m_A} \right) \right] \tag{6.25}$$

when $u(t_j^*) < 0$. In the above expression, $\frac{\partial u(t_j^*)}{\partial \alpha}$ is the sensitivity of the peak control forces, and $\frac{\partial}{\partial \alpha} \left(\frac{1}{m_A} \right)$ is nonzero only when α is the corresponding actuator mass variable.

Chapter VII

OPTIMIZATION

7.1 INTRODUCTION

Various approximation concepts such as structural and control design variable linking presented in Chapter IV, temporary constraint deletion and intermediate design variables (Refs. 34 and 35) are used to replace the original optimization problem stated in Chapter II by a series of explicit approximate problems. With the first order sensitivity information derived in Chapter VI, linear, reciprocal or hybrid approximations can be made with respect to either direct or intermediate design variables, even though the approximate design optimization problems are always solved in an integrated design space that spans the actual structural CSD's and the participation coefficients of the linked control gains. Each approximate optimization problem has its own lower and upper bounds on the design variables determined by given move limits and retains a set of constraints which are active and potentially active for the approximate problem.

7.2 INTERMEDIATE DESIGN VARIABLES

In order to generate a high quality approximate problem intermediate design variables are used. For frame elements it is known that the section properties A, I_y , I_z and J are a good choice for intermediate design variables. This follows from the fact that the elements of the stiffness and the mass matrices are linear functions of these section properties (see Appendix A).

Control design variables are used directly in the generation of the approximate problem because the system matrices are linear functions of the gains. After some numerical experimentation, most behavior constraints used in this work are found to be adequately approximated by the linear approximation with respect to control design variables. So when generating the approximate functions the linear approximation is always chosen for control design variables although the hybrid approximation can be used with respect to intermediate structural design variables.

7.3 TEMPORARY CONSTRAINT DELETION

In order to find a reduced set of constraints for each approximate problem the following rules are used: (1) all constraints which are greater than a given cutoff parameter are retained; and (2) when all the constraints in one specific category, for example when all the peak actuator force constraints are less than the given cutoff parameter, the one which has maximum value among them is retained so that the effect of this specific category will not be neglected.

After determining which constraints are retained for the approximate problem, sensitivities of those retained constraints along with the objective function are calculated analytically as shown in Chapter VI.

7.4 APPROXIMATE PROBLEM

With the information acquired from the analysis and sensitivity analysis phase each approximate optimization problem can be formulated as follows:

Find a design variable vector $\mathbf{Y}$ to minimize

$$\tilde{F}(\mathbf{X}(\mathbf{Y})) \tag{7.1}$$

subject to

$$\tilde{G}_j(\mathbf{X}(\mathbf{Y})) \leq 0\,, \qquad j \in Q_R \tag{7.2}$$

with bounds

$$\tilde{\mathbf{Y}}_i^L \leq \mathbf{Y}_i \leq \tilde{\mathbf{Y}}_i^U \qquad i = 1, \ldots, NDV \tag{7.3}$$

where NDV is the total number of design variables, $\mathbf{Y}$ is a vector of design variables $(NDV \times 1)$, $NIDV$ is the total number of intermediate design variables, $\mathbf{X}(\mathbf{Y})$ is a vector of intermediate design variables $(NIDV \times 1)$, $\tilde{F}(\cdot)$ is an approximate objective function, $\tilde{G}_j(\cdot)$ is the *j-th* approximate constraint, $\tilde{\mathbf{Y}}_i^L$ and $\tilde{\mathbf{Y}}_i^U$ are lower and upper bounds of the *i-th* design variable which are

determined by a given move limit, and Q_R is the retained set of constraints for the approximate problem.

Either linear , reciprocal or hybrid approximation can be used for $\tilde{F}(\cdot)$ and $\tilde{G}_j(\cdot)$. The details of the hybrid approximation follow. Let $\tilde{f}(\cdot)$ be any approximate function ($\tilde{F}(\cdot)$ or $\tilde{G}_j(\cdot)$), then during the approximate optimization cycle $\tilde{f}(\cdot)$ is

$$\begin{aligned}\tilde{f}(\mathbf{X}(\mathbf{Y})) &= f(\mathbf{X}(\mathbf{Y}_o)) + \sum_{k=1}^{NIDV} \frac{\partial f(\mathbf{X}(\mathbf{Y}_o))}{\partial \mathbf{X}_k} B_k(\mathbf{X}(\mathbf{Y})) \\ &= f_o + \sum_{k=1}^{NIDV} C_{ok}\, B_k(\mathbf{X}(\mathbf{Y}))\end{aligned} \tag{7.4}$$

where $\mathbf{Y}_o$, $f_o = f(\mathbf{X}(\mathbf{Y}_o))$, $C_{ok} = \partial f(\mathbf{X}(\mathbf{Y}_o))/\partial \mathbf{X}_k$, $k = 1, \ldots, NIDV$ are values at the beginning of the approximate problem which remain constant during the cycle, and

$$\begin{aligned} B_k(\mathbf{X}(\mathbf{Y})) &= \mathbf{X}_k(\mathbf{Y}) - \mathbf{X}_k(\mathbf{Y}_o), && \text{when } C_{ok} > 0 \\ B_k(\mathbf{X}(\mathbf{Y})) &= -(\mathbf{X}_k(\mathbf{Y}_o))^2\left(\frac{1}{\mathbf{X}_k(\mathbf{Y})} - \frac{1}{\mathbf{X}_k(\mathbf{Y}_o)}\right), && \text{when } C_{ok} < 0 \end{aligned} \tag{7.5}$$

and derivative of $\tilde{f}(\cdot)$ with respect to the *i-th* design variable $\mathbf{Y}_i$ is

$$\frac{\partial \tilde{f}(\mathbf{X}(\mathbf{Y}))}{\partial \mathbf{Y}_i} = \sum_{k=1}^{NIDV} C_{ok} \frac{\partial B_k(\mathbf{X}(\mathbf{Y}))}{\partial \mathbf{Y}_i} \tag{7.6}$$

where

$$\frac{\partial B_k(\mathbf{X}(\mathbf{Y}))}{\partial \mathbf{Y}_i} = \frac{\partial \mathbf{X}_k(\mathbf{Y})}{\partial \mathbf{Y}_i}, \qquad \text{when } C_{ok} > 0$$

$$\frac{\partial B_k(\mathbf{X}(\mathbf{Y}))}{\partial \mathbf{Y}_i} = \left(\frac{\mathbf{X}_k(\mathbf{Y}_o)}{\mathbf{X}_k(\mathbf{Y})}\right)^2 \frac{\partial \mathbf{X}_k(\mathbf{Y})}{\partial \mathbf{Y}_i}, \qquad \text{when } C_{ok} < 0 \tag{7.7}$$

Note that when no intermediate design variables are used, $NIDV = NDV$ and $\mathbf{X}(\mathbf{Y}) = \mathbf{Y}$ or $\mathbf{X}_i = \mathbf{Y}_i$, $i = 1, 2, \ldots, NDV$.

Chapter VIII

NUMERICAL RESULTS

8.1 INTRODUCTION

The control augmented structural optimization solution method described in the previous chapters has been implemented on the IBM 3090 main frame computer at UCLA. Numerical results for several examples, which illustrate the effectiveness of alternative control design variable linking schemes, are presented here. In most example problems, CONMIN (Ref. 36) is used as the optimizer, and it is conservatively assumed that the passive damping is zero ($c_M = c_K = 0$, see Eq. (3.2)), unless otherwise specified. The convergence criterion used in these examples is that the relative change in the objective function values between two sets of consecutive design iterations should be less than 0.1 percent.

8.2 EXAMPLE 1 - CANTILEVER BEAM

The first example is a cantilever beam as shown in Figure 2 free to deflect in plane (E $= 7.1 \times 10^6$ N/cm^2, $\rho = 2.768 \times 10^{-3}$ kg/cm^3). It has a box beam type cross section and is modelled by 10 equal length (100 cm) finite elements resulting in 20 degrees of freedom ($N = 20$). A concentrated mass of 200 kg is located at the middle of the beam and a single translational actuator

($M = 1$) having a mass of 4 kg applies control force $u(t)$ at the tip. A transient half sine pulse (with a magnitude of 4000 N at a frequency of 3.9 Hz) is applied at the tip translational degree of freedom for a time interval $0 \leq t \leq$ 0.1282 seconds. The dimension of the first order state equation (see Eq. (3.10)) is 40 ($2N$), so the total number of complex modes is 40. Transient responses are considered for the time interval $0 \leq t \leq 2$ seconds and the lowest 20 out of the 40 complex modes (according to the absolute value of the imaginary parts of the complex eigenvalues) are used to calculate the transient responses. The normalizing constants for the right hand complex eigenvectors ($d_i's$, see Eq. (5.8)) are chosen to be 10^5.

For each finite element the width (B) and depth (H) are fixed (B = H = 40 cm), but the flange and web thicknesses are free to change (subject to side constraints 0.5 $cm \leq$ T2, T3 $\leq$ 10.0 cm) resulting in two design variables per finite element. Initial thicknesses are all set to 5.0 cm.

Total mass is taken as the objective function and it includes: (1) the fixed mass at midspan (200 kg); (2) the fixed actuator mass at the tip (4 kg); and (3) the variable structural mass. All the finite elements are linked resulting in 2 structural design variables (SDV's). Hybrid approximations in terms of the structural intermediate design variables (sectional properties) are used while the approximations with respect to the control design variables (CDV's) are linear. Behavior constraints are imposed on: (1) the real part of all the retained complex modes ($\sigma_i \leq -0.5$, $i = 1, \ldots 10$): (2) the lowest damped fre-

quency ($\omega_{d_1} \geq 4.0$ Hz); (3) the peak tip displacement, ($|q_{19}(t)| \leq 10.0\ cm$); and (4) the peak actuator force ($|u(t)| \leq 1000$ N).

8.2.1 *Control Design Variable Linking (I)*

In this section, row-wise and column-wise control design variable linking schemes which are described in section 4.3 are applied to the cantilever structure. The maximum possible number of control design variables is relatively small ($M \times 2N = 40$), so all available control design variable linking options are tried (see Table 2). Since there is only one actuator, there are 5 distinct control design variable linking options for the same problem instead of 10 (for $M = 1$ each column of the gain matrix contains only one element, so the options 1, 2, 5, 7 and 6 are identical to 3, 4, 8, 9 and 10, respectively, see Table 2).

Initial startup feedback gains are computed by solving 10 sets of 2×2 Riccati equations corresponding to the lowest 10 normal modes ($r = 10$). The control weighting coefficients $\gamma_i's$ are set to 1/300 and the 2×2 state weighting matrices are chosen to be $[Q_i] = \text{Diag}\ (\omega_i^2, 1)\ i = 1, \ldots, r$ so that the first term of Eq. (4.21) represents a total (strain and kinetic) modal energy.

Five distinct control design variable linking options are imposed on the startup gain matrix from the beginning. Move limits of 50 to 60 percent for structural variables and 90 percent for control variables are used. Iteration

histories and final structural designs are given in Tables 3 and 4 respectively, and are also displayed in Figures 3 and 4.

In case 1 the feedback gain matrix is totally unlinked (or equivalently columns of $[H]$ are linked, Option 1 or 3 of Table 2). The number of control design variables (CDV's) is 40. This case allows complete freedom in the control design variable space and the final design is a near minimum gauge design with respect to the cross sectional dimensions (see Table 4). In case 2 the position part of the feedback gain matrix is fixed and the elements of velocity part are chosen as design variables (or columns of velocity part are linked, Option 2 or 4 of Table 2), resulting in 20 control design variables. In this case the convergence is relatively slow and the optimum mass is high considering the freedom given to the design space. This is because even though the elements of the velocity part of the feedback gain matrix can change freely, the fixed initial position gains are not appropriate. This can be attributed to the fact that when the position gains are fixed at their initial values, the peak displacement and frequency constraints must be satisfied by increasing the structural stiffness (once the peak actuator force constraint has become active). In case 3 the position and velocity parts (or the rows of the position and velocity parts) of the feedback gain matrix are linked (Option 5 or 8 of Table 2), which leaves 2 independent control design variables. The results for this option are remarkable because it takes only 10 analyses to completely converge to a near minimum gauge design using only 4 independent design variables (2 SDV's and 2 CDV's). In case 4 the position part of the feedback gain matrix

is fixed and the velocity part (or the rows of the velocity part) of the feedback gain matrix is linked (Option 7 or 9 of Table 2) which leaves a single control design variable. In case 5 the row of the feedback gain matrix (or the the entire feedback gain matrix) is linked (Option 6 or 10 of Table 2) which leaves also only one control design variable. Cases 4 and 5 exhibit similar convergence histories and final designs except for the position part of the feedback gain matrix (which is frozen in case 4). As one would expect when seeking a minimum mass design, the final web thicknesses in all cases are at the lower bound value (i.e. T3 = 0.5 *cm*, see Table 4 and Figure 4).

For comparison purposes the results for cases 1-5 are summarized in Table 5 along with the active constraints at the final design. Most cases converged smoothly and the maximum difference in the final objective function values achieved was as less than 15 percent. As expected the final design mass becomes larger as more restrictive linking is imposed, but the convergence becomes more robust and the total number of analyses required to obtain convergence is reduced (e.g., see cases 3-5).

8.2.2 *Different Initial Gains for Generating Startup Gain Matrix*

In this section different arbitrary initial feedback gain matrices are used to find startup gain matrices in order to examine the first initializing method (see section 4.2). It will be recalled that this method chooses arbitrary initial control gains to start and then allows a few totally unlinked iterations before imposing any control design variable linking. Four different initial feedback

gain arrangements are chosen and 3 iterations are allowed without any control design variable linking (40 independent CDV's, option 1 or 3 of Table 2). Then the position and velocity parts of the gain matrix are linked (2 independent CDV's, option 5 or 8 of Table 2).

In case 6 the initial gain matrix is null ($[H] = [0]$). In case 7 the initial gain matrix is chosen in a manner similar to that which would be used if direct output feedback control was being employed ($H(1, 19) = 5$ $kg/sec.^2$, $H(1, 39) = 100$ $kg/sec.$, $H(1, i) = 0$, elsewhere). In cases 6 and 7, in addition to the larger move limits for the control design variables (i.e., 190 percent), absolute move limits are used for small elements (namely, for gain elements less than 1 move limits are set to 100) during the unlinked iterations. In case 8 the initial gain matrix is calculated by solving the full order Riccati equation with weighting matrices $[Q] = \text{Diag}\,[\,[K],\ [M]\,]$ and $[R] = \frac{1}{300}[I]$. In case 9 the initial feedback gain matrix is obtained by solving 10 sets of 2×2 Riccati equations followed by three unlinked iterations to generate the startup matrix.

Iteration histories and final structural dimensions are given in Tables 6-7 and Figures 5-6. All four cases converge to similar final mass values. For comparison the results for cases 6-9 are summarized in Table 8 along with the active constraints at the final design. In this example the final web thicknesses in all cases take on their lower bound value (i.e. T3 = 0.5 *cm*, see Figure 6).

The results for cases 6-9 show that the initial gain matrix used to generate a startup gain matrix (via three iterations without any CDV linking) does not

have a significant effect on the final structural design or the minimum mass values achieved. It is important to note that the method used in this section can not be extended to larger problems because as the number of CDV's involved increases (i.e., according to number of CDV's = $M \times 2N$), the three totally unlinked optimization cycles required to generate the startup gain matrix become intractable.

8.3 EXAMPLE 2 - ACOSS FOUR STRUCTURE: CDV LINKING (I)

The second example is the ACOSS FOUR structure shown in Figure 7. Several studies have been made on this model (see Refs. 11, 13-16, 18 and 19) since it represents one of the simplest configurations for a 3 dimensional space structure. It consists of twelve truss elements and has 12 degrees of freedom. Nondimensionalized Young's modulus and mass density are 1 and 0.001 units, respectively. The edges of this tetrahedral truss are 10 units long, and the six supporting links are 2.83 units long. An actuator is located in each of the six supporting links (elements 7 through 12) introducing control forces that act along the supporting links, and 4 nonstructural masses of 2 units each are attached at nodes 1-4. The nodal coordinates are given in Table 9 (from Ref. 11).

The design objective is to minimize the structural mass satisfying given behavior constraints on the closed-loop eigenvalues. Truss member areas are the design variables and no structural linking scheme is used, therefore, the

number of independent structural design variables is 12. Initial truss member areas are given in Table 10 along with the final areas for all 4 cases. Lower and upper limits on the areas are 10 and 1500, respectively. The most restrictive control design variable linking scheme (option number 10 of Table 2) is chosen which leaves only one independent control design variable (elements of the feedback gain matrix are all linked). Hybrid approximation in terms of areas and linear approximation in terms of the control design variable are used to construct a sequence of explicit approximate problems. DOT (Ref. 37) is used as the optimizer.

Initially two control feedback gain matrices (Initial Design A and B) are found by solving full order and 2 × 2 Riccati equations, respectively. Initial design A is found by solving the full order Riccati equations with identity weighting matrices for both states and control forces ($[Q] = [I]_{2N}$, $[R] = [I]_M$, see Eq. (4.3)). In Tables 11 and 12 initial feedback gains, natural frequencies and closed-loop eigenvalues of the initial design A are given. Initial design B is obtained by solving 12 sets of 2 × 2 decoupled Riccati equations for the initial control gains with identity control weighting matrix ($[R_i] = [I]_M$ or $\gamma_i's = 1$), and diagonal 2 × 2 state weighting matrices ($[Q_i]$ = Diag (ω_i^2, 1), $i = 1, \ldots, 12$, see Eq. (4.21)). The normalizing constants $d_i's$ for the right hand eigenvectors (see Eq. (5.8)) are chosen to be 1. Again in Tables 13 and 14 initial feedback gains, natural frequencies and closed-loop eigenvalues are shown. In the following subsections 4 cases are investigated

where different sets of behavior constraints and initial startup control gains are used.

8.3.1 *Inequality Constraints*

In the first two cases, inequality behavior constraints are imposed on the first damping ratio ($\xi_1 \geq 0.15$), and first two damped frequencies ($\omega_{d1} \geq 1.341$ and $\omega_{d2} \geq 1.6$, see Ref. 19). Cases 1 and 2 start from the same member areas but different control gains, namely, from initial design A and B, respectively. Move limits used for the structural variables are fixed at 50 percent, and for the control variable the move limit is reduced by 70 percent after each iteration starting from 70 percent (case 1) and 50 percent (case 2).

Final member areas as well as the final value of the single control variable are given in Table 10. The value of the control design variable represents the ratio of the final feedback gain elements with respect to the initial gain elements, so the actual final feedback gain matrix is the initial feedback gain matrix multiplied by the final control design variable in each case. Natural frequencies and closed-loop eigenvalues of the final designs are given in Tables 15 and 16. In both cases the two damped frequency constraints are active at the final design but the first modal damping factor is not critical (i.e., case 1, $0.16465 > 0.15$ and case 2, $0.16745 > 0.15$).

Iteration histories of cases 1 and 2 are similar to each other (see Table 19 and Figure 8). Total design masses include 8 units for the fixed nonstructural

masses as well as the structural member masses. Final truss areas are shown in Figure 10.

Cases 1 and 2 show similar area distributions and final mass values (see Figure 10) even though the final control gains are different. The final structural masses obtained here (14.52 and 14.12, see Table 10) are lower than the result reported in Ref. 19 (18.56) by more than 20 percent. This reduction in the final mass can be attributed primarily to integration of the structural and control design variables, even though the most restrictive control variable linking option is used. It may be noted that less restrictive control design variable linking options do not reduce the final mass much further in this example.

8.3.2 *Equality Constraints*

The next two cases (cases 3 and 4) are similar to cases 1 and 2 but have different behavior constraints. One inequality constraint and five equality constraints are imposed: the first 4 modes are constrained to have the same damping ratios $\xi_i = 0.1093, i = 1, \ldots, 4$; and the first two damped frequencies are constrained as follows, $\omega_{d1} = 1.34$ and $\omega_{d2} \geq 1.5$ (see Refs. 18 and 15).

Each equality constraint is replaced by 2 inequality constraints that define a small interval, namely $0.1093 \leq \xi_i \leq 0.11, i = 1, \ldots, 4$ and $1.34 \leq \omega_{d1} \leq 1.345$, resulting in 11 inequality constraints. Cases 3 and 4

start from initial design A and B, respectively, and both structural and control design variables have 70 percent move limits.

Final designs, natural frequencies, closed-loop eigenvalues are given in Tables 10, 17 and 18. All the constraints are satisfied with less than 0.5 percent constraint violation.

Iteration histories are shown in Table 19 and also in Figure 9. Final truss areas are shown in Figure 10.

Cases 3 and 4 also show similar area distributions and final mass values (see Figure 10). And the final structural masses obtained here (15.18 and 14.94, see Table 10) are lower than the results reported in in Ref. 18 (24.01) by more than 35 percent. Between cases 3 and 4 it is seen that case 4 which uses 2 × 2 Riccati equation solutions to generate the startup gains converges much faster (see Figure 9).

8.4 EXAMPLE 3 - ANTENNA STRUCTURE: CDV LINKING (I)

The third example is an antenna structure consisting of eight aluminium beams (E = 7.3×10^6 N/cm^2, $\rho = 2.77 \times 10^{-3}$ kg/cm^3, $v = 0.325$) which have thin walled hollow box beam cross sections (see Figure 11). This structure is constrained to move vertically (**Y** - direction) only, so each nodal point has 3 degrees of freedom (translation, bending and torsion) resulting in the total 18 degrees of freedom ($N = 18$). Four translational actuators ($M = 4$) weighing

4 *kg* each are attached to nodes 3, 5, 6 and 7. These actuators are oriented so that the force they generate acts in the vertical direction (degrees of freedom 4, 10, 13 and 16). Two ramp type transient loads are applied to the node 3 at the same time. One is a vertical force ($f_1(t)$) and the other is a torsional moment ($f_2(t)$) with respect to finite elements 1 and 2 which gives anti symmetric exitation. These loads are given as follows:

$$f_1(t) = 333.3\,t \quad \text{N}, \quad f_2(t) = 10.0 \times f_1(t) \quad \text{N} \cdot cm$$

for $0 \leq t \leq 0.3$ seconds, and $f_1(t) = f_2(t) = 0$ for $t > 0.3$ seconds (see Figure 11). Transient responses are considered for the time interval $0 \leq t \leq 2$ seconds and 20 out of 36 complex modes are used to calculate the peak response values. The normalizing constants $d_i's$ for the right hand eigenvectors (see Eq. (5.8)) are chosen to be 10^5.

Flange and web thicknesses are constrained to be the same, so there are three structural design variables for each finite element (B, H and T = T2 = T3, see Option 11 of Table 1). Structural linking is also used to make the structure remain symmetric with respect to the **XY** plane, which results in the total 15 independent structural design variables. The initial structure is uniform (B = H = 20.0 *cm*, T = 0.5 *cm*), and the side constraints are 10.0 *cm* ≤ B, H ≤ 25.0 *cm*, and 0.1 *cm* ≤ T ≤ 1.0 *cm*.

Move limits of 30 percent for both structural variables and control variables are used. Behavior constraints are imposed on: (1) the real part of all the retained complex modes ($\sigma_i \leq -0.5$); (2) the fourth and fifth damped fre-

quencies ($\omega_{d_4} \geq 8.0$ Hz, $\omega_{d_5} \geq 9.25$ Hz); (3) the peak displacement of nodes 2, 4, 5 and 7 ($| q_i(t) | \leq 1.0\ cm$, $i = 1, 7, 10$ and 16); and (4) the peak actuator force ($| u_j(t) | \leq 8.5$ N, $j = 1, 2, 3$ and 4).

Initial feedback gains are computed by solving 10 sets of 2×2 Riccati equations with the control weighting coefficients $\gamma_i's = 1/400$ and the state weighting matrices $[Q_i] = \text{Diag}\ (\omega_i^2, 1)$ $i = 1, \ldots, 10$. In Figure 12, the initial closed-loop eigenvalues ($\lambda_i = \sigma_i + j\omega_{d_i}$) obtained by solving 10 sets of 2×2 Riccati equations are compared with those obtained from a full order Riccati equation solution (with weighting matrices $[Q] = \text{Diag}\ [\ [K],\ [M]\ ]$ and $[R] = \frac{1}{400}[I]$, see Eq. (4.3)), and as can be seen from the plot, these two solution methods give almost the same values for the lowest 10 modes.

Row-wise and column-wise control design variable linking schemes are investigated for this example. The maximum number of control design variables is relatively large ($M \times 2N = 144$). In this example since $M = 4$ rather than unity, there exist 10 distinct control design variable options. Ten different control design variable linking schemes (see Table 2) are imposed on the the same initial startup gains from the beginning.

Iteration histories are shown in Table 20 and Figure 13 and final structural designs are given in Table 21 and Figure 14. Design masses include the fixed actuator mass ($4 \times 4 = 16\ kg$) as well as the variable structural mass.

As the freedom in the design space is reduced by imposing more restrictive control design variable linking schemes (from case 1 to case 10), it can be

clearly seen from the results that: (1) the number of independent control variables in the optimization loop decreases (from 144 to 1); (2) the optimum mass increases (from 163.11 *kg* to 206.06 *kg*); (3) the total number of iterations decreases and the convergence becomes more robust.

Even though there is more than 20 percent of difference in the optimum mass between case 1 and case 10, all cases show a similar trend in the final structural design. Namely, widths and depths of finite elements 1, 2, 5 and 6 take on their upper bound values and thicknesses of elements 3, 4, 7, and 8 move to their lower bound values (see Table 21 and Figure 14).

Final mass values and active constraint sets for the final designs achieved in cases 1-10 are summarized in Table 22. In all cases damped frequency, peak response and peak control force constraints are active.

This example problem investigates the effect of row-wise and column-wise linking schemes on: (1) the minimum mass achievable; and (2) convergence characteristics of the optimization procedure. Generally as more linking is imposed, the final mass increases and the design converges faster and more smoothly. In Figure 15 optimum masses are compared with the number of independent control variables according to the distinct control design variable linking options chosen.

8.5 EXAMPLE 4 - ANTENNA STRUCTURE: CDV LINKING (II)

This example is the same as the previous example (Example 3) except that here the block type control design variable linking schemes introduced in section 4.4 are investigated.

8.5.1 *Linking on* [H]

Cases 1-10 select participation coefficients $\alpha_i's$ of $[H^o]^{(i)}$ (see Eq. (4.33)) as design variables. These $\alpha_i's$ are further linked so that in each case the number of independent control design variables is different. The basic scheme employed here is to treat the first $(K-1)$ variables $\alpha_1, \ldots, \alpha_{K-1}$ as independent and then link all the remaining variables $\alpha_K = \alpha_{K+1} = \cdots = \alpha_{10}$ so that the total number of independent control design variables after linking is K. For example, when $K=1$ there is only one independent design variable after linking, since $\alpha_1 = \alpha_2 = \cdots = \alpha_{10}$. When $K=2$ there are two independent design variables after linking, namely α_1 and $\alpha_2 = \alpha_3 = \cdots = \alpha_{10}$. Finally when $K=10$ there will be ten independent design variables after linking, namely the participation coefficients of the ten basis matrices in Eq. (4.33).

Iteration histories for cases 1-10 are given numerically in Table 23 and the results for cases 1, 2, 4, 6 and 10 are presented graphically in Figure 16. Final structural designs are displayed in Table 24 and in Figure 17.

8.5.2 *Linking on* $[Hp]$ *and* $[Hv]$

Cases 11-20 are the same as cases 1-10 except that the position and velocity parts of the gain matrix are separated. Namely, the $\alpha_i's$ of both $[H_p^o]^{(i)}$ and $[H_v^o]^{(i)}$ (see Eq. (4.34)) are candidates for design variables, so that the maximum number of independent control design variables after linking is doubled from 10 to 20. Iteration histories and final structural designs are given in Tables 25-26 and Figures 18-19.

As the freedom in the design space is increased by choosing more independent control design variables (from case 1 to case 10 and from case 11 to 20), it can be clearly seen from the results that the optimum mass decreases. Table 27 summarizes the critical constraint sets ($-0.03 \leq G_j \leq 0.0004$) at the final designs. The fourth damped frequency (ω_{d_4}) , the peak displacement at node 7 (q_{16}) and the peak control force at node 7 (u_4) are critical in all 20 cases.

It is important to note that even with only one or two independent control design variables (case 1 and case 11), the final objective mass values obtained (206.06 *kg* and 204.16 *kg*) are about 15% lower than the result reported in Ref. 25 (241.97 *kg*). This can be attributed to the fact that in Ref. 25 the control gains are not independent design variables since, for any particular set of structural design variables, they are determined from the solution of an LQR subproblem.

In Figure 20 final masses are compared with the number of independent control variables (case 1 of Example 3 which has 144 independent CDV's is

also shown as a reference solution). Compared to the results for Example 3, based on the column-wise or row-wise linking schemes, the new block type (basis matrix) linking method (see section 4.4) gives much better results, in the sense that with the same or fewer independent control design variables significantly lower final design mass can be obtained (compare Figures 15 and 20).

8.6 EXAMPLE 5 - ANTENNA STRUCTURE: ADDITIONAL PROBLEMS

In this section additional problems using the same antenna structure as in Examples 3 and 4 are investigated. All the cases in this section use the same startup gains and the same control design variable linking scheme as in case 10 of Example 4 (namely, startup gains are calculated by solving 10 sets of 2 × 2 Riccati equations and $\alpha_1, \ldots, \alpha_{10}$ are independent CDV's, see Eq. (4.33)) except for some additional constraints and/or special features.

8.6.1 *Additional Constraints*

Three cases are considered which have additional behavior constraints. Case 1 is identical to case 10 of Example 4 except that this case has an additional constraint on the control effort such that CE $\leq$ 20 $N^2 \cdot sec$. The 4×4 control weighting matrix $[R_{CE}]$ is chosen to be the identity matrix (see Eq. (5.21)). Case 2 is identical to case 10 of Example 4 except that in this case additional constraints are imposed on the accelerations in the vertical direction at nodes 2, 4, 5 and 7 ($| a_k(t) | \leq 100\ cm/\sec^2$, $k = 1, 7, 10$ and 16). In case

3 both control effort and acceleration constraints described above are imposed at the same time, in addition to all the other constraints.

Iteration histories and final structural dimensions are given numerically in Tables 28-29. and displayed graphically in Figures 21 and 24. Table 36 shows final mass and critical constraint set results for these three cases. Final mass values are increased compared with that for case 10 of Example 4 (170.92 *kg*) and this can be attributed primarily to the presence of additional behavior constraints. It is interesting to note that in cases 2 and 3, where acceleration constraints are considered and found active at the final design, a different type of structural design is found, namely one where all the widths (B) take on their upper bound values instead of the depths (H) (see Table 29. and Figure 24).

8.6.2 *Updating Fixed Ratios and Truncation of the Gain Matrices*

Cases 4 and 5 are the same as case 10 of Example 4 except that feedback gain matrices are modified in order to update the fixed ratios (case 4) or to prevent higher uncontrolled modes from being destabilized (case 5). In case 4 the fixed ratios built into the initial startup gain matrix are updated by solving 2×2 Riccati equations again at the beginning of each iteration. When 2×2 Riccati equations are re-solved, weighting matrices are adjusted such that the real parts of the closed-loop eigenvalues remain invariant between the updating (see Appendix C). In case 5 components of the feedback gain matrix which excite uncontrolled higher modes are eliminated by using the method presented in Appendix D.

Iteration histories and final structural dimensions are given in Tables 30-31 and Figures 22 and 24. Final masses are similar to each other, differing by less than 3 percent difference. In Table 32 the final closed-loop eigenvalues are compared with those of case 10 of Example 4. Most of the uncontrolled higher modes (modes 11 to 18) are unstable in case 10 of Example 4, but in cases 4 and 5 they are marginally stable.

8.6.3 *Lumped Mass Design Elements*

In this subsection the actuator mass constraints described in section 5.5 are included and actuator masses are treated as independent design variables (i.e., variable lumped mass design elements). The exponent in Eq. (5.33) is set to be unity ($c_2 = 1$), namely, the relation between the peak control force and the required actuator mass is assumed to be proportional with the coefficient c_1.

Three runs are made with different values of c_1. In case 6 the coefficient c_1 is chosen such that an actuator of 4 *kg* mass can produce control force of 8.5 N (i.e., $c_1 = 4\ kg\ /\ 8.5$ N) to provide requirements similar to those in case 10 of Example 4, where constraints are given on the peak control forces (8.5 N) for the fixed mass actuators (4 *kg*). In case 7 more restrictive actuator mass constraints are used such that actuators with 8 *kg* mass are needed to produce control forces of 8.5 N (i.e., $c_1 = 8\ kg\ /\ 8.5$ N). And in case 8, c_1 is chosen such that actuators of 2 *kg* mass are enough to generate control forces of 8.5 N (i.e., $c_1 = 2\ kg\ /\ 8.5$ N).

Iteration histories, final structural and actuator mass values are given in Tables 33-35 and Figures 23-24. As expected, case 6 converged to a final design similar to that found in case 10 of Example 4, and cases 7 and 8 converged to higher and lower final objective mass values, respectively, consistent with the higher and lower values used for c_1.

Final mass results for all the cases in this section are summarized along with the active constraint sets in Table 36.

8.7 EXAMPLE 6 - GRILLAGE STRUCTURE: CDV LINKING (II)

The final example treated here is the 4 by 6 planar grillage structure (see Figure 25) which was previously studied in Refs. 9 and 25. It consists of a lattice of 10 aluminium frame members placed on 2 foot centers and cantilevered from two fixed supports by 2 foot long flexible beams (E = 10.5×10^6 psi, $\rho = 0.1$ lb/in^3, $\nu = 0.3$). Each solid rectangular member is 2.0 in wide (fixed) and has an initial depth (variable) of 0.25 in. The members are oriented so that the width dimensions lie in the plane of the structure (**XZ** plane). The grillage is modelled using 40 finite elements each of which is 2 foot long and the total number of degrees of freedom is 72 (3 per node at 24 nodes). A small amount of passive damping ($c_M = 0$, $c_K = 0.00005$, see Eq. (3.2)), which gives passive damping ratios between 0.0059 % (1st mode) and 0.36 % (20th mode) to the uncontrolled initial structure, is assumed to exist. Four torque actuators are placed to provide control torque in the directions as

shown in Figure 25. The mass of each actuator (1.296×10^{-3} lb·sec^2/in) is modelled as a fixed nonstructural mass. Initial control gains are obtained by solving 25 sets of 2 × 2 decoupled Riccati equations with diagonal control weighting matrices $[R_i] = \frac{1}{200}$ Diag [2, 2, 1, 1] and diagonal 2 × 2 state weighting matrices $[Q_i]$ = Diag (ω_i^2, 1), $i = 1, \ldots, 25$ (see Eq. (4.21)). Initial open-loop and closed-loop eigenvalues are given in Table 37. Transient responses are considered for a time period $0 \leq t \leq 3$ seconds and the lowest 40 out of 144 complex modes are used.

The total mass is minimized and the grillage is subjected to a transient loading at node 3 in the **Y** direction which is a half sine pulse of magnitude 0.2 lb and frequency 7 rad/sec. Structural design variable linking is used to impose symmetry with respect to the **XY** plane on the structure and as a result there are 8 independent structural design variables (see Figure 25). Lower and upper limits on the member depths are 0.1 and 1.0 in, respectively. In this example behavior constraints are imposed on: (1) the modal damping factors of the first 20 modes ($\xi_i \geq 1\%$, $i = 1, \ldots, 20$) ; (2) the transient displacements at nodes 1-6, 7, 13, 19, 12, 18, and 24 in the **Y** - direction (i.e., $q(t) \leq 0.2$ in); and (3) the transient control torques of all actuators ($u(t) \leq 2.5$ lb·in).

At the initial structural and control design, all the damping ratio and control force constraints are satisfied, but transient displacement constraints are infeasible by as much as 68 %. Hybrid approximation in terms of depths of the members and linear approximation in terms of the control design variables are used to generate approximate optimization problems.

In this example the number of elements in the feedback gain matrix is very large ($M \times 2N = 4 \times 2{\cdot}72 = 576$), so it is almost impossible to use all the gain elements directly as independent design variables. Six cases are investigated which are similar to cases 1-10 of Example 4, namely, the participation coefficients $\alpha_i's$ of $[H^o]^{(i)}$ (see Eq. (4.33)) are control system design variables. These $\alpha_i's$ are further linked so that in each case the number of independent control design variables is different (see Table 38).

Iteration histories are given numerically in Table 40 and graphically in Figure 26. Final member depths are given in Table 39 and Figure 27. In all the cases depth of member 3 (node 13-18) has its lower bound value, and in cases 5 and 6 depths of members 5 (node 1-19) and 10 (node 6-24) also have lower bound values in addition to member 3. In Figure 28 final mass values achieved in each of the six cases are compared with the number of independent control design variables used. Similar observations to those made about previous examples can be made, namely, as the number of independent control design variables is increased from 1 to 20, the final objective mass value decreases (from 0.1191 to 0.1039, a 12.8 % reduction), but the total number of analyses required for the convergence tends to increase. The final closed-loop complex eigenvalues and modal damping factors are given in Table 41.

In all the cases transient displacement constraints at node 1 and the transient control force constraints on actuator 3 and 4 are active at the final design in addition to the critical damping ratio constraints (noted in Table 41).

Chapter IX

CONCLUSIONS AND RECOMMENDATIONS

9.1 CONCLUSIONS

A method has been presented to integrate the design space for structural/control system optimization problems in the case of linear state feedback control.

When linear state feedback control is used in the integrated structural/control optimization problem, the usual approach is to treat structural design variables as the only independent variables in the optimization loop. The control gains are subordinated by using the solution to the linear optimal control problem to implicitly represent the "optimal" control gains corresponding to any given set of structural design variables. In this approach the control gains are in effect dependent variables that can be determined for any particular structural "plant" once the state and control weighting matrices are specified. In other words, there is no design space freedom on the control system design unless the state and control weighting matrices involve some candidates for independent design variables which are free to change during optimization. While some studies suggest to use coefficients of the weighting matrices or control effort as independent design variables in optimization (see Refs. 22, 23), this is a rather indirect approach and it does not represent a truly integrated formulation of the structural/control system optimization problem.

The method presented here treats elements of the feedback gain matrix directly as independent design variables together with the structural sizing variables and actuator mass variables. In order to reduce the number of independent control design variables, the conventional structural design variable linking idea is extended to the elements of the feedback gain matrix introducing several alternative linking schemes. Also a method for generating effective initial startup control gains, which avoids the burden of solving the full order Riccati equations (see Section 4.2), is presented.

The integrated structural/control system design problem is posed as a general nonlinear mathematical programming problem. The objective is to minimize the total mass of the integrated system. Constraints on dynamic stability, damped frequency, control effort, peak transient displacement, acceleration and control force, and actuator mass are considered. By assuming that the external transient disturbances are represented in terms of a truncated Fourier series and polynomial terms, all the transient responses and their sensitivities are derived explicitly in closed form.

The general optimization problem is solved through the iterative construction and solution of a sequence of explicit approximate problems based on various approximation concepts including new control design variable linking schemes. Each approximate problem is solved using the feasible direction method implemented in CONMIN (Ref. 36) or the modified feasible direction method in DOT (Ref. 37).

The methodology summarized in this report has been implemented in a research computer program, and numerical results for several illustrative example problems have been presented. The number of analyses required to achieve convergence (based on a 0.1 percent objective function diminishing returns criterion) in most example problems ranged from 8 to 20 and significant improvement in the final design objective function values have been achieved compared to previously reported results.

The antenna example was particularly useful as a test-bed for examining the alternative control design variable linking schemes introduced here, since it involves multiple actuators and moderate model size. These results confirm that providing more design freedom by increasing the number of independent control design variables (after linking) makes it possible to achieve lower objective function values. The trade-off between reduced objective function value and increased control variable design freedom is clearly illustrated in Figure 15 (row-wise and column-wise CDV linking schems) and in Figure 20 (block type CDV linking schemes). It should be noted that as the number of independent control variables increases, the number of analyses required for convergence tends to increase. Although the full extent of the benefit is problem dependent, it is often possible to achieve significant reductions in the final objective function value by incorporating only a small number of independent control design variables into the integrated design space.

The design variable linking idea has been successfully extended to integrated structural/control optimization problems, based on full state linear

feedback control. In the context of this class of problems, design variable linking makes it possible to treat structural design variables (SDV's), actuator mass variables and control design variables (CDV's) simultaneously without having to deal with prohibitively large numbers of design variables. Furthermore, the 2 × 2 decoupled Riccati equation solution method makes it possible to obtain good startup values for the elements of the gain matrix without the computational burden of having to solve a full order ($2N \times 2N$) Riccati equation. The method presented shows promise in the sense that it offers the prospect of being able to exploit the benefits of full state feedback and true integration without having to: (1) repeatedly solve large $2N \times 2N$ Riccati equations; (2) deal with extremely large numbers of independent design variables.

9.2 RECOMMENDATIONS

The method presented in this work can be used to optimize frame/truss structures augmented by a linear state feedback controller. While this work represents an important step towards the goal of integrating the structural and the control system design processes, several improvements and extensions can be made which will lead to increased efficiency and broader applicability.

Since the majority of the time for each design iteration lies in the analysis (analysis and sensitivity analysis), reducing the total number of analyses required for the convergence will lead to significant reductions in the total cost.

The key to fewer design iterations is the construction of more accurate approximate optimization problems so that larger move limits on the design variables can be used during each stage. One way to improve the accuracy of the approximations is to use intermediate response quantities such as modal energies when constructing explicit approximations for the real (σ) and imaginary (ω_d) parts of complex eigenvalues (see Ref. 9).

Another important factor in the total cost of optimization is the time required for each analysis. If the order of the model is reduced by using appropriate basis vectors (for example natural modes of the structure), the analysis cost can be significantly reduced.

Currently a full order finite element model of the structure is used for the controller design (in other words, elements of the feedback gain matrix, $[H]$, are optimized in the physical coordinate system) assuming all the dynamic displacements and velocities are directly available. However, for practical purposes an observer or a state estimator is required to reconstruct the state values from the sensor outputs. When the observer is constructed for the full order model the task is rather difficult, since it can increase the order of the entire set of dynamic equations up to $4N$. Once the original model is reduced as mentioned above, building the observer becomes much more tractable. When an observer is used, the same linking idea can be applied to the observer gains. It should be noted that when the observer gains are also used as independent design variables, various linking schemes can be used for the observer gains. Furthermore, it will be necessary to consider additional constraints, for

example the real parts of the observer poles should have values that are more negative than the real parts of the controller poles (this will make the estimator errors decay faster than the controlled states).

In Appendix C a method is presented for updating the fixed ratios between gain matrix elements (associated with a particular linking scheme), while constraining the real parts of the closed-loop eigenvalues ($\sigma_i's$) to be unchanged during the update. When modal damping ratios ($\xi_i's$) are constrained rather than $\sigma_i's$, the possibility of a similar updating scheme needs to be investigated.

Other areas for further investigation which will be important for the solution of more realistic problems include consideration of: (1) stress constraints (both static and dynamic); (2) multiple loading conditions; (3) overdamped modes (pure real closed-loop eigenvalues); (4) sensor/actuator location issues and/or observability and controllability requirements; and (5) sensor/actuator time delay effects.

REFERENCES

1. Nurre, G.S., Ryan, R.S., Scofield, H.N. and Sims, J.L., "Dynamics and Control of Large Space Structures," *Journal of Guidance, Control and Dynamics,* Vol.7, No.5, Sept.-Oct. 1984, pp.512-526.

2. Haftka, R.T., Martinovic, Z.N. and Hallauer, W.L., "Enhanced Vibration Controllability by Minor Structural Modification," *AIAA Journal,* Vol.23, No.8, Aug. 1985, pp.1260-1266.

3. Junkins, J.L., Bodden, D.S. and Turner, J.D., "A Unified Approach to Structure and Control System Design Iteration," *Proceedings of the 4th International Conference on Applied Numerical Modeling,* Tainan, Taiwan, Dec. 1984, pp.483-490.

4. Junkins, J.L. and Rew, D.W., "Unified Optimization of Structures and Controllers," *Large Space Structures: Dynamics and Control,* edited by Atluri, S.N. and Amos, A.K., Springer-Verlag, Berlin, 1988, pp.323-353.

5. Lim, K.B. and Junkins, J.L., "Robustness Optimization of Structural and Controller Parameters," *Journal of Guidance and Control,* Vol.12, No.1, Jan.-Feb., 1989, pp.89-96.

6. Lust, R.V. and Schmit, L.A., "Control-Augmented Structural Synthesis," *AIAA Journal,* Vol.26, No.1, Jan. 1988, pp.86-94.

7. Lust, R.V. and Schmit, L.A., "Control Augmented Structural Synthesis," NASA CR-4132, April 1988.

8. Thomas, H.L., "Improved Approximations for Simultaneous Structural and Control System Synthesis," Ph. D. Dissertation, University of California, Los Angeles, 1990.

9. Thomas, H.L., Sepulveda A.E. and Schmit, L.A., "Improved Approximations for Control Augmented Structural Synthesis," *AIAA Journal,* Vol. 30, No. 1, January 1992, pp.171-179.

10. McLaren, M.D. and Slater, G.L., "A Covariance Approach to Integrated Control/Structure Optimization," *AIAA Dynamics Specialist Conference,* AIAA-90-1211-CP, Long Beach, CA, April 5-6 1990 pp.189-205.

11. Khot, N.S., Venkayya, V.B. and Eastep, F.E., "Optimal Structural Modifications to Enhance the Active Vibration Control of Flexible Structures," *AIAA Journal,* Vol.24, No.8, Aug. 1986, pp.1368-1374.

12. Venkayya, V.B. and Tischler, V.A., "Frequency Control and Its Effect on the Dynamic Response of Flexible Structures," *AIAA Journal,* Vol.23, No.11, Nov. 1985, pp.1768-1774.

13. Khot, N.S. and Grandhi, R.V., "An Integrated Approach to Structure and Control Design of Space Structures," *Recent Developments in Structural Optimization,* edited by Cheng, F.Y., ASCE Publication, 1986, pp.26-39

14. Khot, N.S., Grandhi, R.V. and Venkayya, V.B., "Structures and Control Optimization of Space Structures," *Proceedings of the AIAA/ASME/ASCE/AHS 28th Structures, Structural Dynamics and Material Conference,* Monterey, CA, April 1987, pp.850-860.

15. Grandhi, R.V., "Structural and Control Optimization of Space Structures," *Computers and Structures,* Vol.31, No.2, 1989, pp.139-150.

16. Khot, N.S., "Minimum Weight and Optimal Control Design of Space Structures," *Computer Aided Optimal Design: Structural and Mechanical Systems,* NATO ASI Series, Vol.F27, edited by Mota Soares, C.A., Springer-Verlag, Berlin, 1987, pp.389-403.

17. Khot, N.S., Öz H., Grandhi, R.V., Eastep, F.E. and Venkayya, V.B., "Optimal Structural Design With Control Gain Norm Constraints," *AIAA Journal,* Vol.26, No.5, May 1988, pp.604-611.

18. Khot, N.S., "Structural/Control Optimization to Improve the Dynamic Response of Space Structures," *Computational Mechanics,* Springer-Verlag, Vol.3, 1988, pp.179-186.

19. Grandhi, R.V., Haq, I. and Khot, N.S., "Enhanced Robustness in Integrated Structural/Control Systems Design," *Proceedings of the AIAA/ASME/ASCE/AHS/ASC Structures, Structural Dynamics and Materials Conference,* Long Beach, CA, April 1990, Part I, pp.268-276.

20. Belvin, W.K. and Park, K.C., "Structural Tailoring and Feedback Control Synthesis: An Interdisciplinary Approach," *Proceedings of the AIAA/ASME/ASCE/AHS 29th Structures, Structural Dynamics and Material Conference,* Williamsburg, VA, April 18-20, 1988, pp.1-8.

21. Miller, D.F. and Shim, J., "Gradient-Based Combined Structural and Control Optimization," *Journal of Guidance,* Vol.10, No.3, May-June 1987, pp.291-298.

22. Becus, G.A., Lui, C.Y., Venkayya, V.B. and Tischler, V.A., "Simultaneous Structural and Control Optimization via Linear Quadratic Regulator Eigenstructure Assignment," *Proceedings of the 58th Shock and Vibration Symposium,* Huntsville, AL, Oct. 1987, pp.225-232.

23. Onoda, J. and Haftka, R.T., "An Approach to Structure/Control Simultaneous Optimization for Large Flexible Spacecraft," *AIAA Journal,* Vol.25, No.8, Aug. 1987, pp.1133-1138.

24. Sepulveda, A. E., "Optimal Placement of Actuators and Sensors in Control Augmented Structural Optimization," Ph. D. Dissertation, University of California, Los Angeles, 1990.

25. Sepulveda, A. E. and Schmit, L.A., "Optimal Placement of Actuators and Sensors in Control Augmented Structural Optimization," *International Journal for Numerical Methods in Engineering,* Vol. 32, No. 6, October 1991, pp.1165-1187.

26. Jin, I.M. and Schmit, L.A., "Control Design Variable Linking for Optimization of Structural/Control Systems," *AIAA Journal,* Vol.30, No.7, July 1992, pp.1892-1900.

27. Jin, I.M. and Schmit, L.A., "Improved Control Design Variable Linking for Optimization of Structural/Control Systems," *Aerospace Design Conference,* AIAA-92-1241, Irvine, CA, Feb. 3-6, 1992.

28. Kwakernaak, H. and Sivan, R., "Linear Optimal Control Systems," Wiley, 1972.

29. Lim, K.B., Junkins, J.L. and Wang, B.P., "Re-examination of Eigenvector Derivatives," *Journal of Guidance,* Vol.10, No.6, Nov.-Dec. 1987, pp.581-587.

30. Grandhi, R.V., Haftka, R.T. and Watson, L.T., "Design-Oriented Identification of Critical Times in Transient Response," *AIAA Journal,* Vol.24, No.4, Apr. 1986, pp.649-656.

31. Padula, S.L., James, B.B., Graves, P.C., and Woodward, S.E., "Multidisciplinary Optimization of Controlled Space Structures With Global Sensitivity Equations," NASA Technical Paper 3130, 1991.

32. Nelson, R.B., "Simplified Calculation of Eigenvector Derivatives," *AIAA Journal,* Vol.14, No.9, Sept. 1976, pp.1201-1205.

33. Sutter, T.R., Camarda, C.J., Walsh, J.L. and Adelman, H.M., "Comparison of Several Methods for Calculating Vibration Mode Shape Derivatives," *AIAA Journal,* Vol.26, No.12, Dec. 1988, pp.1506-1511.

34. Schmit, L.A. and Farshi, B., "Some Approximation Concepts for Efficient Structural Synthesis," *AIAA Journal,* Vol.12, May 1974, pp.692-699.

35. Schmit, L.A.,Jr., and Miura, H., "Approximation Concepts for Efficient Structural Synthesis," NASA CR-2552, March 1976.

36. Vanderplaats, G.N., "CONMIN - A FORTRAN Program for Constrained Function Minimization," NASA TM X-62682, Aug. 1973.

37. Vanderplaats, G.N. and Hansen, S.R., DOT Users Manual, Version 2.04, VMA Engineering, 1989.

38. Balas, M.J., "Active Control of Flexible Systems," *Journal of Optimization Theory and Applications,* Vol.25, No.3, July 1978, pp.415-436.

Appendix A

ELEMENT STIFFNESS AND MASS MATRICES FOR SPACE FRAME ELEMENT

For a 3 dimensional frame element shown in Figure 1 the vector of the e-th element nodal degrees of freedom in the local coordinates is

$$\{ q^e \}^T = [u_1,\ v_1,\ w_1,\ \theta_{x1},\ \theta_{y1},\ \theta_{z1},\ u_2,\ v_2,\ w_2,\ \theta_{x2},\ \theta_{y2},\ \theta_{z2}] \qquad (A.1)$$

where u, v, and w are displacements along **x**, **y**, and **z** axes, θ_x, θ_y and θ_z are rotations about **x**, **y**, and **z** axes, respectively, and subscripts 1 and 2 represent each end point 1 and 2. Then the element stiffness matrix is

$$[K]^e = \frac{E}{l}\begin{bmatrix}
A & 0 & 0 & 0 & 0 & 0 & -A & 0 & 0 & 0 & 0 & 0 \\
 & 12I_z/l^2 & 0 & 0 & 0 & 6I_z/l & 0 & -12I_z/l^2 & 0 & 0 & 0 & 6I_z/l \\
 & & 12I_y/l^2 & 0 & -6I_y/l & 0 & 0 & 0 & -12I_y/l^2 & 0 & -6I_y/l & 0 \\
 & & & GJ/E & 0 & 0 & 0 & 0 & 0 & -GJ/E & 0 & 0 \\
 & & & & 4I_y & 0 & 0 & 0 & 6I_y/l & 0 & 2I_y & 0 \\
 & & & & & 4I_y & 0 & 6I_y/l & 0 & 0 & 0 & 2I_z \\
 & & & & & & A & 0 & 0 & 0 & 0 & 0 \\
 & & & & & & & 12I_z/l^2 & 0 & 0 & 0 & -6I_z/l \\
 & & & & Sym. & & & & 12I_y/l^2 & 0 & 6I_y/l & 0 \\
 & & & & & & & & & GJ/E & 0 & 0 \\
 & & & & & & & & & & 4I_y & 0 \\
 & & & & & & & & & & & 4I_z
\end{bmatrix} \qquad (A.2)$$

where E is the Young's modulus, G is the shear modulus, A is the area, l is the length, GJ is the torsional rigidity, and I_y and I_z are the area moment of inertia of the cross section with respect to the centroidal principal axes **y** and **z**, respectively.

The element mass matrix is

$$[M]^e = \frac{\rho A l}{420}\begin{bmatrix}
140 & 0 & 0 & 0 & 0 & 0 & 70 & 0 & 0 & 0 & 0 & 0 \\
 & 156 & 0 & 0 & 0 & 22l & 0 & 54 & 0 & 0 & 0 & 13l \\
 & & 156 & 0 & -22l & 0 & 0 & 0 & 54 & 0 & 13l & 0 \\
 & & & 140I_p/A & 0 & 0 & 0 & 0 & 0 & 70I_p/A & 0 & 0 \\
 & & & & 4l^2 & 0 & 0 & 0 & -13l & 0 & -3l^2 & 0 \\
 & & & & & 4l^2 & 0 & 13l & 0 & 0 & 0 & -3l^2 \\
 & & & & & & 140 & 0 & 0 & 0 & 0 & 0 \\
 & & & & & & & 156 & 0 & 0 & 0 & 22l \\
 & & & & Sym. & & & & 156 & 0 & 22l & 0 \\
 & & & & & & & & & 140I_p/A & 0 & 0 \\
 & & & & & & & & & & 4l^2 & 0 \\
 & & & & & & & & & & & 4l^2
\end{bmatrix} \qquad (A.3)$$

where ρ is the mass density and I_p is the polar area moment of inertia of the cross section.

Appendix B

SOLUTION OF 2 × 2 RICCATI EQUATION

Equation (4.23) can be written in equivalent form as

$$\begin{bmatrix} p_{11}^i & p_{12}^i \\ p_{12}^i & p_{22}^i \end{bmatrix}\begin{bmatrix} 0 & 1 \\ -\omega_i^2 & -c_i \end{bmatrix} + \begin{bmatrix} 0 & -\omega_i^2 \\ 1 & -c_i \end{bmatrix}\begin{bmatrix} p_{11}^i & p_{12}^i \\ p_{12}^i & p_{22}^i \end{bmatrix} + \begin{bmatrix} Q_{11}^i & 0 \\ 0 & Q_{22}^i \end{bmatrix}$$
$$- \begin{bmatrix} p_{11}^i & p_{12}^i \\ p_{12}^i & p_{22}^i \end{bmatrix}\begin{bmatrix} [0] \\ \{v_i\}^T [b] \end{bmatrix} \frac{1}{\gamma_i} [I] \begin{bmatrix} [0] & [b]^T \{v_i\} \end{bmatrix} \begin{bmatrix} p_{11}^i & p_{12}^i \\ p_{12}^i & p_{22}^i \end{bmatrix} = [0] \tag{B.1}$$

where the 2 × 2 matrix $[P_i]$ is positive definite (i.e., $p_{11}^i > 0$, $p_{22}^i > 0$ and $p_{11}^i p_{22}^i - (p_{12}^i)^2 > 0$) and $Q_{11}^i, Q_{22}^i \geq 0, \gamma_i > 0$.

Since the above equation is symmetric, there are 3 independent scalar equations as follows:

$$W_i (p_{12}^i)^2 + 2\omega_i^2 p_{12}^i - Q_{11}^i = 0 \tag{B.2.a}$$

$$W_i (p_{22}^i)^2 + 2c_i p_{22}^i - Q_{22}^i - 2p_{12} = 0 \tag{B.2.b}$$

$$W_i p_{12}^i p_{22}^i - p_{11}^i + c_i p_{12}^i + \omega_i^2 p_{22}^i = 0 \tag{B.2.c}$$

where

$$W_i = \frac{1}{\gamma_i} \{v_i\}^T [b] [b]^T \{v_i\} > 0 \tag{B.3}$$

From Eq. (B.2),

$$p_{12}^{i} = \frac{-\omega_i^2 \pm \sqrt{\omega_i^4 + W_i Q_{11}^{i}}}{W_i} \qquad (B.4.a)$$

$$p_{22}^{i} = \frac{-c_i \pm \sqrt{c_i^2 + W_i Q_{22}^{i} + 2 W_i p_{12}^{i}}}{W_i} \qquad (B.4.b)$$

$$p_{11}^{i} = -\frac{1}{W_i} c_i \omega_i^2 \pm \frac{1}{W_i}\sqrt{\left(\omega_i^4 + W_i Q_{11}^{i}\right)\left(c_i^2 + W_i Q_{22}^{i} - 2\omega_i^2 \pm \sqrt{\omega_i^4 + W_i Q_{11}^{i}}\right)} \qquad (B.4.c)$$

Since $p_{22}^{i} > 0$ and $c_i \geq 0$ the minus sign in front of the square root in Eq. (B.4.b) is dropped and since $p_{11}^{i} > 0$ the minus signs of Eq. (B.4.c) disappear so that a unique solution for $[P_i]$ can be determined as follows:

$$p_{12}^{i} = \frac{-\omega_i^2 + \sqrt{\omega_i^4 + W_i Q_{11}^{i}}}{W_i} \qquad (B.5.a)$$

$$p_{22}^{i} = \frac{-c_i + \sqrt{c_i^2 + W_i Q_{22}^{i} + 2 W_i p_{12}^{i}}}{W_i} \qquad (B.5.b)$$

$$p_{11}^{i} = -\frac{1}{W_i} c_i \omega_i^2 + \frac{1}{W_i}\sqrt{\left(\omega_i^4 + W_i Q_{11}^{i}\right)\left(c_i^2 + W_i Q_{22}^{i} - 2\omega_i^2 + 2\sqrt{\omega_i^4 + W_i Q_{11}^{i}}\right)} \qquad (B.5.c)$$

Appendix C

UPDATING FIXED RATIOS OF CONTROL GAINS

As mentioned in Section 4.2, solving for the initial feedback gain matrix and imposing some kind of linking on the feedback gains fixes the relative values of those elements through the final stage. When the decoupled Riccati equation solution method presented in subsection 4.2.2 is used, this problem can be relaxed.

When the 2 × 2 Riccati equations are solved again for a different structure, there should be some rule to choose weighting matrices $[Q_i]$ and $[R_i]$ of Eq. (4.21). Considering that the real parts of the eigenvalues ($\sigma_i's$) play an important role on the dynamic responses as well as themselves are the behavior constraints, the scheme presented here has focused on the continuity of the $\sigma_i's$ during the resolution of the feedback gain matrix.

First, the further assumption is made that the coupling effects of Eq. (4.27) on the closed-loop eigenvalues are negligible. Then neglecting the right hand side of Eq. (4.27), the *i-th* equation for the complex eigenvalue λ_i becomes

$$\lambda_i^2 + \left(c_i + W_i p_{22}^i\right)\lambda_i + \left(\omega_i^2 + W_i p_{12}^i\right) = 0 \qquad (C.1)$$

where

$$W_i = \frac{1}{\gamma_i}\{v_i\}^T [b][b]^T \{v_i\} \qquad (C.2)$$

$$p_{12}^{i} = \frac{-\omega_i^2 + \sqrt{\omega_i^4 + W_i Q_{11}^{i}}}{W_i} \qquad (C.3)$$

$$p_{22}^{i} = \frac{-c_i + \sqrt{c_i^2 + W_i Q_{22}^{i} - 2\omega_i^2 + 2\sqrt{\omega_i^4 + W_i Q_{11}^{i}}}}{W_i} \qquad (C.4)$$

Then the *i-th* closed-loop eigenvalue λ_i becomes (assuming underdamped motion)

$$\begin{aligned} \lambda_i &= \sigma_i \pm j\omega_{d_i} \\ &= \frac{-\left(c_i + W_i p_{22}^{i}\right) \pm j\sqrt{4\left(\omega_i^2 + W_i p_{12}^{i}\right) - \left(c_i + W_i p_{22}^{i}\right)^2}}{2} \end{aligned} \qquad (C.5)$$

From Eq. (C.2)-(C.5) noting that $\{v_i\}$, $[b]$, ω_i^2 and c_i are fixed for a given structure, the complex eigenvalues λ_i can be assigned arbitrarily by adjusting W_i, p_{12}^{i} and p_{22}^{i} or equivalently γ_i, Q_{11}^{i} and Q_{22}^{i}.

The ratio between the state weighting matrix $[Q_i] = \text{Diag}\,(Q_{11}^{i}, Q_{22}^{i})$ and the control weighting matrix $[R_i] = \gamma_i [I]$ determines the relative magnitude of states and control forces. This means that the ratio between $[Q_i]$ and $[R_i]$ (or Q_{11}^{i}, Q_{22}^{i} and γ_i) will determine the damping effect in the *i-th* mode, so by changing only γ_i the real part of the closed-loop eigenvalue can be assigned (within some bounds).

The foregoing observations suggest that for some iterations (for example for every K iterations) the fixed ratios within the feedback gain matrix can be updated by changing the $\gamma_i's$ in a manner which forces the real part of the

closed-loop eigenvalues to coincide with the approximate real part of the eigenvalues ($\tilde{\sigma}_i's$) from the previous iteration, i.e. from Eqs. (C.5) and (C.4)

$$\begin{aligned}\tilde{\sigma}_i &= -\frac{c_i + W_i p_{22}^i}{2} \\ &= -\frac{1}{2}\sqrt{c_i^2 + W_i Q_{22}^i - 2\omega_i^2 + 2\sqrt{\omega_i^4 + W_i Q_{11}^i}}\end{aligned} \tag{C.6}$$

or

$$W_i = \frac{1}{\left(Q_{22}^i\right)^2}\left(X + 2Q_{11}^i - 2\sqrt{Q_{11}^i X + \left(Q_{22}^i\right)^2 + \omega_i^4\left(Q_{22}^i\right)^2}\right) \tag{C.7}$$

where

$$X = Q_{22}^i\left(4\tilde{\sigma}_i^2 + 2\omega_i^2 - c_i^2\right)$$

Then from Eq. (C.2)

$$\gamma_i = \frac{1}{W_i}\{v_i\}^T[b][b]^T\{v_i\} \tag{C.8}$$

With a new set of $\gamma_i's$ the decoupled Riccati equations are solved again so that the relative values of the elements in the gain matrix are updated according to the changing structure preserving continuity of the real parts of the complex eigenvalues between the iterations. When all the $\gamma_i's$ converge to the previous values, this updating option can be turned off.

Appendix D

ABOUT SPILLOVER EFFECT

In this appendix the existence of spillover effect (see Ref. 38) of the formulation used in this study is investigated. Consider Eqs. (4.1) and (3.9) again for convenience

$$[M]\{\ddot{q}\} + [C]\{\dot{q}\} + [K]\{q\} = [b]\{u\} \tag{D.1}$$

$$\{u\} = -[H_p]\{q\} - [H_v]\{\dot{q}\} \tag{D.2}$$

The nodal degree of freedom vector, $\{q\}$, can be written without any truncation as follows (compare with Eq. (4.9)):

$$\{q\} = [V_C]\{z_C\} + [V_U]\{z_U\} \tag{D.3}$$

where $\{z_C\}$ is the $r \times 1$ controlled normal coordinate vector, $[V_C]$ is the $N \times r$ eigenmatrix consisting of the controlled r normal eigenvectors, $\{z_U\}$ is the $(N-r)\times 1$ uncontrolled normal coordinate vector, and $[V_U]$ is the $N \times (N-r)$ eigenmatrix corresponding to uncontrolled modes $\{z_U\}$.

Eigenmatrices $[V_C]$ and $[V_U]$ in Eq. (D.3) can be normalized such that

$$\begin{aligned} [V_C]^T[M][V_C] &= [I], \qquad [V_U]^T[M][V_U] = [I] \\ [V_C]^T[M][V_U] &= [0], \qquad [V_U]^T[M][V_C] = [0] \end{aligned} \tag{D.4}$$

and

$$
\begin{aligned}
&[V_C]^T [C] [V_C] = [C_C], \qquad [V_C]^T [K] [V_C] = [\Lambda_C] \\
&[V_U]^T [C] [V_U] = [C_U], \qquad [V_U]^T [K] [V_U] = [\Lambda_U]
\end{aligned} \tag{D.5}
$$

Substituting Eq. (D.3) into Eq. (D.1) and premultiplying by $[V_C]^T$ and $[V_U]^T$ results in

$$
\{ \ddot{z}_C \} + [C_C] \{ \dot{z}_C \} + [\Lambda_C] \{ z_C \} = [V_C]^T [b] \{ u \} \tag{D.6}
$$

$$
\{ \ddot{z}_U \} + [C_U] \{ \dot{z}_U \} + [\Lambda_U] \{ z_U \} = [V_U]^T [b] \{ u \} \tag{D.7}
$$

On the right hand side of Eq. (D.7), $[V_U]^T [b] \neq [0]$, which means there exists control spillover.

Substituting Eq. (D.3) into Eq. (D.2) leads to

$$
\begin{aligned}
\{ u \} = &- \left([H_p] [V_C] \{ z_C \} + [H_v] [V_C] \{ \dot{z}_C \} \right) \\
&- \left([H_p] [V_U] \{ z_U \} + [H_v] [V_U] \{ \dot{z}_U \} \right)
\end{aligned} \tag{D.8}
$$

On the right hand side of Eq. (D.8), those matrices in front of the uncontrolled modes are not zero (i.e., $[H_p] [V_U] \neq [0]$, $[H_v] [V_U] \neq [0]$) which can be interpreted as observation spillover.

As can be seen from Eqs. (D.7) and (D.8), there exist both control and observation spillover. According to Ref. 38, the closed-loop system has potential instability when the system has both observation and control spillover and it is more important to eliminate observation spillover in order to avoid instability. Therefore, the desired control input, $\{ u^* \}$, should contain only controlled modes, $\{ z_C \}$, namely

$$\{u^*\} = -[H_p][V_C]\{z_C\} - [H_v][V_C]\{\dot{z}_C\} \tag{D.9}$$

Premultiplying $[V_C]^T[M]$ to Eq. (D.3) and using relations in Eq. (D.4) results in

$$\{z_C\} = [V_C]^T[M]\{q\} \tag{D.10}$$

Substituting Eq. (D.10) into Eq. (D.9) gives

$$\begin{aligned}\{u^*\} &= -[H_p][V_C][V_C]^T[M]\{q\} - [H_v][V_C][V_C]^T[M]\{\dot{q}\} \\ &= -[H_p^*]\{q\} - [H_v^*]\{\dot{q}\}\end{aligned} \tag{D.11}$$

where

$$[H_p^*] = [H_p][V_C][V_C]^T[M] \tag{D.12}$$

and

$$[H_v^*] = [H_v][V_C][V_C]^T[M] \tag{D.13}$$

In summary, destabilization of uncontrolled higher modes can be prevented by using the truncated feedback gain matrices shown above since these matrices are orthogonal to the uncontrolled higher modes $[V_U]$ and will eliminate observation spillover.

Appendix E

CLOSED FORM SOLUTION OF TRANSIENT ANALYSIS

E.1 CLOSED FORM RESPONSE CALCULATION

Eq. (5.17) can be written in explicit closed form as

$$\eta_i(t) = \{\psi_i\}^T[E]\left(\sum_{k=1}^{N_\Omega}\left(IC_k\{FC\}_k + IS_k\{FS\}_k\right) + \sum_{p=0}^{N_P} IP_p\{FP\}_p\right) + e^{\lambda_i t}\eta_i(0) \qquad \text{when } 0 \le t \le t_f \tag{E.1}$$

$$\eta_i(t) = e^{\lambda_i (t - t_f)}\eta_i(t_f) \qquad \text{when } t > t_f$$

where

$$IC_k \equiv \int_0^t e^{\lambda_i(t-\tau)}\cos\Omega_k\tau\, d\tau = \frac{1}{\Omega_k^2 + \lambda_i^2}\left(\lambda_i e^{\lambda_i t} + \Omega_k \sin\Omega_k t - \lambda_i \cos\Omega_k t\right) \tag{E.2}$$

$$IS_k \equiv \int_0^t e^{\lambda_i(t-\tau)}\sin\Omega_k\tau\, d\tau = \frac{1}{\Omega_k^2 + \lambda_i^2}\left(\Omega_k e^{\lambda_i t} - \Omega_k \cos\Omega_k t - \lambda_i \sin\Omega_k t\right) \tag{E.3}$$

$$IP_p \equiv \int_0^t e^{\lambda_i(t-\tau)}\tau^p\, d\tau \tag{E.4}$$

When $p = 0$ (which corresponds to a step input),

$$IP_0 \equiv \int_0^t e^{\lambda_i(t-\tau)}\,d\tau = \frac{1}{\lambda_i}\left(e^{\lambda_i t} - 1\right) \tag{E.5}$$

and when $p = 1$ (which corresponds to a ramp input),

$$IP_1 \equiv \int_0^t e^{\lambda_i(t-\tau)}\,\tau\,d\tau = \frac{1}{\lambda_i}\left(\frac{1}{\lambda_i}e^{\lambda_i t} - t - \frac{1}{\lambda_i}\right) \tag{E.6}$$

The above expressions can be derived by integration by parts. It should be noted that for a given set of design variables, $\eta_i(t_f)$ needs to be calculated only once and for $t > t_f$ the second formula of Eq. (E.1) is used.

E.2 CLOSED FORM RESPONSE SENSITIVITY CALCULATION

Differentiating Eq. (E.1) with respect to α yields

$$\begin{aligned}
\frac{\partial\eta_i(t)}{\partial\alpha} = {} & \left(\frac{\partial\{\psi_i\}^T}{\partial\alpha}[E] + \{\psi_i\}^T\frac{\partial[E]}{\partial\alpha}\right) \\
& \times\left(\sum_{k=1}^{N_\Omega}\left(IC_k\{FC\}_k + IS_k\{FS\}_k\right) + \sum_{p=0}^{N_P} IP_p\{FP\}_p\right) \\
& + \{\psi_i\}^T[E] \\
& \times\left(\sum_{k=1}^{N_\Omega}\left(\frac{\partial IC_k}{\partial\alpha}\{FC\}_k + \frac{\partial IS_k}{\partial\alpha}\{FS\}_k\right) + \sum_{p=0}^{N_P}\frac{\partial IP_p}{\partial\alpha}\{FP\}_p\right) \\
& + \frac{\partial\lambda_i}{\partial\alpha}t\,e^{\lambda_i t}\eta_i(0) + e^{\lambda_i t}\frac{\partial\eta_i(0)}{\partial\alpha}, \qquad \text{when } 0 \le t \le t_f
\end{aligned} \tag{E.7}$$

$$\frac{\partial\eta_i(t)}{\partial\alpha} = \frac{\partial\lambda_i}{\partial\alpha}(t-t_f)\,e^{\lambda_i(t-t_f)}\eta_i(t_f) + e^{\lambda_i(t-t_f)}\frac{\partial\eta_i(t_f)}{\partial\alpha}, \quad \text{when } t > t_f$$

where

$$\begin{aligned}
\frac{\partial IC_k}{\partial \alpha} &\equiv \frac{\partial}{\partial \alpha}\int_0^t e^{\lambda_i(t-\tau)}\cos\Omega_k\tau\,d\tau \\
&= \frac{\partial \lambda_i}{\partial \alpha}\int_0^t e^{\lambda_i(t-\tau)}(t-\tau)\cos\Omega_k\tau\,d\tau \\
&= \frac{\partial \lambda_i}{\partial \alpha}\frac{1}{\Omega_k^2+\lambda_i^2}\left(t\lambda_i e^{\lambda_i t}+e^{\lambda_i t}-\cos\Omega_k t-2\lambda_i IC_k\right)
\end{aligned} \tag{E.8}$$

$$\begin{aligned}
\frac{\partial IS_k}{\partial \alpha} &\equiv \frac{\partial}{\partial \alpha}\int_0^t e^{\lambda_i(t-\tau)}\sin\Omega_k\tau\,d\tau \\
&= \frac{\partial \lambda_i}{\partial \alpha}\int_0^t e^{\lambda_i(t-\tau)}(t-\tau)\sin\Omega_k\tau\,d\tau \\
&= \frac{\partial \lambda_i}{\partial \alpha}\frac{1}{\Omega_k^2+\lambda_i^2}\left(t\Omega_k e^{\lambda_i t}-\sin\Omega_k t-2\lambda_i IS_k\right)
\end{aligned} \tag{E.9}$$

$$\begin{aligned}
\frac{\partial IP_0}{\partial \alpha} &\equiv \frac{\partial}{\partial \alpha}\int_0^t e^{\lambda_i(t-\tau)}\,d\tau \\
&= \frac{\partial \lambda_i}{\partial \alpha}\int_0^t e^{\lambda_i(t-\tau)}(t-\tau)\,d\tau \\
&= \frac{\partial \lambda_i}{\partial \alpha}\left(t e^{\lambda_i t}-\frac{1}{\lambda_i}e^{\lambda_i t}+\frac{1}{\lambda_i}\right)
\end{aligned} \tag{E.10}$$

$$\begin{aligned}
\frac{\partial IP_1}{\partial \alpha} &\equiv \frac{\partial}{\partial \alpha}\int_0^t e^{\lambda_i(t-\tau)}\tau\,d\tau \\
&= \frac{\partial \lambda_i}{\partial \alpha}\int_0^t e^{\lambda_i(t-\tau)}(t-\tau)\tau\,d\tau \\
&= \frac{\partial \lambda_i}{\partial \alpha}\frac{1}{\lambda_i^2}\left[t+\left(t-\frac{2}{\lambda_i}\right)e^{\lambda_i t}+\frac{2}{\lambda_i}\right]
\end{aligned} \tag{E.11}$$

Again the above expressions can be derived using integration by parts.

TABLE 1

Choice of Structural Design Variables

Option	Design Variables	Linking within an Element
1	B and H	NA
2	H	B = α H
3	B	NA
4	H	NA
5	B, H, T2 and T3	NA
6	T2 and T3	NA
7	T2 and T3	B = α T3, H = β T2
8	T3	T2 = α T3
9	T2	NA
10	T3	NA
11	B, H and T3	T2 = α T3
12	H, T2 and T3	B = α H
13	H and T3	B = α H, T2 = β T3

α, β : preassigned constants
NA : no linking within a cross section.
n.b. : options 5-13 apply to the box beam type element only. (see Figure 1)

TABLE 2

Control Design Variable Linking Options

Option	Description	Design Variables	No. of D.V.'s
1	totally unlinked	elements of $[H]$	M × 2N
2	$[H_p]$ fixed, $[H_v]$ unlinked	elements of $[H_v]$	M × N
3	columns of $[H]$ linked	coefficients of columns of $[H]$	2N
4	$[H_p]$ fixed, columns of $[H_v]$ linked	coefficients of columns of $[H_v]$	N
5	rows of $[H_p]$ and $[H_v]$ linked	coefficients of rows of $[H_p]$ and $[H_v]$	2M
6	rows of $[H]$ linked	coefficients of rows of $[H]$	M
7	$[H_p]$ fixed, rows of $[H_v]$ linked	coefficients of rows of $[H_v]$	M
8	$[H_p]$, $[H_v]$ linked	coefficients of $[H_p]$, $[H_v]$	2
9	$[H_p]$ fixed, $[H_v]$ linked	coefficient of $[H_v]$	1
10	$[H]$ linked	coefficient of $[H]$	1

$[H]$: M × 2N feedback gain matrix
$[H_p]$: position part of $[H]$ (M × N)
$[H_v]$: velocity part of $[H]$ (M × N)

TABLE 3

Iteration History for Example 1: Cantilever Beam, Cases 1-5
Control Design Variable Linking (I)

Total Mass(kg)

Analysis	Case 1	Case 2	Case 3	Case 4	Case 5
1	2141.6	2141.6	2141.6	2141.6	2141.6
2	1351.1	1352.1	1351.4	1453.5	1453.6
3	833.30	841.33	841.18	956.15	956.45
4	595.18	896.81	598.67	658.18	658.57
5	502.20	621.41	502.45	533.76	534.30
6	461.45	519.07	460.13	485.52	486.13
7	444.36	479.59	435.03	472.54	473.19
8	428.04	467.22	428.93	472.54	473.19
9	427.74	463.20	428.93	472.54	473.19
10	423.71	455.93	428.93		
11	423.70	454.28			
12	423.67	454.18			
13		453.07			
14		452.20			
15		451.95			
16		451.94			

TABLE 4

Final Cross Sectional Dimensions for Example 1: Cantilever Beam, Cases 1-5
Control Design Variable Linking (I)

Final Cross Sectional Dimensions(cm)

	Case 1	Case 2	Case 3	Case 4	Case 5
T2	0.5046	0.6356	0.5290	0.7310	0.7340
T3	0.5000°	0.5000°	0.5000°	0.5000°	0.5000°

° indicates lower bound value

TABLE 5

Summary of Example 1: Cantilever Beam, Cases 1-5
Control Design Variable Linking (I)

	Case 1	Case 2	Case 3	Case 4	Case 5
CDV Linking Option*	1 or 3	2 or 4	5 or 8	7 or 9	6 or 10
No. of Total Analyses	12	16	10	9	9
Final Active Constraints	ω_d q u	ω_d u	ω_d q u	σ_{10} ω_d	σ_{10} ω_d
Number of CDV	40	20	2	1	1
Final Mass (kg)	423.67	451.94	428.93	472.54	473.19

* : See Table 2

TABLE 6

Iteration History for Example 1: Cantilever Beam, Cases 6-9
Different Initial Feedback Gains

Total Mass(kg)

Analysis	Case 6	Case 7	Case 8	Case 9
1	2141.6	2141.6	2141.6	2141.6
2	1891.0	1433.9	2151.5	1559.4
3	927.12	1035.4	1644.0	1091.8
4	549.12	774.95	1170.6	780.60
5	512.22	595.87	836.46	582.35
6	465.22	491.20	622.14	456.71
7	437.93	458.57	489.56	435.84
8	429.40	431.84	444.44	428.09
9	429.40	431.84	434.64	427.81
10	429.40	431.84	434.64	428.63
11			434.64	428.63
12				428.63

TABLE 7

Final Cross Sectional Dimensions for Example 1: Cantilever Beam, Cases 6-9
Different Initial Feedback Gains

Final Cross Sectional Dimensions(cm)

	Case 6	Case 7	Case 8	Case 9
T2	0.5311	0.5424	0.5554	0.5276
T3	0.5000[a]	0.5000[a]	0.5000[a]	0.5000[a]

[a] indicates lower bound value

TABLE 8

Summary of Example 1: Cantilever Beam, Cases 6-9
Different Initial Feedback Gains

	Case 6	Case 7	Case 8	Case 9
Initial Gains	$[H] = [0]$	direct output	Full Riccati	2×2 Riccati
No. of Unlinked Iterations	3	3	3	3
No. of Total Analyses	10	10	11	12
Final Active Constraints	$\omega_d\ q\ u$	$\omega_d\ q\ u$	$\sigma_{10}\ \omega_d\ q\ u$	$\omega_d\ q\ u$
Final Mass (kg)	429.40	431.84	434.64	428.63

TABLE 9

Nodal Point Coordinates for Example 2: ACOSS FOUR

Node	X	Y	Z*
1	0.0	0.0	8.165
2	−5.0	−2.8868	0.0
3	5.0	−2.8868	0.0
4	0.0	5.7735	0.0
5	−6.0	−1.1547	−2.0
6	−4.0	−4.6188	−2.0
7	4.0	−4.6188	−2.0
8	6.0	−1.1547	−2.0
9	−2.0	5.7735	−2.0
10	2.0	5.7735	−2.0

* : the origin (0,0,0) lies in the plane of nodes 2,3 and 4
(2 units shift in Z coordinate origin from Ref. 11)

TABLE 10

Initial and Final Cross Sectional Areas of Truss Elements for Example 2: ACOSS FOUR

Element (Nodes)	Initial A and B	Final Case 1	Final Case 2	Final Case 3	Final Case 4
1 (1-2)	1000.	258.2	251.7	258.6	290.4
2 (2-3)	1000.	164.8	162.6	260.1	243.8
3 (1-3)	100.	153.3	149.3	168.5	134.9
4 (1-4)	100.	152.4	149.4	101.4	131.8
5 (2-4)	1000.	165.8	162.6	243.5	245.0
6 (3-4)	1000.	282.8	274.5	291.2	286.9
7 (2-5)	100.	162.4	156.4	76.2	78.9
8 (2-6)	100.	161.6	156.5	137.9	72.8
9 (3-7)	100.	102.9	82.0	110.3	98.4
10 (3-8)	100.	219.8	225.1	102.1	110.2
11 (4-9)	100.	103.8	81.9	94.2	99.6
12 (4-10)	100.	219.6	225.1	166.8	107.9
Structural Mass	43.697	14.518	14.124	15.177	14.935
Control Design Variable	1.0	5.2283*	2.8781**	2.9479*	1.5385**
Number of Analyses Required	-	11	12	13	8

* : represents the ratio of the final feedback gain with respect to the initial gain of Design A (See Table 11)
** : represents the ratio of the final feedback gain with respect to the initial gain of Design B (See Table 13)

TABLE 11

Feedback Gains of Initial Design A for Example 2: ACOSS FOUR
(Feedback Gain Calculated by Solving Full Order Riccati Equations with Weighting Matrices $[Q] = [I]_{2N}$ and $[R] = [I]_M$)

Position Gains

Node	Direction	Actuator 1	Actuator 2	Actuator 3	Actuator 4	Actuator 5	Actuator 6
	X	-0.17112	-0.15531	0.04389	-0.00572	0.01124	-0.02256
1	Y	-0.08062	-0.10785	-0.01233	-0.02279	0.04415	0.00646
	Z	-0.23050	-0.23037	-0.00667	-0.15163	-0.00672	-0.15156
	X	0.50329	0.35341	-0.26035	0.19237	-0.15928	0.15346
2	Y	0.11764	0.37713	-0.03369	0.06621	-0.20857	0.13342
	Z	0.27425	0.27412	-0.14808	0.04077	-0.14804	0.04074
	X	-0.37381	-0.12643	0.07734	-0.17505	-0.02042	-0.01554
3	Y	0.21863	0.23719	0.14667	-0.09655	0.07495	-0.13230
	Z	0.07594	0.03240	0.08307	0.05708	0.04116	-0.02841
	X	0.14220	0.00236	0.05463	-0.12230	0.16562	-0.17110
4	Y	-0.22824	-0.43309	-0.05519	0.05272	-0.00637	-0.10331
	Z	0.03239	0.07595	0.04116	-0.02840	0.08307	0.05707

Velocity Gains

	X	0.33432	-0.01836	-0.23952	-0.53569	0.34669	-0.30211
1	Y	-0.21421	0.39664	0.53864	-0.03958	-0.47675	-0.44411
	Z	-0.19287	-0.19284	0.16896	0.08101	0.16895	0.08103
	X	0.84740	-0.10095	0.01224	0.01220	0.12992	-0.09151
2	Y	-0.60568	1.03660	0.14295	-0.11270	-0.06087	0.06691
	Z	1.12920	1.12920	-0.01356	0.01441	-0.01355	0.01440
	X	-0.08273	-0.16078	0.47486	-0.52061	0.17640	-0.17019
3	Y	-0.09619	0.20450	0.85744	-0.81356	0.05456	-0.05683
	Z	-0.00656	0.00742	0.84300	0.82788	0.01139	0.01026
	X	0.09672	-0.12468	0.13546	-0.13433	0.97992	-0.96481
4	Y	-0.24152	-0.02350	0.12552	-0.11899	-0.01753	-0.04402
	Z	0.00741	-0.00656	0.01139	0.01026	0.84299	0.82788

TABLE 12

Natural Frequencies, Closed-Loop Eigenvalues and Modal Damping Ratios for Initial Design A in Example 2: ACOSS FOUR

Mode Number	Natural Frequency (ω^2)	Closed-loop Eigenvalue ($\sigma \pm j\omega_d$)	Damping Ratio (ξ)
1	1.8010	−0.05196 ± j 1.34173	0.03869
2	2.7715	−0.07716 ± j 1.66395	0.04632
3	8.3563	−0.15106 ± j 2.88766	0.05224
4	8.7465	−0.16782 ± j 2.95366	0.05673
5	11.548	−0.20178 ± j 3.39314	0.05936
6	17.678	−0.25698 ± j 4.19752	0.06111
7	21.735	−0.25094 ± j 4.65595	0.05382
8	22.613	−0.24350 ± j 4.74958	0.05120
9	72.923	−0.20643 ± j 8.53709	0.02417
10	85.574	−0.19523 ± j 9.24860	0.02110
11	105.78	−0.15129 ± j10.28381	0.01471
12	166.55	−0.05871 ± j12.90510	0.00455

TABLE 13

Feedback Gains of Initial Design B for Example 2: ACOSS FOUR
(Feedback Gain Calculated by Solving 12 Sets of 2 × 2 Riccati Equations with Weighting Matrices $[Q_i] = \text{Diag}\,(\omega_i^2,\ 1)$ and $[R_i] = [I]_M$)

Position Gains

Node	Direction	Actuator 1	Actuator 2	Actuator 3	Actuator 4	Actuator 5	Actuator 6
1	X	-0.00027	-0.00040	-0.00009	-0.00015	0.00008	-0.00011
	Y	-0.00031	-0.00008	0.00015	-0.00004	-0.00015	-0.00011
	Z	-0.00078	-0.00078	-0.00005	0.00001	-0.00005	0.00001
2	X	0.17636	-0.17577	-0.00057	0.00059	-0.00008	0.00009
	Y	-0.30476	0.30509	0.00024	-0.00023	-0.00062	0.00063
	Z	0.35224	0.35224	0.00014	-0.00019	0.00014	-0.00019
3	X	-0.00044	0.00087	0.17609	-0.17614	-0.00008	0.00013
	Y	-0.00013	0.00026	0.30499	-0.30492	0.00070	-0.00069
	Z	-0.00003	-0.00003	0.35173	0.35169	0.00010	0.00006
4	X	0.00066	-0.00033	0.00057	-0.00053	0.35215	-0.35211
	Y	0.00062	-0.00031	-0.00042	0.00046	-0.00001	-0.00007
	Z	-0.00003	-0.00003	0.00010	0.00006	0.35173	0.35169

Velocity Gains

Node	Direction	Actuator 1	Actuator 2	Actuator 3	Actuator 4	Actuator 5	Actuator 6
1	X	0.48833	-0.05431	-0.35118	-0.87244	0.55421	-0.50961
	Y	-0.34465	0.59525	0.84274	-0.08477	-0.72551	-0.71314
	Z	-0.39794	-0.39787	0.30804	0.11272	0.30801	0.11277
2	X	1.63810	-0.19273	0.00299	0.07450	0.21374	-0.13354
	Y	-1.16800	2.00250	0.24509	-0.19719	-0.11992	0.16311
	Z	2.18680	2.18680	-0.03887	0.05238	-0.03886	0.05237
3	X	-0.22706	-0.30616	0.94046	-0.99591	0.30379	-0.29970
	Y	-0.16336	0.36588	1.64910	-1.58520	0.14310	-0.11673
	Z	0.00539	0.00812	1.62040	1.59280	0.03972	0.01485
4	X	0.16378	-0.25501	0.27585	-0.25098	1.89820	-1.87060
	Y	-0.44813	-0.11487	0.19162	-0.20122	-0.01018	-0.06976
	Z	0.00811	0.00541	0.03972	0.01484	1.62040	1.59280

TABLE 14

Natural Frequencies, Closed-Loop Eigenvalues and Modal Damping Ratios for Initial Design B in Example 2: ACOSS FOUR

Mode Number	Natural Frequency (ω^2)	Closed-loop Eigenvalue ($\sigma \pm j\omega_d$)	Damping Ratio (ξ)
1	1.8010	$-0.08264 \pm$ j 1.34786	0.06120
2	2.7715	$-0.13181 \pm$ j 1.67555	0.07843
3	8.3563	$-0.28566 \pm$ j 2.90017	0.09802
4	8.7465	$-0.31846 \pm$ j 2.96470	0.10680
5	11.548	$-0.38801 \pm$ j 3.40683	0.11316
6	17.678	$-0.49915 \pm$ j 4.20444	0.11789
7	21.735	$-0.49119 \pm$ j 4.64576	0.10514
8	22.613	$-0.47814 \pm$ j 4.72990	0.10058
9	72.923	$-0.41002 \pm$ j 8.50867	0.04813
10	85.574	$-0.38734 \pm$ j 9.21960	0.04198
11	105.78	$-0.30212 \pm$ j10.26629	0.02942
12	166.55	$-0.11446 \pm$ j12.88505	0.00888

TABLE 15

Natural Frequencies, Closed-Loop Eigenvalues and Modal Damping Ratios for Final Design of Case 1 in Example 2: ACOSS FOUR

Mode Number	Natural Frequency (ω^2)	Closed-loop Eigenvalue ($\sigma \pm j\omega_d$)	Damping Ratio (ξ)
1	1.7917	$-0.22511 \pm$ j 1.34857*	0.16465
2	2.5221	$-0.16755 \pm$ j 1.59354*	0.10456
3	7.7894	$-0.45422 \pm$ j 2.90936	0.15426
4	8.3369	$-0.17110 \pm$ j 2.91693	0.05856
5	13.329	$-0.26529 \pm$ j 3.72512	0.07104
6	21.781	$-1.31127 \pm$ j 4.39815	0.28571
7	24.304	$-1.06505 \pm$ j 4.73268	0.21955
8	33.428	$-1.64435 \pm$ j 5.54856	0.28414
9	37.101	$-0.32458 \pm$ j 6.05921	0.05349
10	44.278	$-1.72945 \pm$ j 6.22344	0.26775
11	45.840	$-1.47318 \pm$ j 6.40279	0.22423
12	48.746	$-1.69234 \pm$ j 6.67545	0.24574

* : critical constraints

TABLE 16

Natural Frequencies, Closed-Loop Eigenvalues and Modal Damping Ratios for Final Design of Case 2 in Example 2: ACOSS FOUR

Mode Number	Natural Frequency (ω^2)	Closed-loop Eigenvalue ($\sigma \pm j\omega_d$)	Damping Ratio (ξ)
1	1.6850	$-0.22690 \pm$ j 1.33431*	0.16764
2	2.4551	$-0.15342 \pm$ j 1.59436*	0.09579
3	6.8799	$-0.62833 \pm$ j 2.90255	0.21157
4	8.1448	$-0.16614 \pm$ j 2.92190	0.05677
5	13.008	$-0.25024 \pm$ j 3.71749	0.06716
6	18.175	$-1.38884 \pm$ j 3.96390	0.33066
7	22.033	$-1.09006 \pm$ j 4.23768	0.24912
8	32.395	$-1.76219 \pm$ j 5.42404	0.30899
9	35.531	$-0.21716 \pm$ j 5.96693	0.03637
10	44.649	$-1.92262 \pm$ j 6.05257	0.30275
11	44.946	$-1.57552 \pm$ j 6.45964	0.23696
12	49.007	$-1.81167 \pm$ j 6.66486	0.26231

* : critical constraints

TABLE 17

Natural Frequencies, Closed-Loop Eigenvalues and Modal Damping Ratios for Final Design of Case 3 in Example 2: ACOSS FOUR

Mode Number	Natural Frequency (ω^2)	Closed-loop Eigenvalue ($\sigma \pm j\omega_d$)	Damping Ratio (ξ)
1	1.7695	−0.14827 ± j 1.33906*	0.11006*
2	2.2701	−0.16543 ± j 1.49824*	0.10975*
3	6.8825	−0.29043 ± j 2.65129	0.10889*
4	8.3137	−0.32120 ± j 2.91758	0.10943*
5	10.390	−0.25878 ± j 3.22166	0.08007
6	18.333	−0.73126 ± j 4.20431	0.17136
7	23.871	−0.76931 ± j 4.79604	0.15838
8	27.481	−0.52110 ± j 5.18450	0.10001
9	32.038	−0.73261 ± j 5.56344	0.13056
10	34.259	−0.88063 ± j 5.78363	0.15053
11	40.272	−0.88313 ± j 6.29546	0.13892
12	47.972	−0.23151 ± j 6.78034	0.03412

* : critical constraints

TABLE 18

Natural Frequencies, Closed-Loop Eigenvalues and Modal Damping Ratios for Final Design of Case 4 in Example 2: ACOSS FOUR

Mode Number	Natural Frequency (ω^2)	Closed-loop Eigenvalue ($\sigma \pm j\omega_d$)	Damping Ratio (ξ)
1	1.7527	−0.14811 ± j 1.33743*	0.11007*
2	2.1804	−0.16354 ± j 1.49360*	0.10884*
3	6.7730	−0.29237 ± j 2.65644	0.10940*
4	7.5292	−0.30754 ± j 2.81009	0.10879*
5	8.8137	−0.41410 ± j 3.02121	0.13579
6	16.516	−0.74291 ± j 4.02792	0.18138
7	23.311	−0.77221 ± j 4.77106	0.15977
8	24.868	−0.69572 ± j 4.96686	0.13872
9	27.885	−0.65279 ± j 5.20579	0.12442
10	30.156	−0.78313 ± j 5.34630	0.14493
11	36.127	−0.76335 ± j 5.85341	0.12932
12	47.773	−0.24766 ± j 6.76245	0.03660

* : critical constraints

TABLE 19

Iteration History for Example 2: ACOSS FOUR, Cases 1-4

Total Mass(*)

Analysis	Case 1	Case 2	Case 3	Case 4
1	51.6970	51.6970	51.6970	51.6970
2	45.2192	47.0839	50.0280	25.6928
3	40.5850	43.4828	33.0527	24.2318
4	29.9721	32.6651	31.6158	23.3435
5	23.9877	25.7153	28.1675	22.9081
6	22.8540	22.4004	26.2944	22.9354
7	22.5623	22.3012	25.0935	22.9354
8	22.4889	22.2166	24.1897	22.9354
9	22.5179	22.1845	23.6746	
10	22.5179	22.1586	23.6389	
11	22.5179	22.1404	23.1769	
12		22.1236	23.1769	
13			23.1769	

* : total mass includes 8 units of nonstructural mass in addition to structural mass.

TABLE 20

Iteration History for Example 3: Antenna Structure, Cases 1-10
Control Design Variable Linking (I)

Total Mass(kg)

Analysis	Case 1 (144*)	Case 2 (72*)	Case 3 (36*)	Case 4 (18*)	Case 5 (8*)
1	502.14	502.14	502.14	502.14	502.14
2	462.20	462.39	466.52	462.25	455.96
3	345.34	343.47	349.71	351.13	359.45
4	254.17	259.92	261.19	263.19	283.10
5	213.91	218.31	235.33	230.47	231.57
6	184.11	191.87	210.26	213.59	212.83
7	174.34	176.98	199.19	200.50	204.21
8	168.93	170.94	192.61	195.82	200.82
9	169.35	167.01	193.88	194.60	198.91
10	165.61	166.99	190.74	192.95	198.71
11	164.42	165.43	188.11	191.28	198.45
12	164.08	165.03	185.03	189.94	198.01
13	164.17	164.84	185.75	189.03	197.42
14	163.99	164.64	184.26	187.51	196.93
15	163.76	164.39	182.27	186.92	196.46
16	163.20	164.19	180.79	186.66	196.32
17	163.10	164.10	179.90	186.50	196.31
18	163.11	164.05	179.79	186.34	
19			179.64		

Analysis	Case 6 (4*)	Case 7 (4*)	Case 8 (2*)	Case 9 (1*)	Case 10 (1*)
1	502.14	502.14	502.14	502.14	502.14
2	469.64	465.14	485.24	474.45	484.61
3	367.65	361.18	383.18	374.55	387.64
4	293.90	280.72	302.66	291.97	297.69
5	237.33	231.87	241.31	234.26	240.14
6	218.09	212.22	216.56	214.15	215.05
7	205.11	204.82	208.12	207.01	208.60
8	201.28	201.05	206.07	207.00	206.33
9	200.51	200.69	205.78	204.60	206.07
10	200.35	200.63	204.22	204.47	206.06
11	200.27	200.59	204.19	204.46	206.06
12			204.16		

* : number of independent control design variables

TABLE 21

Final Cross Sectional Dimensions for Example 3: Antenna Structure, Cases 1-10
Control Design Variable Linking (I)

Case		Final Cross Sectional Dimensions(cm) Element 1	Element 2	Element 3,4	Element 5,6	Element 7,8
1	B	25.00[b]	25.00[b]	23.24	25.00[b]	19.31
	H	25.00[b]	25.00[b]	25.00[b]	25.00[b]	25.00[b]
	T	0.1000[a]	0.1108	0.1000[a]	0.1935	0.1000[a]
2	B	25.00[b]	25.00[b]	24.11	25.00[b]	18.68
	H	25.00[b]	25.00[b]	25.00[b]	25.00[b]	24.99
	T	0.1046	0.1129	0.1000[a]	0.1908	0.1000[a]
3	B	25.00[b]	25.00[b]	17.68	25.00[b]	18.87
	H	25.00[b]	25.00[b]	24.41	25.00[b]	25.00[b]
	T	0.1393	0.1263	0.1000[a]	0.2202	0.1000[a]
4	B	25.00[b]	25.00[b]	16.67	25.00[b]	18.56
	H	25.00[b]	25.00[b]	21.92	25.00[b]	25.00[b]
	T	0.1454	0.1213	0.1000[a]	0.2490	0.1000[a]
5	B	25.00[b]	25.00[b]	21.55	25.00[b]	13.82
	H	25.00[b]	25.00[b]	25.00[b]	25.00[b]	25.00[b]
	T	0.1748	0.1152	0.1000[a]	0.2526	0.1000[a]
6	B	25.00[b]	25.00[b]	22.04	25.00[b]	10.84
	H	25.00[b]	25.00[b]	25.00[b]	25.00[b]	24.83
	T	0.2166	0.1496	0.1000[a]	0.2134	0.1000[a]
7	B	25.00[b]	25.00[b]	20.95	25.00[b]	12.08
	H	25.00[b]	25.00[b]	25.00[b]	25.00[b]	24.86
	T	0.2054	0.1360	0.1000[a]	0.2323	0.1000[a]
8	B	25.00[b]	25.00[b]	19.04	25.00[b]	14.43
	H	25.00[b]	25.00[b]	25.00[b]	25.00[b]	25.00[b]
	T	0.1790	0.1115	0.1000[a]	0.2832	0.1000[a]
9	B	25.00[b]	25.00[b]	18.47	25.00[b]	14.50
	H	25.00[b]	25.00[b]	25.00[b]	25.00[b]	25.00[b]
	T	0.1752	0.1129	0.1000[a]	0.2883	0.1000[a]
10	B	25.00[b]	25.00[b]	19.13	25.00[b]	15.80
	H	25.00[b]	25.00[b]	25.00[b]	25.00[b]	25.00[b]
	T	0.1904	0.1000[a]	0.1000[a]	0.2815	0.1000[a]

[a] indicates lower bound value

[b] indicates upper bound value

TABLE 22

Summary of Example 3: Antenna Structure, Cases 1-10
Control Design Variable Linking (I)

Case Number(*)	Final Mass, kg (**)	Critical Constraints			
		$Re(\lambda)$	$Imag(\lambda)$	peak displacement	peak control force
1(144)	163.11(18)	σ_6 σ_{10}	ω_{d_4}	q_{10} q_{16}	u_1 u_2 u_3 u_4
2 (72)	164.05(18)	-	ω_{d_4}	q_{10} q_{16}	u_1 u_3 u_4
3 (36)	179.64(19)	σ_4	ω_{d_4}	q_{10} q_{16}	u_1 u_2 u_3 u_4
4 (18)	186.34(18)	σ_4 σ_{10}	ω_{d_4} ω_{d_5}	q_{10} q_{16}	u_1 u_2 u_3 u_4
5 (8)	196.31(17)	σ_8 σ_9	ω_{d_4}	q_{10} q_{16}	u_1 u_3 u_4
6 (4)	200.27(11)	-	ω_{d_4}	q_{10} q_{16}	u_1 u_3 u_4
7 (4)	200.59(11)	-	ω_{d_4}	q_{16}	u_1 u_3 u_4
8 (2)	204.16(12)	-	ω_{d_4}	q_{16}	u_3 u_4
9 (1)	204.46(11)	-	ω_{d_4}	q_{16}	u_3 u_4
10 (1)	206.05(10)	-	ω_{d_4}	q_{10} q_{16}	u_3 u_4

* : number of independent control design variables
** : number of total analyses

TABLE 23

Iteration History for Example 4: Antenna Structure, Linking on $[H]$
Control Design Variable Linking (II)

Total Mass(kg)

Analysis	Case 1 (1*)	Case 2 (2*)	Case 3 (3*)	Case 4 (4*)	Case 5 (5*)
1	502.14	502.14	502.14	502.14	502.14
2	484.61	470.88	471.87	444.12	454.83
3	387.64	328.11	328.47	303.50	346.62
4	297.69	260.67	254.76	233.56	268.66
5	240.14	217.39	214.99	193.83	215.70
6	215.05	199.59	200.57	178.76	185.24
7	208.60	193.04	192.60	174.18	175.46
8	206.33	191.20	190.47	173.05	176.56
9	206.07	190.90	190.23	172.50	173.25
10	206.06	190.80	190.14	172.46	172.66
11	206.06	190.70	189.94	172.46	172.46
12			189.85		172.37
13			189.81		172.32

Analysis	Case 6 (6*)	Case 7 (7*)	Case 8 (8*)	Case 9 (9*)	Case 10 (10*)
1	502.14	502.14	502.14	502.14	502.14
2	453.14	449.81	450.11	453.15	469.10
3	299.54	293.56	294.62	307.14	350.45
4	228.72	217.54	218.41	228.31	268.09
5	187.80	184.73	180.21	188.59	215.51
6	175.65	176.29	174.64	175.95	181.84
7	173.27	173.07	174.70	173.41	173.50
8	172.41	172.28	174.38	172.68	171.19
9	172.29	171.93	173.93	171.10	171.02
10	172.17	171.80	171.27	170.84	170.96
11		171.73	170.97	170.70	170.92
12			170.84	170.65	
13			170.81		

* : number of independent control design variables

TABLE 24

Final Cross Sectional Dimensions for Example 4:
Antenna Structure, Linking on [H], Control Design Variable Linking (II)

Final Cross Sectional Dimensions(cm)

Case		Element 1	Element 2	Element 3,4	Element 5,6	Element 7,8
	B	25.00[b]	25.00[b]	19.62	25.00[b]	15.51
1	H	25.00[b]	25.00[b]	25.00[b]	25.00[b]	25.00[b]
	T	0.1899	0.1000[a]	0.1000[a]	0.2816	0.1000[a]
	B	25.00[b]	25.00[b]	19.78	25.00[b]	24.94
2	H	25.00[b]	25.00[b]	25.00[b]	23.05	22.23
	T	0.1830	0.1326	0.1000[a]	0.2103	0.1000[a]
	B	25.00[b]	25.00[b]	20.03	25.00[b]	22.86
3	H	25.00[b]	25.00[b]	25.00[b]	23.37	21.94
	T	0.1869	0.1413	0.1000[a]	0.2012	0.1000[a]
	B	25.00[b]	25.00[b]	20.90	25.00[b]	20.51
4	H	25.00[b]	25.00[b]	25.00[b]	25.00[b]	25.00[b]
	T	0.1000[a]	0.1000[a]	0.1000[a]	0.2356	0.1000[a]
	B	25.00[b]	25.00[b]	18.85	25.00[b]	23.70
5	H	25.00[b]	25.00[b]	25.00[b]	25.00[b]	25.00[b]
	T	0.1025	0.1036	0.1000[a]	0.2287	0.1000[a]
	B	25.00[b]	25.00[b]	18.72	25.00[b]	21.03
6	H	25.00[b]	25.00[b]	25.00[b]	25.00[b]	25.00[b]
	T	0.1000[a]	0.1107	0.1000[a]	0.2330	0.1000[a]
	B	25.00[b]	25.00[b]	17.65	25.00[b]	20.47
7	H	25.00[b]	25.00[b]	24.89	25.00[b]	25.00[b]
	T	0.1000[a]	0.1165	0.1000[a]	0.2318	0.1000[a]
	B	25.00[b]	25.00[b]	14.95	25.00[b]	23.42
8	H	25.00[b]	25.00[b]	23.00	25.00[b]	25.00[b]
	T	0.1073	0.1244	0.1000[a]	0.2203	0.1000[a]
	B	25.00[b]	25.00[b]	14.62	25.00[b]	22.12
9	H	25.00[b]	25.00[b]	22.36	25.00[b]	25.00[b]
	T	0.1013	0.1319	0.1000[a]	0.2267	0.1000[a]
	B	25.00[b]	25.00[b]	19.96	25.00[b]	20.29
10	H	25.00[b]	25.00[b]	25.00[b]	25.00[b]	25.00[b]
	T	0.1000[a]	0.1058	0.1000[a]	0.2296	0.1000[a]

[a] indicates lower bound value

[b] indicates upper bound value

TABLE 25

Iteration History for Example 4: Antenna Structure, Linking on $[H_p]$ and $[H_v]$, Control Design Variable Linking (II)

Total Mass(kg)

Analysis	Case 11 (2*)	Case 12 (4*)	Case 13 (6*)	Case 14 (8*)	Case 15 (10*)
1	502.14	502.14	502.14	502.14	502.14
2	485.24	482.76	462.89	420.35	470.72
3	383.18	343.98	339.86	288.81	326.51
4	302.66	276.53	260.17	229.95	247.00
5	241.31	225.43	222.33	196.72	207.82
6	216.56	200.56	202.26	180.59	185.02
7	208.12	189.44	191.17	174.55	173.76
8	206.07	187.41	186.95	172.76	171.10
9	205.78	186.31	185.45	171.64	171.25
10	204.22	185.54	183.60	170.30	170.49
11	204.19	185.21	181.66	170.41	169.99
12	204.16	185.13	181.23	170.37	169.80
13		185.09	180.70		169.64
14			178.65		169.55
15			178.06		
16			177.86		
17			177.31		
18			176.72		
19			176.67		
20			176.56		

* : number of independent control design variables

TABLE 25

Iteration History for Example 4: Antenna Structure,
Linking on $[H_p]$ and $[H_v]$, Control Design Variable Linking (II), Continued

Total Mass(kg)

Analysis	Case 16 (12*)	Case 17 (14*)	Case 18 (16*)	Case 19 (18*)	Case 20 (20*)
1	502.14	502.14	502.14	502.14	502.14
2	475.80	474.66	474.47	466.40	434.64
3	301.89	304.10	304.66	304.00	287.18
4	228.23	230.32	231.61	226.62	224.61
5	188.16	197.86	197.41	185.11	183.32
6	175.46	178.77	178.20	174.03	172.69
7	174.21	172.28	172.25	172.93	171.31
8	173.71	171.81	171.09	172.39	169.42
9	172.95	169.76	170.49	172.02	166.81
10	171.19	171.33	170.21	171.80	166.79
11	170.91	170.02	169.72	170.04	166.22
12	170.69	169.07	169.16	169.67	165.66
13	169.68	167.59	167.78	169.37	165.61
14	169.49	166.91	167.26	169.17	166.50
15	168.38	166.23	167.00	168.92	165.30
16	167.40	166.17	166.65	167.74	165.14
17	167.01	166.01	166.29	166.91	164.95
18	166.85		165.69	165.84	164.86
19	166.76		165.46	165.64	164.80
20			165.34	165.49	
21			165.29	165.38	

* : number of independent control design variables

TABLE 26

Final Cross Sectional Dimensions for Example 4:
Linking on $[H_p]$ and $[H_v]$, Control Design Variable Linking (II)

Case		Final Cross Sectional Dimensions(cm) Element 1	Element 2	Element 3,4	Element 5,6	Element 7,8
11	B	25.00[b]	25.00[b]	18.99	25.00[b]	14.13
	H	25.00[b]	25.00[b]	25.00[b]	25.00[b]	25.00[b]
	T	0.1777	0.1149	0.1000[a]	0.2835	0.1000[a]
12	B	25.00[b]	25.00[b]	19.57	25.00[b]	25.00[b]
	H	25.00[b]	25.00[b]	25.00[b]	22.84	22.14
	T	0.1687	0.1361	0.1000[a]	0.2032	0.1000[a]
13	B	25.00[b]	25.00[b]	13.22	25.00[b]	25.00[b]
	H	25.00[b]	25.00[b]	25.00[b]	23.70	24.65
	T	0.1239	0.1259	0.1000[a]	0.2271	0.1000[a]
14	B	25.00[b]	25.00[b]	22.11	25.00[b]	20.00
	H	25.00[b]	25.00[b]	25.00[b]	25.00[b]	25.00[b]
	T	0.1000[a]	0.1021	0.1000[a]	0.2256	0.1000[a]
15	B	25.00[b]	25.00[b]	19.45	25.00[b]	21.32
	H	25.00[b]	25.00[b]	24.70	25.00[b]	25.00[b]
	T	0.1000[a]	0.1051	0.1000[a]	0.2246	0.1000[a]
16	B	25.00[b]	25.00[b]	13.02	25.00[b]	24.32
	H	25.00[b]	25.00[b]	24.12	24.93	25.00[b]
	T	0.1000[a]	0.1341	0.1000[a]	0.2082	0.1000[a]
17	B	25.00[b]	25.00[b]	13.64	25.00[b]	24.70
	H	25.00[b]	25.00[b]	24.06	25.00[b]	25.00[b]
	T	0.1000[a]	0.1289	0.1000[a]	0.2061	0.1000[a]
18	B	25.00[b]	25.00[b]	15.33	25.00[b]	25.00[b]
	H	25.00[b]	25.00[b]	23.14	25.00[b]	25.00[b]
	T	0.1000[a]	0.1213	0.1000[a]	0.2047	0.1000[a]
19	B	25.00[b]	25.00[b]	14.99	25.00[b]	24.29
	H	25.00[b]	25.00[b]	23.31	25.00[b]	25.00[b]
	T	0.1000[a]	0.1186	0.1000[a]	0.2084	0.1000[a]
20	B	25.00[b]	25.00[b]	14.91	25.00[b]	24.62
	H	25.00[b]	25.00[b]	22.93	25.00[b]	25.00[b]
	T	0.1000[a]	0.1205	0.1000[a]	0.2054	0.1000[a]

[a] indicates lower bound value

[b] indicates upper bound value

TABLE 27

Summary of Example 4: Antenna Structure, Cases 1-20
Control Design Variable Linking (II)

Case Number(*)	Final Mass, kg (**)	Critical Constraints			
		$Re(\lambda)$	$Imag(\lambda)$	peak displacement	peak control force
1 (1)	206.06(11)	-	ω_{d_4}	q_{16}	u_4
2 (2)	190.70(11)	σ_8 σ_9	ω_{d_4} ω_{d_5}	q_{16}	u_4
3 (3)	189.81(13)	$\sigma_4 \sigma_8 \sigma_9$	ω_{d_4} ω_{d_5}	q_{16}	u_4
4 (4)	172.46(11)	σ_3 σ_4 σ_8	ω_{d_4}	q_{16}	u_4
5 (5)	172.32(13)	$\sigma_3 \sigma_4 \sigma_8$	ω_{d_4}	q_{16}	u_4
6 (5)	172.17(10)	σ_8	ω_{d_4}	q_{16}	u_4
7 (7)	171.73(11)	σ_8	ω_{d_4}	q_{16}	u_3 u_4
8 (8)	170.81(13)	σ_8	ω_{d_4} ω_{d_5}	q_{16}	u_3 u_4
9 (9)	170.77(12)	σ_7 σ_8	ω_{d_4} ω_{d_5}	q_{16}	u_3 u_4
10(10)	170.92(11)	-	ω_{d_4}	q_{16}	u_3 u_4
11 (2)	204.16(12)	-	ω_{d_4}	q_{16}	u_3 u_4
12 (4)	185.09(13)	σ_8 σ_9	ω_{d_4} ω_{d_5}	q_{16}	u_4
13 (6)	176.56(20)	σ_4 σ_8 σ_9	ω_{d_4} ω_{d_5}	q_{16}	u_4
14 (8)	170.37(12)	σ_8	ω_{d_4}	q_{16}	u_4
15(10)	169.55(14)	σ_4 σ_8	ω_{d_4}	q_{16}	u_4
16(12)	166.76(19)	σ_3 σ_4 σ_8	ω_{d_4} ω_{d_5}	q_{16}	u_3 u_4
17(14)	166.01(17)	σ_3 σ_4	ω_{d_4} ω_{d_5}	q_{16}	u_3 u_4
18(16)	165.29(21)	σ_4	ω_{d_4} ω_{d_5}	q_{16}	u_1 u_3 u_4
19(18)	165.38(21)	σ_4 σ_7 σ_8	ω_{d_4} ω_{d_5}	q_{16}	u_3 u_4
20(20)	164.80(19)	σ_4 σ_7	ω_{d_4} ω_{d_5}	q_{16}	u_1 u_3 u_4

* : number of independent control design variables
** : number of total analyses

TABLE 28

Iteration History for Example 5: Antenna Structure, Additional Constraints

Total Mass(kg)

Analysis	Case 1 Control Effort Constraint	Case 2 Acceleration Constraints	Case 3 Control Effort & Acceleration Constraints
1	502.14	502.14	502.14
2	475.98	446.92	476.33
3	369.44	345.03	375.87
4	281.91	305.57	309.06
5	242.58	286.80	286.28
6	222.34	277.24	276.98
7	216.91	276.31	273.76
8	215.93	276.01	273.24
9	214.42	275.55	272.95
10	213.99	275.23	272.72
11	213.71	274.91	271.76
12		274.60	270.65
13		274.45	270.50
14		274.06	270.44
15		268.62	270.38
16		268.38	
17		268.03	
18		267.94	
19		267.88	

TABLE 29

Final Cross Sectional Dimensions for Example 5:
Antenna Structure, Additional Constraints

Case		Final Cross Sectional Dimensions(cm) Element 1	Element 2	Element 3,4	Element 5,6	Element 7,8
1	B	25.00[b]	25.00[b]	16.94	25.00[b]	18.55
	H	25.00[b]	25.00[b]	25.00[b]	25.00[b]	25.00[b]
	T	0.2476	0.1027	0.1000[a]	0.2452	0.1000[a]
2	B	25.00[b]	25.00[b]	25.00[b]	25.00[b]	25.00[b]
	H	22.50	22.56	25.00[b]	23.92	22.40
	T	0.2935	0.2656	0.2432	0.1255	0.1552
3	B	25.00[b]	25.00[b]	25.00[b]	25.00[b]	25.00[b]
	H	25.00[b]	22.15	25.00[b]	24.11	22.41
	T	0.2841	0.2793	0.2405	0.1278	0.1532

[a] indicates lower bound value

[b] indicates upper bound value

TABLE 30

Iteration History for Example 5: Antenna Structure
Re-solving 2 × 2 Riccati Equations and Truncation of Gain Matrix

Total Mass(kg)

Analysis	Case 4 Re-solving 2 × 2 Riccati Equations	Case 5 Truncation of Gain Matrix
1	502.14	502.14
2	469.10	469.10
3	366.71	350.41
4	281.45	268.57
5	220.83	214.43
6	190.46	181.03
7	177.59	172.36
8	174.16	170.64
9	174.02	171.37
10	175.31	171.25
11	175.05	170.89
12	174.96	170.85
13	174.79	170.72
14	174.77	170.71
15	174.74	170.69

TABLE 31

Final Cross Sectional Dimensions for Example 5:
Re-solving 2 × 2 Riccati Equations and Truncation of Gain Matrix

Case		Final Cross Sectional Dimensions(cm) Element 1	Element 2	Element 3,4	Element 5,6	Element 7,8
4	B	25.00[b]	25.00[b]	16.58	25.00[b]	23.67
	H	25.00[b]	25.00[b]	24.63	25.00[b]	25.00[b]
	T	0.1025	0.1000[a]	0.1000[a]	0.2446	0.1000[a]
5	B	25.00[b]	25.00[b]	18.71	25.00[b]	23.11
	H	25.00[b]	25.00[b]	24.33	25.00[b]	25.00[b]
	T	0.1000[a]	0.1000[a]	0.1000[a]	0.2296	0.1000[a]

[a] indicates lower bound value

[b] indicates upper bound value

TABLE 32

Final Closed-Loop Eigenvalues for Example 5:
Re-solving 2 × 2 Riccati Equations and Truncation of Gain Matrix

$\lambda_i = \sigma_i + j\omega_{di}\ (\xi_i,\ \%)$

Mode Number	Case 10 of Example 4	Case 4 Re-solving 2 × 2 Riccati Equations	Case 5 Truncation of Gain Matrix
1	−2.73 ± j 1.61	−2.52 ± j 2.24	−2.77 ± j 1.56
2	−1.86 ± j 4.97	−1.54 ± j 5.01	−1.20 ± j 5.04
3	−.683 ± j 23.7	−.504 ± j 23.7	−.739 ± j 23.6
4	−.519 ± j 50.1	−.499 ± j 50.1	−.528 ± j 50.1
5	−.866 ± j 64.7	−.505 ± j 63.1	−.906 ± j 63.2
6	−1.08 ± j 103.	−.846 ± j 102.	−1.34 ± j 102.
7	−.933 ± j 184.	−.647 ± j 184.	−.507 ± j 184.
8	−.623 ± j 241.	−.501 ± j 238.	−.514 ± j 238.
9	−2.50 ± j 320.	−.938 ± j 319.	−2.98 ± j 320.
10	−2.25 ± j 324.	−1.40 ± j 325.	−1.72 ± j 324.
11	.977 ± j 428.	$-.353 \times 10^{-2}$ ± j 428.	$.110 \times 10^{-3}$ ± j 427.
12	.076 ± j 619.	$.127 \times 10^{-2}$ ± j 617.	$-.462 \times 10^{-6}$ ± j 618.
13	.183 ± j 637.	$-.227 \times 10^{-2}$ ± j 627.	$-.387 \times 10^{-4}$ ± j 626.
14	.203 ± j 681.	$-.425 \times 10^{-2}$ ± j 684.	$.395 \times 10^{-4}$ ± j 681.
15	.121 ± j 1015.	$-.313 \times 10^{-3}$ ± j 995.	$.438 \times 10^{-7}$ ± j 1000.
16	−.121 ± j 1128.	$.131 \times 10^{-2}$ ± j 1124.	$-.670 \times 10^{-6}$ ± j 1121.
17	.504 ± j 1268.	$.245 \times 10^{-3}$ ± j 1294.	$.287 \times 10^{-6}$ ± j 1286.
18	.339 ± j 1375.	$-.378 \times 10^{-2}$ ± j 1380.	$.971 \times 10^{-7}$ ± j 1378.

TABLE 33

Iteration History for Example 5: Antenna Structure
Variable Mass Design Elements

Total Mass(kg)

Analysis	Case 6 $c_1 = 4\,kg\,/\,8.5$ N	Case 7 $c_1 = 8\,kg\,/\,8.5$ N	Case 8 $c_1 = 2\,kg\,/\,8.5$ N
1	502.14	502.14	502.14
2	476.98	476.82	465.89
3	354.56	364.94	336.41
4	270.96	293.55	259.58
5	213.92	233.84	210.89
6	184.34	193.69	178.03
7	173.01	182.61	168.24
8	171.14	183.93	167.14
9	170.62	181.46	166.37
10	170.34	180.47	165.27
11	170.23	180.39	165.13
12	170.17	180.37	165.03

TABLE 34

Final Cross Sectional Dimensions for Example 5: Antenna Structure Variable Mass Design Elements

Final Cross Sectional Dimensions(cm)

Case		Element 1	Element 2	Element 3,4	Element 5,6	Element 7,8
6	B	25.00[b]	25.00[b]	18.26	25.00[b]	22.80
	H	25.00[b]	25.00[b]	25.00[b]	25.00[b]	25.00[b]
	T	0.1000[a]	0.1000[a]	0.1000[a]	0.2330	0.1000[a]
7	B	25.00[b]	25.00[b]	25.00[b]	25.00[b]	25.00[b]
	H	25.00[b]	25.00[b]	25.00[b]	25.00[b]	25.00[b]
	T	0.1000[a]	0.1580	0.1000[a]	0.1728	0.1000[a]
8	B	25.00[b]	25.00[b]	13.98	25.00[b]	21.38
	H	25.00[b]	25.00[b]	22.28	25.00[b]	25.00[b]
	T	0.1191	0.1000[a]	0.1000[a]	0.2382	0.1000[a]

[a] indicates lower bound value

[b] indicates upper bound value

TABLE 35

Final Actuator Masses for Example 5: Antenna Structure Variable Mass Design Elements

Actuator Mass(kg)

Actuator Number	Case 6 $c_1 = 4\ kg\ /\ 8.5$ N	Case 7 $c_1 = 8\ kg\ /\ 8.5$ N	Case 8 $c_1 = 2\ kg\ /\ 8.5$ N
1	2.700	4.641	1.489
2 and 4	4.006	7.958	2.001
3	3.920	7.773	1.974

TABLE 36

Summary of Example 5: Antenna Structure, Cases 1-8
Additional Problems

Case Number	Final Mass, kg (**)	Critical Constraints				
		$Re(\lambda)$	$Imag(\lambda)$	peak displacement	peak control force	additional
Case 10 of Example 4	170.92(11)	-	ω_{d_4}	q_{16}	u_3 u_4	NA
1	213.71(11)	σ_3 σ_4 σ_5	ω_{d_4}	q_{10} q_{16}	-	CE
2	267.88(19)	σ_9	ω_{d_4} ω_{d_5}	q_{16}	u_2 u_3 u_4	a_7
3	270.38(15)	σ_3 σ_8	ω_{d_4} ω_{d_5}	q_{16}	-	CE a_7
4	174.74(15)	σ_3 σ_4 σ_5 σ_8	ω_{d_4}	q_{16}	u_4	NA
5	170.69(15)	σ_7 σ_8	ω_{d_4}	q_{16}	u_3 u_4	NA
6	170.17(12)	-	ω_{d_4}	q_{16}	u_3 u_4	m_A
7	180.37(12)	σ_3 σ_4 σ_7 σ_8	ω_{d_4} ω_{d_5}	q_{16}	u_3 u_4	m_A
8	165.03(12)	σ_8	ω_{d_4}	q_{16}	u_3 u_4	m_A

** : number of total analyses
NA : not applicable

TABLE 37

Initial Complex Eigenvalues, Grillage Structure

$\lambda_i = \sigma_i + j\omega_{di}$ (ξ_i, %)

Mode Number	Open-Loop	Closed-Loop
1	−.0001 ± j 2.29 (.006)	−.874 ± j 2.31 (35.4)
2	−.001 ± j 7.05 (.018)	−.431 ± j 7.06 (6.09)
3	−.007 ± j 16.4 (.041)	−1.87 ± j 17.3 (10.8)
4	−.009 ± j 18.6 (.047)	−.762 ± j 17.6 (4.33)
5	−.018 ± j 27.1 (.069)	−1.36 ± j 27.2 (5.00)
6	−.039 ± j 39.5 (.099)	−.878 ± j 39.9 (2.20)
7	−.040 ± j 39.9 (.100)	−2.00 ± j 40.1 (4.97)
8	−.062 ± j 49.7 (.124)	−3.76 ± j 49.2 (7.64)
9	−.091 ± j 60.2 (.150)	−1.90 ± j 60.1 (3.15)
10	−.119 ± j 68.9 (.172)	−2.01 ± j 69.0 (2.92)
11	−.135 ± j 73.6 (.184)	−2.58 ± j 74.0 (3.49)
12	−.146 ± j 76.5 (.191)	−.840 ± j 75.6 (1.11)
13	−.231 ± j 96.0 (.240)	−2.03 ± j 95.8 (2.11)
14	−.267 ± j 103. (.259)	−1.39 ± j 103. (1.35)
15	−.281 ± j 106. (.265)	−2.26 ± j 106. (2.13)
16	−.316 ± j 112. (.281)	−1.41 ± j 112. (1.26)
17	−.353 ± j 119. (.297)	−2.04 ± j 119. (1.72)
18	−.413 ± j 129. (.321)	−1.66 ± j 128. (1.29)
19	−.505 ± j 142. (.355)	−2.81 ± j 142. (1.98)
20	−.524 ± j 145. (.362)	−1.65 ± j 145. (1.14)

TABLE 38

Independent Control Design Variables, Grillage Structure

	Case 1	Case 2	Case 3	Case 4	Case 5	Case 6
CDV's	$\alpha_1 = \cdots = \alpha_{25}$	α_1, $\alpha_2 = \cdots = \alpha_{25}$	α_1, α_2, $\alpha_3 = \cdots = \alpha_{25}$	$\alpha_1, \ldots, \alpha_4$, $\alpha_5 = \cdots = \alpha_{25}$	$\alpha_1, \ldots, \alpha_9$, $\alpha_{10} = \cdots = \alpha_{25}$	$\alpha_1, \ldots, \alpha_{19}$, $\alpha_{20} = \cdots = \alpha_{25}$
Number of Indep. CDV's	1	2	3	5	10	20

TABLE 39

Final Structural Variables, Grillage Structure

Depths (*cm*)

Design Variable Number	Case 1	Case 2	Case 3	Case 4	Case 5	Case 6
1	0.2849	0.2768	0.2510	0.2392	0.2557	0.2466
2	0.1698	0.1806	0.1936	0.1985	0.1191	0.1125
3	0.1000°	0.1000°	0.1000°	0.1000°	0.1000°	0.1000°
4	0.1953	0.1973	0.1769	0.1788	0.1908	0.1560
5	0.1502	0.1479	0.1429	0.1373	0.1000°	0.1000°
6	0.3656	0.3626	0.3670	0.3691	0.3701	0.4128
7	0.2299	0.2180	0.2221	0.2222	0.1622	0.1137
8	0.4724	0.5021	0.4951	0.4719	0.5880	0.5573

° indicates lower bound value

TABLE 40

Iteration Histories, Grillage Structure

Total Mass ($lb \cdot sec^2/in$)

Analysis	Case 1 (1*)	Case 2 (2*)	Case 3 (3*)	Case 4 (5*)	Case 5 (10*)	Case 6 (20*)
1	0.1294	0.1294	0.1294	0.1294	0.1294	0.1294
2	0.1448	0.1433	0.1440	0.1442	0.1442	0.1468
3	0.1332	0.1327	0.1369	0.1353	0.1352	0.1366
4	0.1272	0.1295	0.1317	0.1258	0.1261	0.1298
5	0.1231	0.1256	0.1238	0.1222	0.1257	0.1223
6	0.1211	0.1247	0.1206	0.1212	0.1215	0.1168
7	0.1211	0.1200	0.1185	0.1197	0.1182	0.1163
8	0.1198	0.1189	0.1172	0.1178	0.1170	0.1139
9	0.1192	0.1189	0.1166	0.1170	0.1145	0.1114
10	0.1192	0.1188	0.1172	0.1174	0.1136	0.1103
11	0.1194		0.1173	0.1173	0.1126	0.1103
12	0.1191		0.1172	0.1171	0.1111	0.1089
13	0.1191		0.1177	0.1162	0.1107	0.1088
14			0.1173	0.1162	0.1111	0.1080
15			0.1168	0.1162	0.1099	0.1065
16			0.1170	0.1159	0.1098	0.1053
17			0.1169	0.1158	0.1098	0.1047
18			0.1169	0.1159	0.1093	0.1044
19				0.1160	0.1091	0.1039
20				0.1158	0.1091	0.1036
21				0.1157	0.1093	0.1042
22				0.1157	0.1083	0.1041
23					0.1080	0.1040
24					0.1082	0.1039
25					0.1083	
26					0.1082	
27					0.1083	

* : number of independent control design variables

TABLE 41

Final Closed-Loop Eigenvalues, Grillage Structure

$\lambda_i = \sigma_i + j\omega_{di}$ (ξ_i, %)

Mode Number	Case 1	Case 2	Case 3
1	−1.58 ± j 4.85 (30.9)	−1.62 ± j 5.03 (30.7)	−1.89 ± j 5.14 (34.4)
2	−.438 ± j 9.76 (4.49)	−.321 ± j 9.93 (3.23)	−.103 ± j 9.90 (1.04)
3	−2.26 ± j 20.4 (11.0)	−1.75 ± j 20.4 (8.53)	−2.36 ± j 20.0 (11.7)
4	−1.53 ± j 24.7 (6.17)	−1.08 ± j 25.4 (4.25)	−2.10 ± j 24.7 (8.50)
5	−2.53 ± j 30.5 (8.26)	−2.08 ± j 31.0 (6.70)	−2.58 ± j 29.9 (8.58)
6	−.415 ± j 38.9 (1.06)	−.404 ± j 39.6 (1.02*)	−.423 ± j 38.7 (1.09)
7	−2.24 ± j 40.1 (5.59)	−1.96 ± j 39.9 (4.91)	−2.62 ± j 39.2 (6.66)
8	−1.36 ± j 50.7 (2.68)	−1.87 ± j 51.5 (3.63)	−15.5 ± j 47.9 (30.7)
9	−15.4 ± j 51.7 (28.6)	−10.9 ± j 53.2 (20.1)	−2.44 ± j 51.2 (4.75)
10	−2.49 ± j 55.1 (4.51)	−1.98 ± j 54.9 (3.60)	−3.14 ± j 52.3 (5.99)
11	−1.14 ± j 62.4 (1.83)	−.674 ± j 63.6 (1.06)	−.995 ± j 62.3 (1.60)
12	−.634 ± j 63.3 (1.00*)	−.638 ± j 63.9 (1.00*)	−.625 ± j 62.3 (1.00*)
13	−3.38 ± j 74.1 (4.55)	−2.56 ± j 75.0 (3.40)	−2.54 ± j 74.0 (3.42)
14	−.944 ± j 93.1 (1.01*)	−.934 ± j 91.7 (1.02*)	−.975 ± j 88.5 (1.10)
15	−17.5 ± j 97.6 (17.7)	−11.8 ± j 100. (11.7)	−20.7 ± j 95.4 (21.2)
16	−2.26 ± j 104. (2.16)	−2.88 ± j 101. (2.85)	−3.96 ± j 99.3 (3.99)
17	−3.28 ± j 105. (3.12)	−4.61 ± j 105. (4.40)	−2.13 ± j 99.9 (2.13)
18	−2.67 ± j 106. (2.51)	−1.08 ± j 105. (1.03*)	−1.04 ± j 101. (1.03*)
19	−1.21 ± j 120. (1.01*)	−1.24 ± j 121. (1.03*)	−1.20 ± j 119. (1.01*)
20	−1.43 ± j 142. (1.01*)	−1.49 ± j 140. (1.06)	−1.36 ± j 135. (1.00*)

* indicate critical damping ratio constraints ($0.999 \leq \xi_i \leq 1.03$)

TABLE 41

Final Closed-Loop Eigenvalues, Grillage Structure, Continued

$\lambda_i = \sigma_i + j\omega_{di}\ (\xi_i,\ \%)$

Mode Number	Case 4	Case 5	Case 6
1	−2.08 ± j 5.19 (37.1)	−2.22 ± j 5.92 (35.1)	−1.85 ± j 6.56 (27.1)
2	−.100 ± j 9.76 (1.02*)	−.115 ± j 10.5 (1.09)	−.112 ± j 10.7 (1.05)
3	−10.4 ± j 19.9 (46.2)	−1.16 ± j 22.2 (5.21)	−.209 ± j 20.3 (1.03*)
4	−1.44 ± j 22.0 (6.55)	−4.02 ± j 22.6 (17.5)	−6.55 ± j 22.2 (28.3)
5	−2.71 ± j 30.0 (9.01)	−1.92 ± j 28.6 (6.70)	−.724 ± j 26.2 (2.77)
6	−.384 ± j 38.1 (1.01*)	−.397 ± j 37.0 (1.07)	−11.4 ± j 35.1 (30.9)
7	−2.01 ± j 38.8 (5.19)	−1.27 ± j 38.6 (3.30)	−.605 ± j 35.4 (1.71)
8	−13.7 ± j 48.3 (27.2)	−12.0 ± j 45.8 (25.4)	−.397 ± j 37.3 (1.07)
9	−2.24 ± j 50.5 (4.42)	−.534 ± j 48.3 (1.10)	−.666 ± j 44.3 (1.50)
10	−3.07 ± j 51.7 (5.92)	−.615 ± j 48.7 (1.26)	−.479 ± j 47.9 (1.00*)
11	−.627 ± j 61.8 (1.02*)	−.525 ± j 52.2 (1.00*)	−.496 ± j 48.4 (1.02*)
12	−.948 ± j 62.7 (1.51)	−.648 ± j 56.1 (1.15)	−.539 ± j 52.8 (1.02*)
13	−2.23 ± j 72.7 (3.06)	−3.55 ± j 65.0 (5.45)	−1.93 ± j 54.6 (3.54)
14	−.881 ± j 86.6 (1.02*)	−.749 ± j 72.7 (1.03*)	−3.35 ± j 66.1 (5.06)
15	−19.4 ± j 96.7 (19.7)	−2.08 ± j 77.5 (2.68)	−37.0 ± j 66.3 (48.8)
16	−2.12 ± j 97.2 (2.19)	−2.63 ± j 79.0 (3.32)	−.742 ± j 71.9 (1.03*)
17	−3.81 ± j 98.4 (3.87)	−12.6 ± j 85.6 (14.5)	−7.59 ± j 75.7 (9.97)
18	−.986 ± j 98.7 (1.00*)	−1.62 ± j 99.0 (1.63)	−1.04 ± j 90.5 (1.15)
19	−1.19 ± j 117. (1.01*)	−2.36 ± j 110. (2.15)	−1.35 ± j 95.1 (1.42)
20	−1.40 ± j 135. (1.04)	−1.33 ± j 133. (1.00*)	−1.34 ± j 131. (1.02*)

* indicate critical damping ratio constraints ($0.999 \leq \xi_i \leq 1.03$)

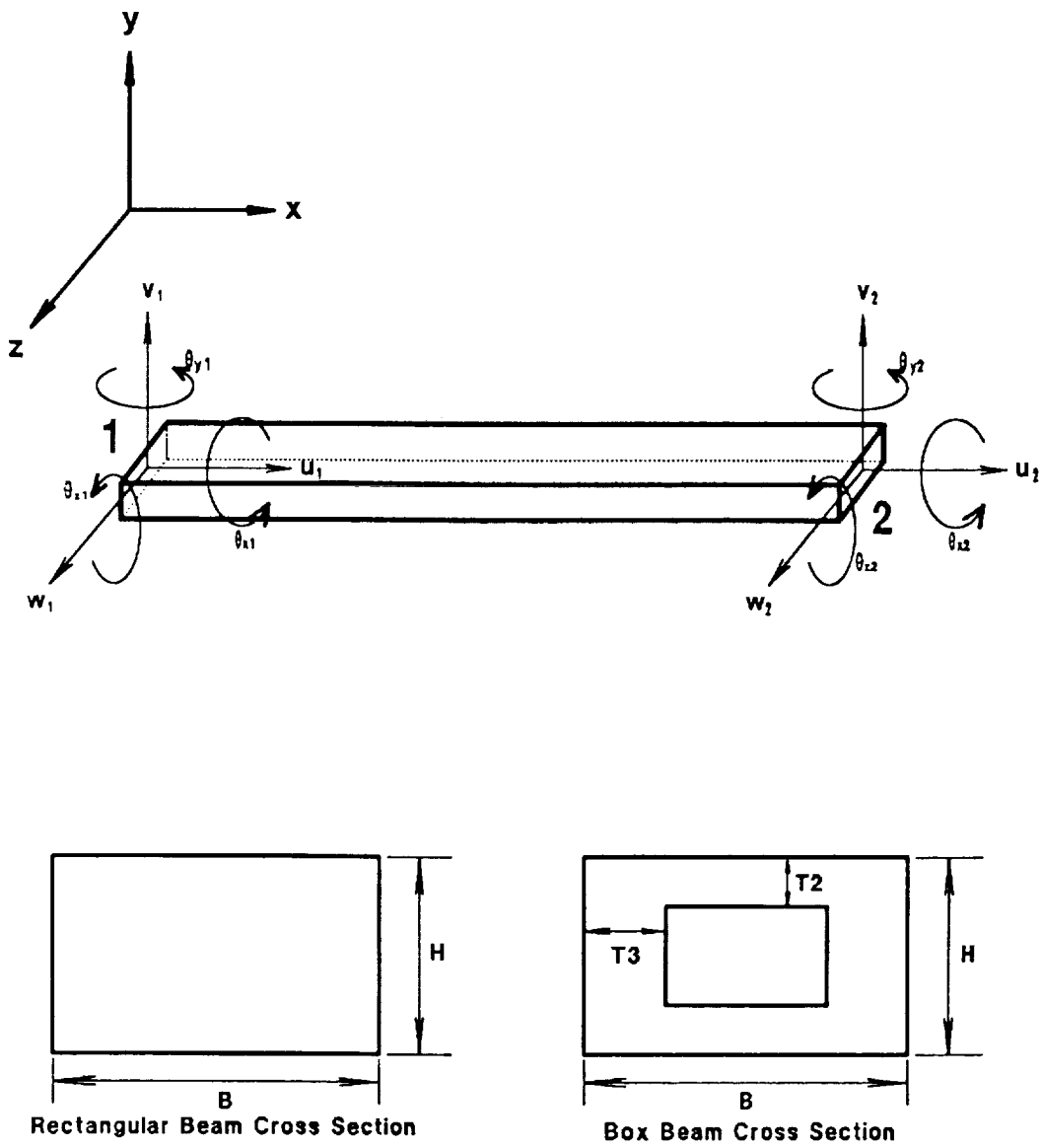

Figure 1: Three Dimensional Frame Element and Its Cross Sections

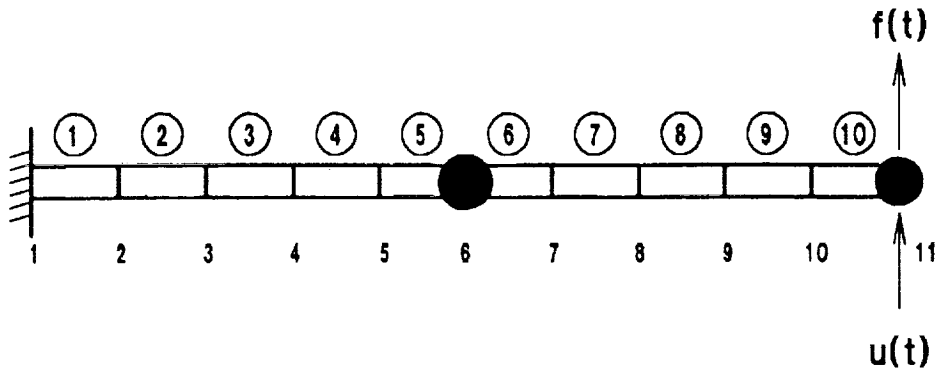

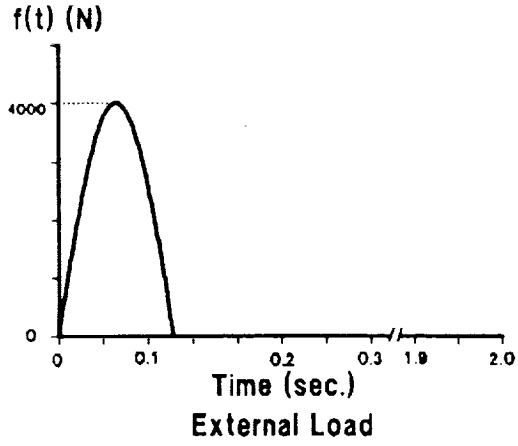

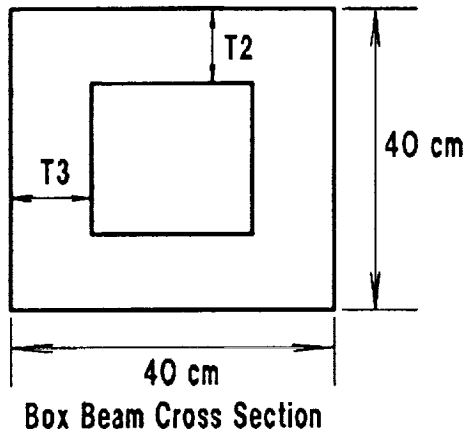

Figure 2: Example 1 - Cantilever Beam

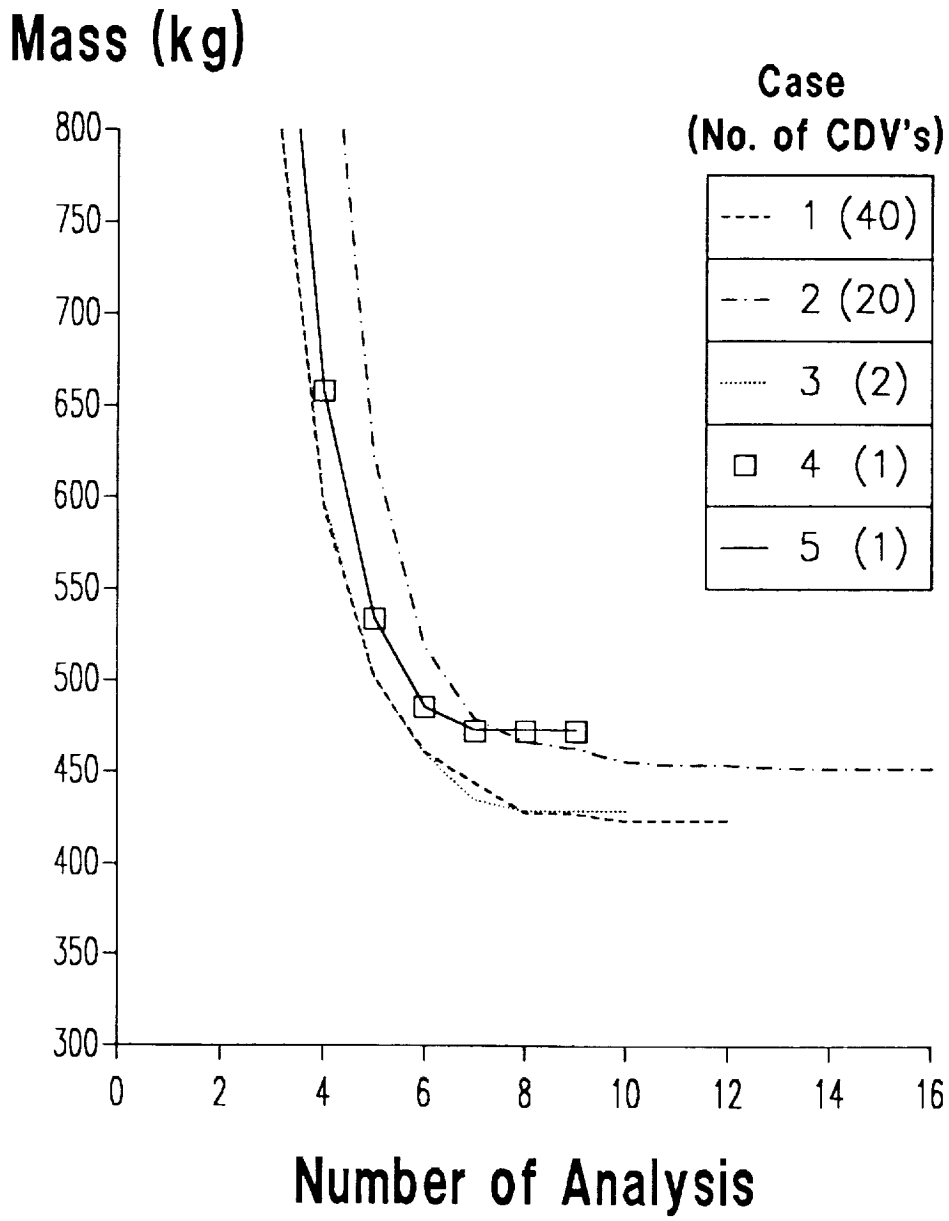

Figure 3: Iteration History for Example 1 - Cantilever Beam, Cases 1-5, Control Design Variable Linking (I)

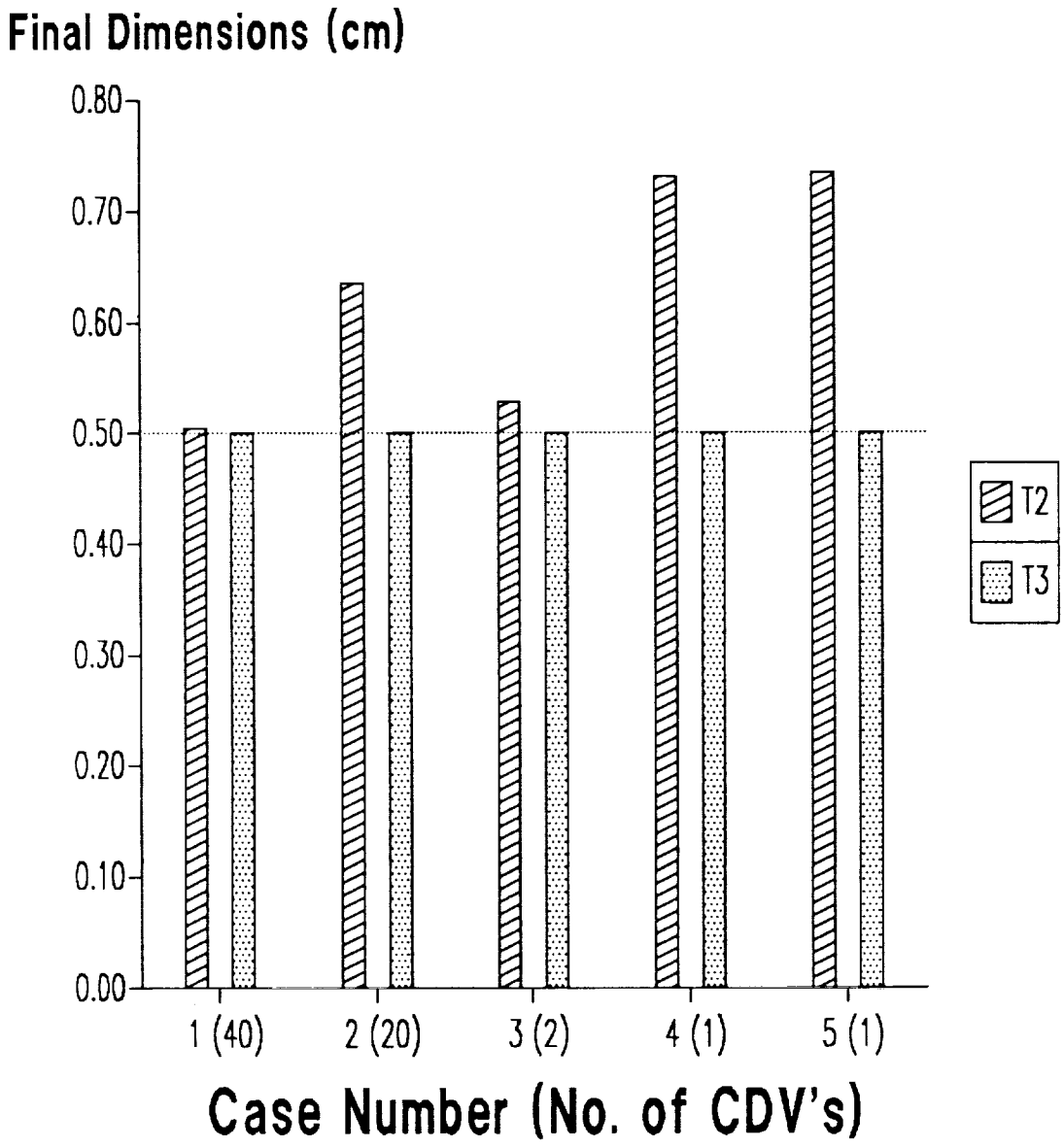

Figure 4: Final Cross Sectional Dimensions for Example 1 - Cantilever Beam, Cases 1-5, Control Design Variable Linking (I)

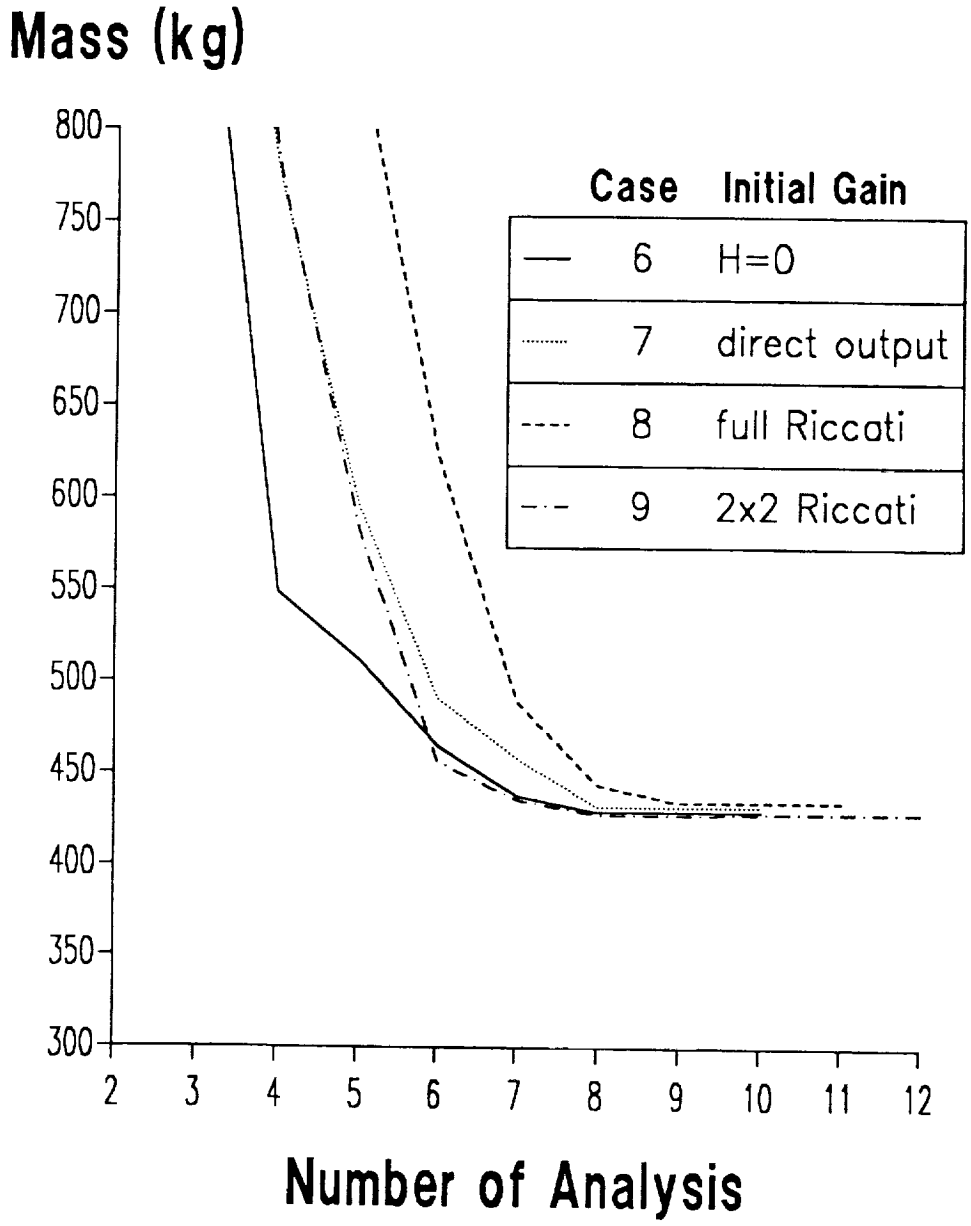

Figure 5: Iteration History for Example 1 - Cantilever Beam, Cases 6-9, Different Initial Feedback Gains

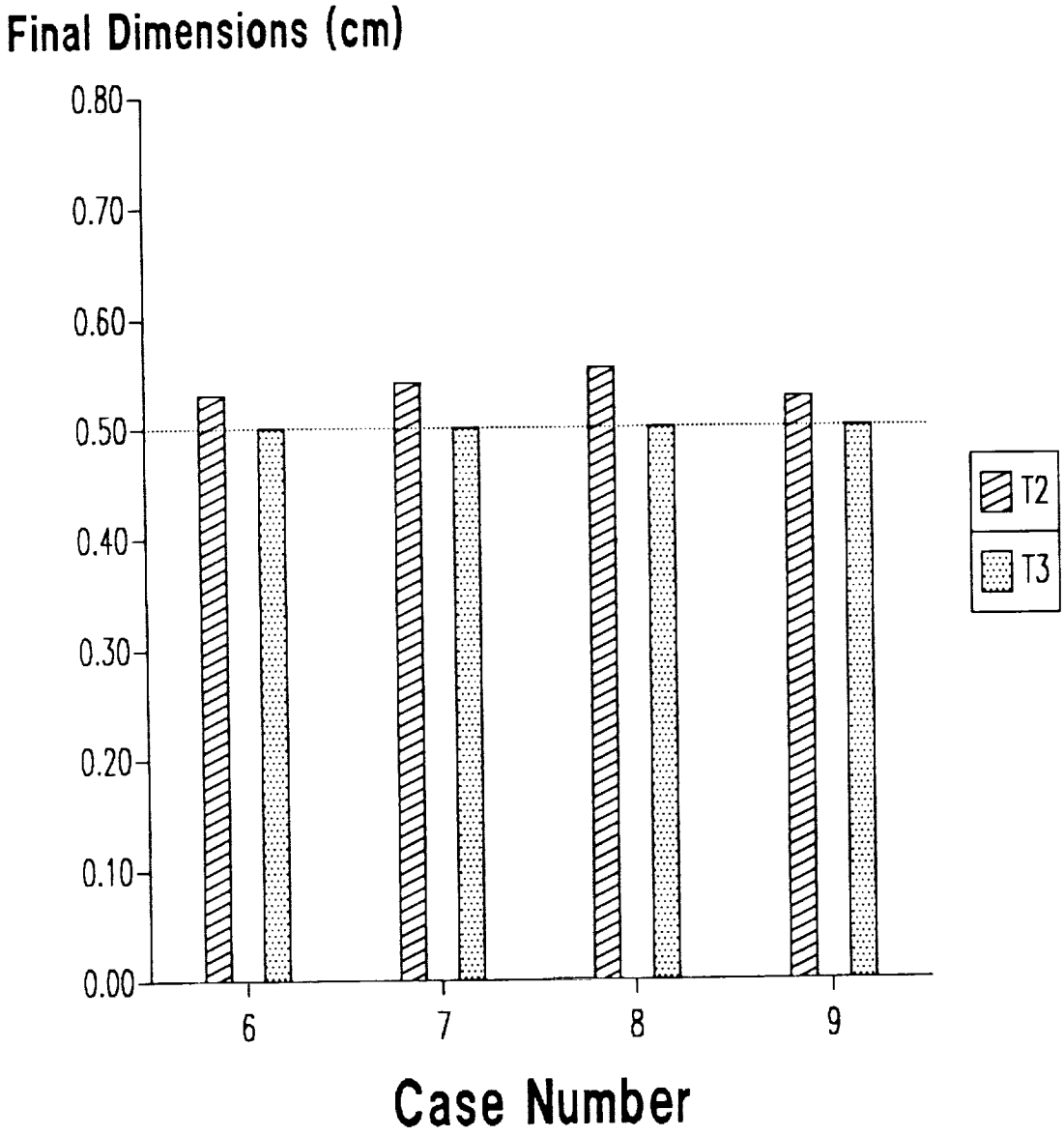

Figure 6: Final Cross Sectional Dimensions for Example 1 - Cantilever Beam, Cases 6-9, Different Initial Feedback Gains

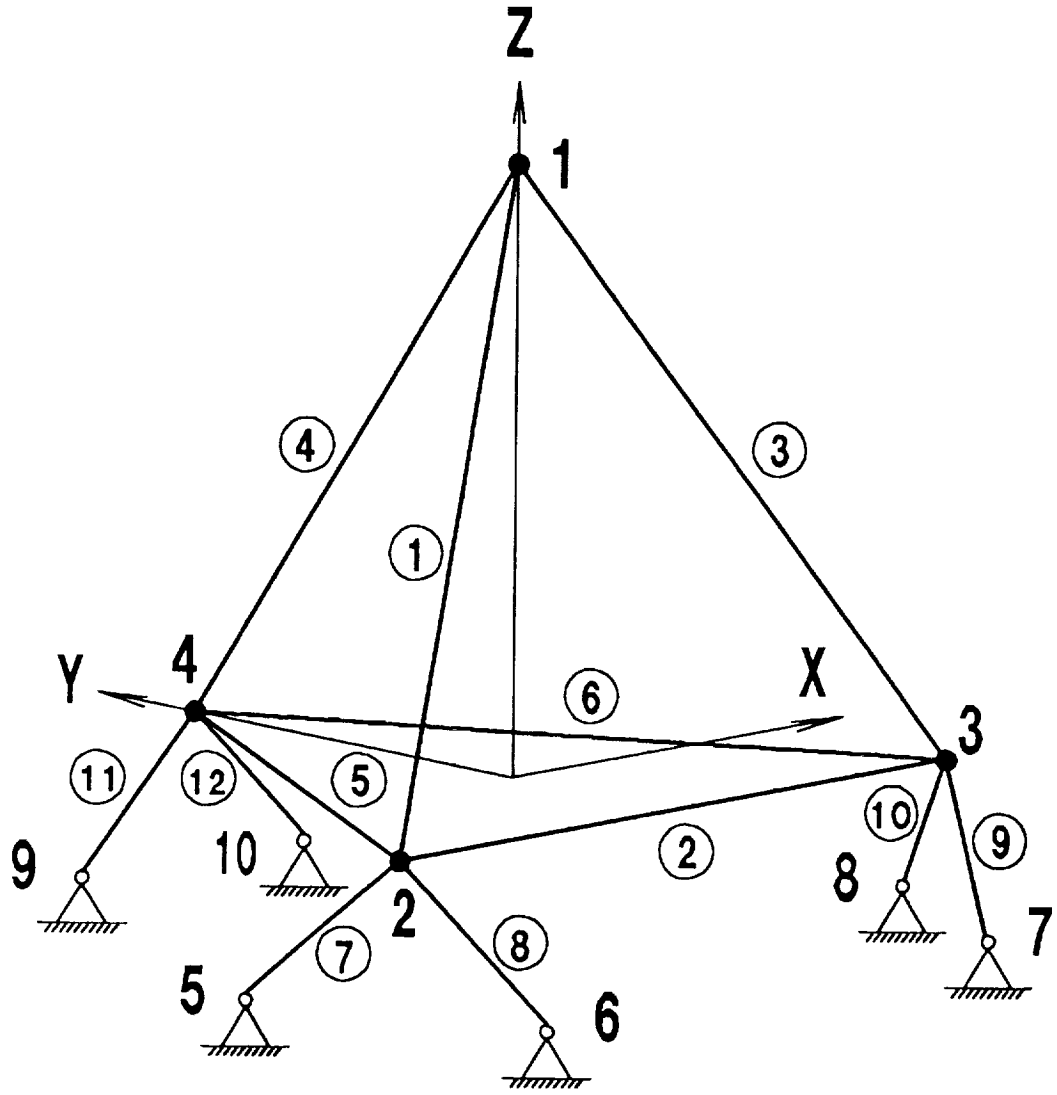

Figure 7: Example 2 - ACOSS FOUR Structure

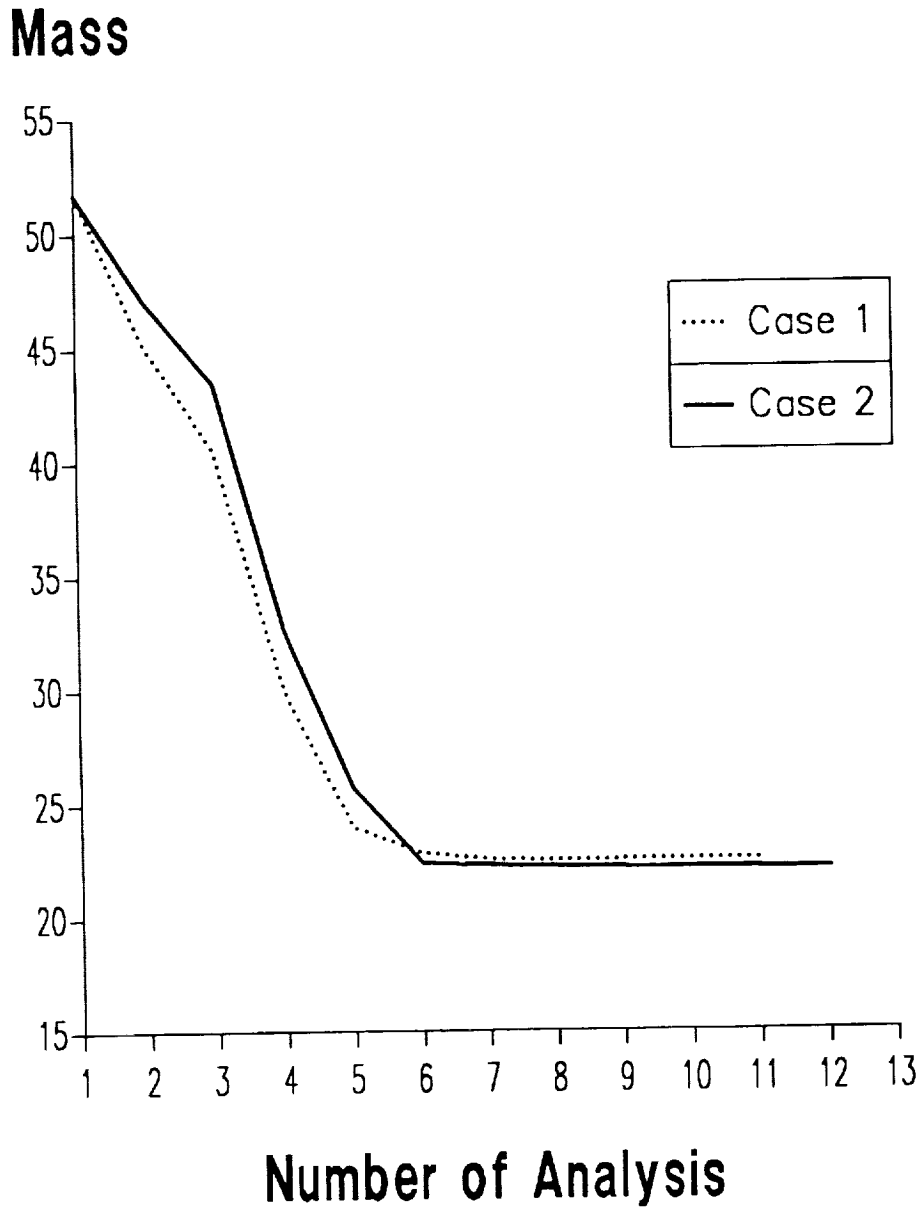

Figure 8: Iteration Histories for Example 2 - ACOSS FOUR, Cases 1 and 2 ($\omega_{d1} \geq 1.341$, $\omega_{d2} \geq 1.6$, $\xi_1 \geq 0.15$)

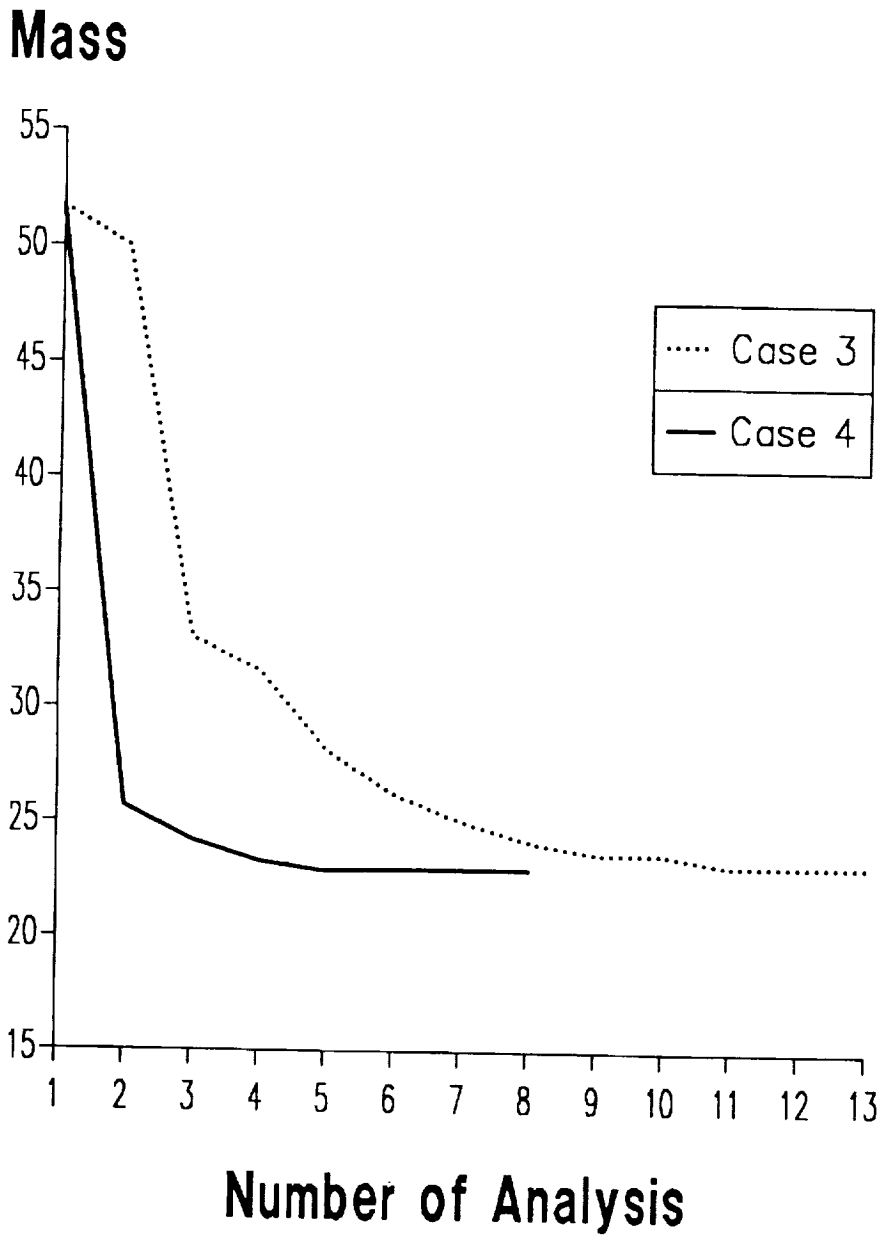

Figure 9: Iteration Histories for Example 2 - ACOSS FOUR, Cases 3 and 4 ($1.34 \leq \omega_{d1} \leq 1.345,\ \omega_{d2} \geq 1.5,\ 0.1093 \leq \xi_i \leq 0.11,\ i = 1, \ldots, 4$)

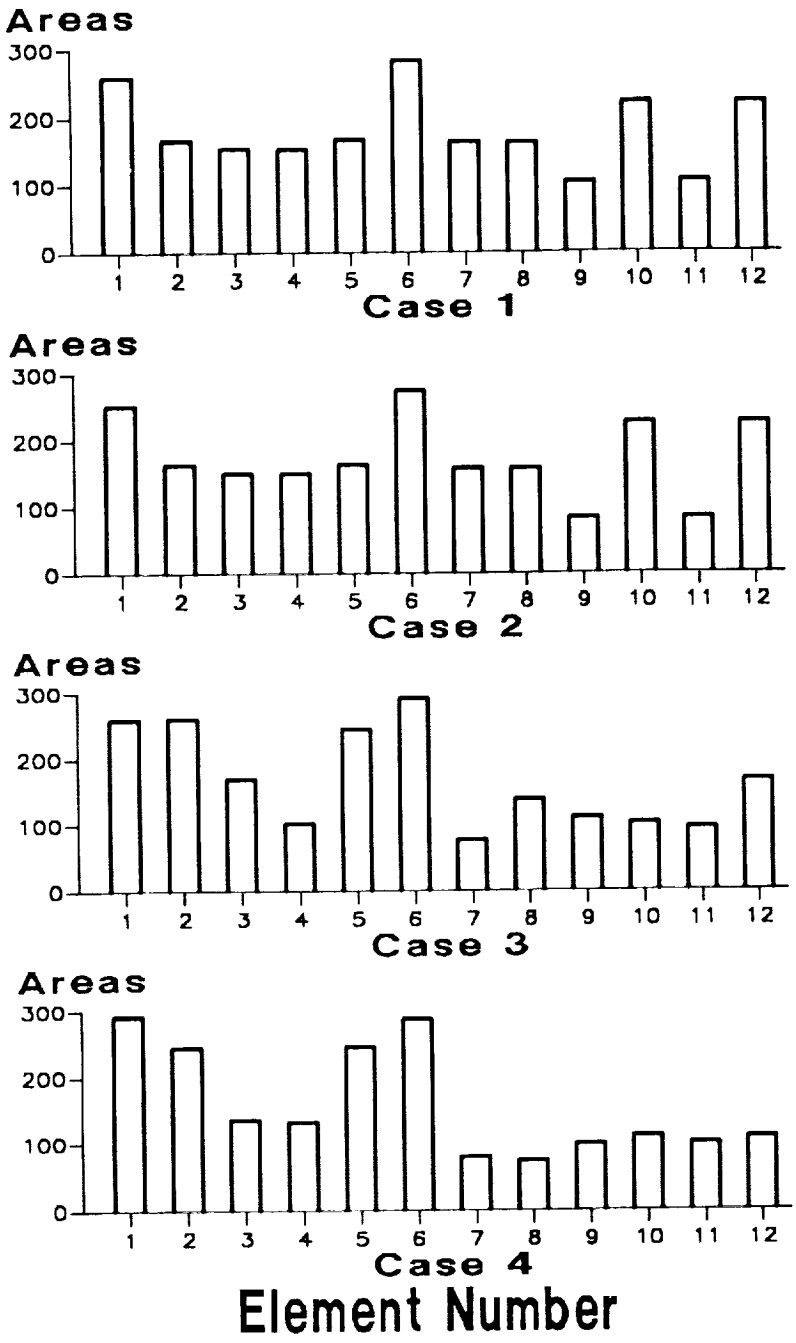

Figure 10: Final Truss Areas for Example 2 - ACOSS FOUR

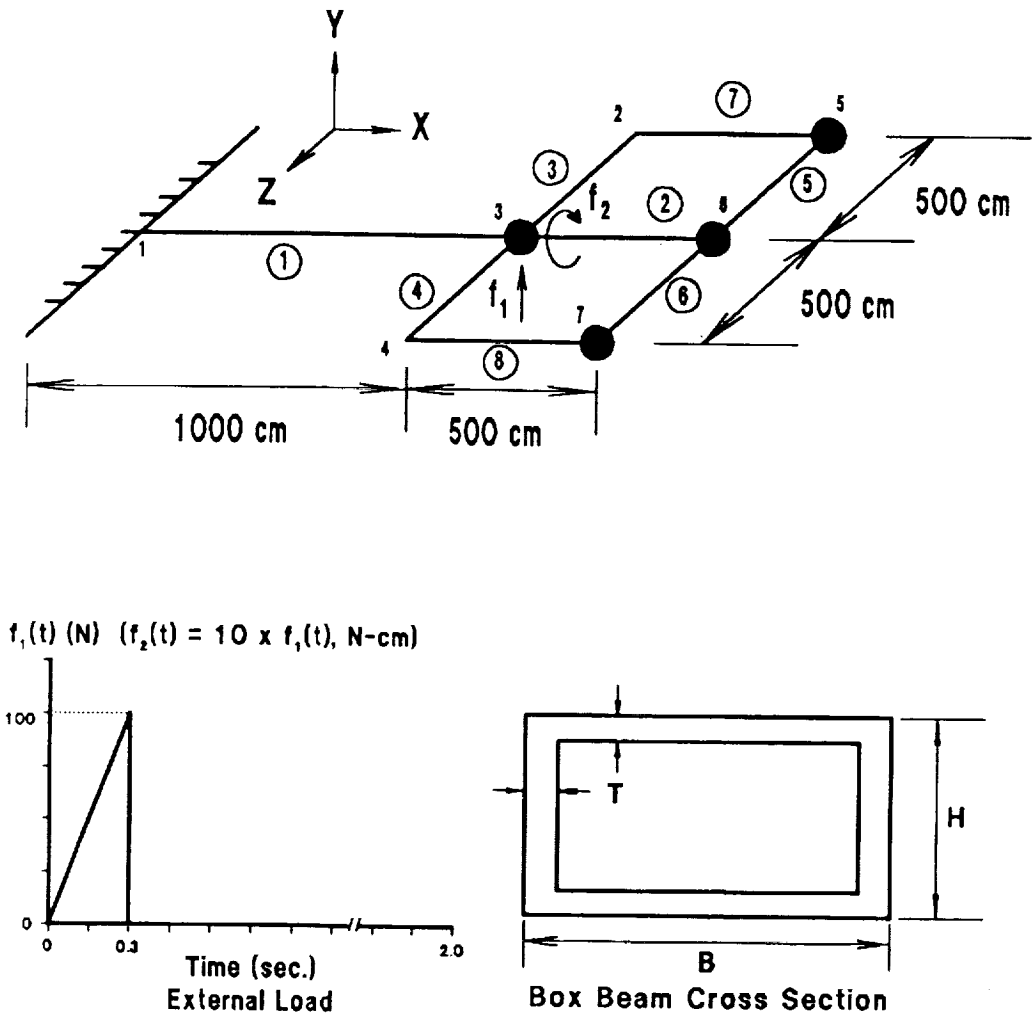

Figure 11: Example 3 - Antenna Structure

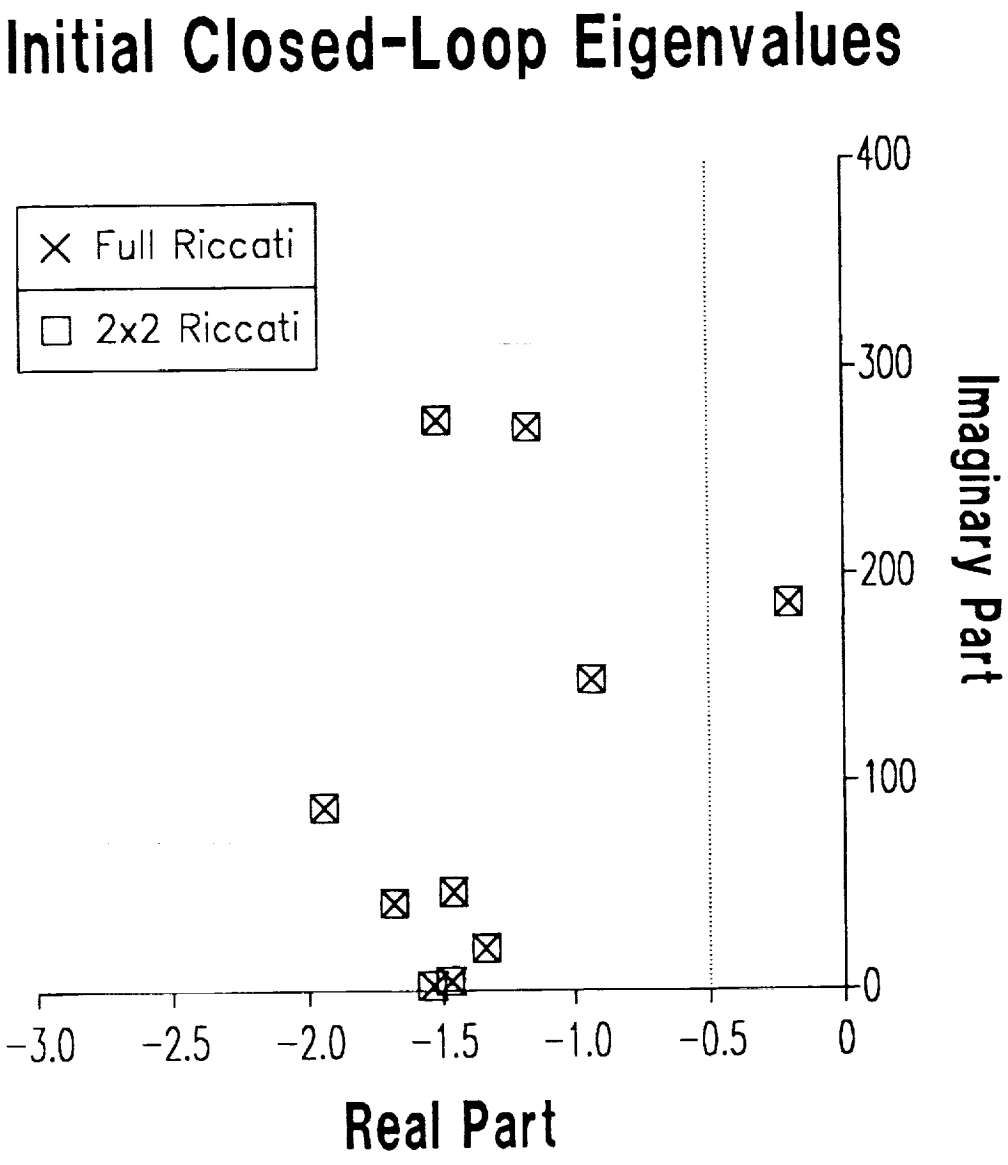

Figure 12: Comparison of Initial Closed-Loop Eigenvalues for Example 3 - Antenna Structure

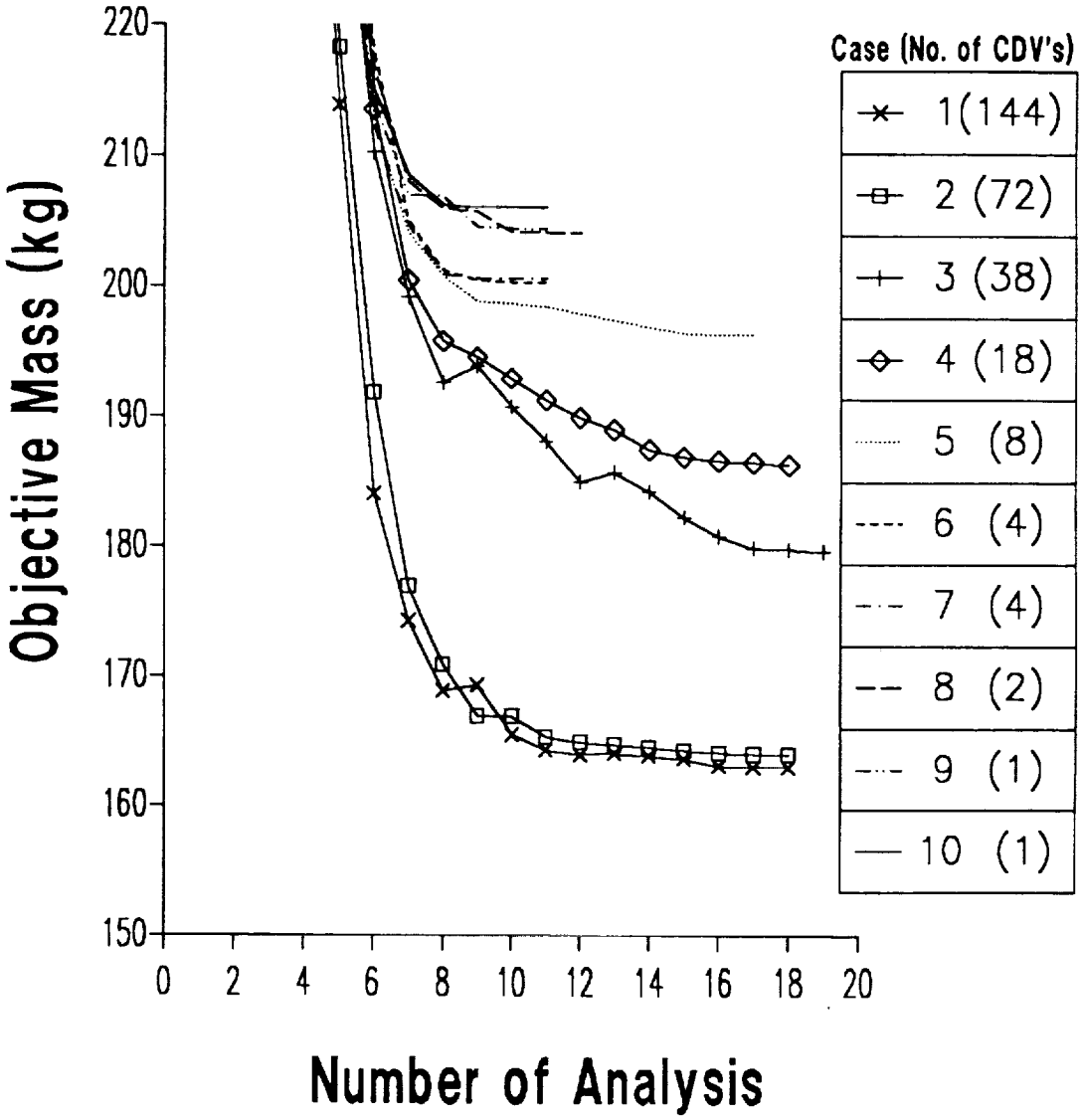

Figure 13: Iteration History for Example 3 - Antenna Structure, Cases 1-10, Control Design Variable Linking (I)

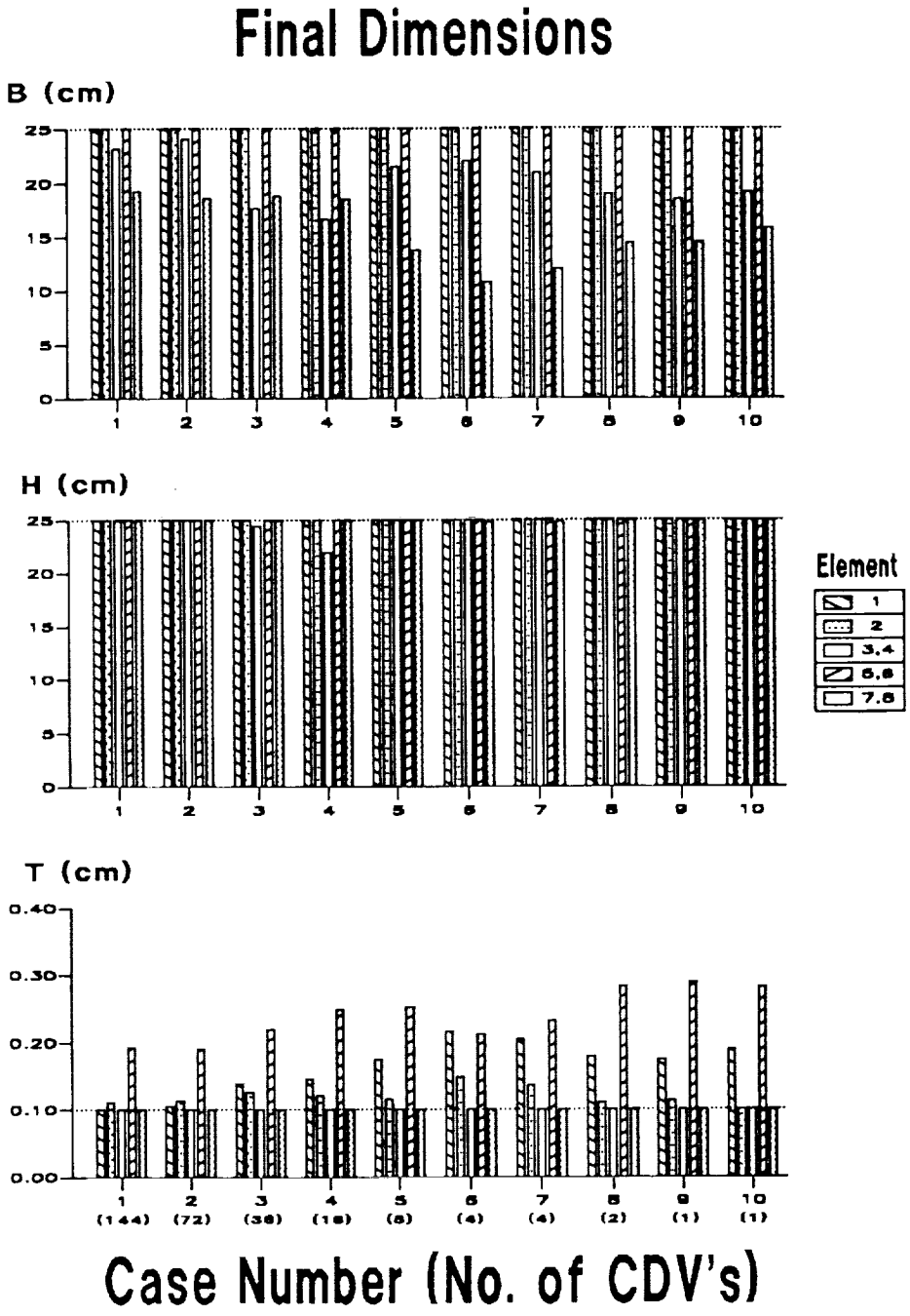

Figure 14: Final Structural Dimensions for Example 3 - Antenna Structure, Cases 1-10, Control Design Variable Linking (I)

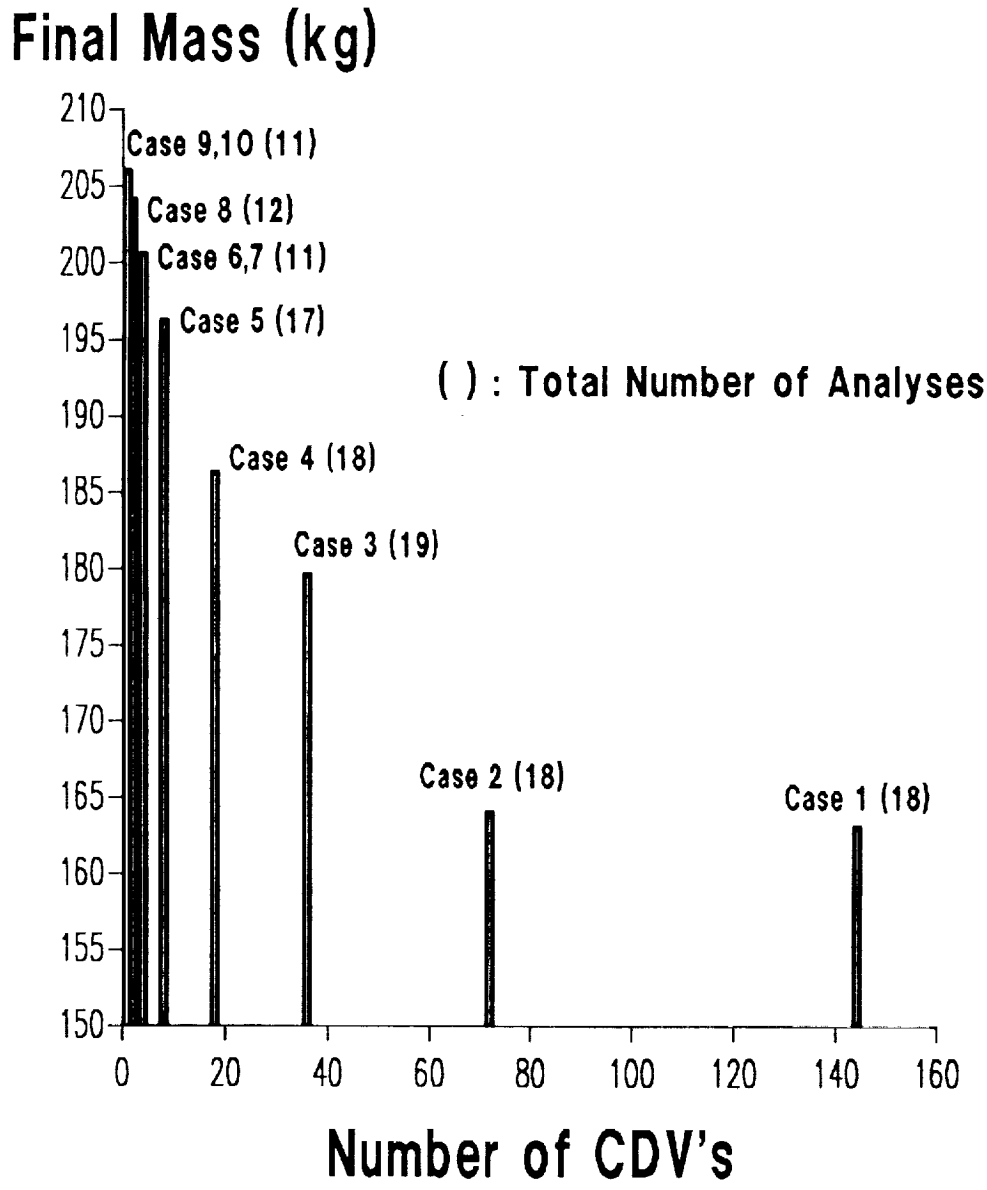

Figure 15: Number of Independent CDV vs. Final Mass - Example 3, Antenna Structure, Cases 1-10, Control Design Variable Linking (I)

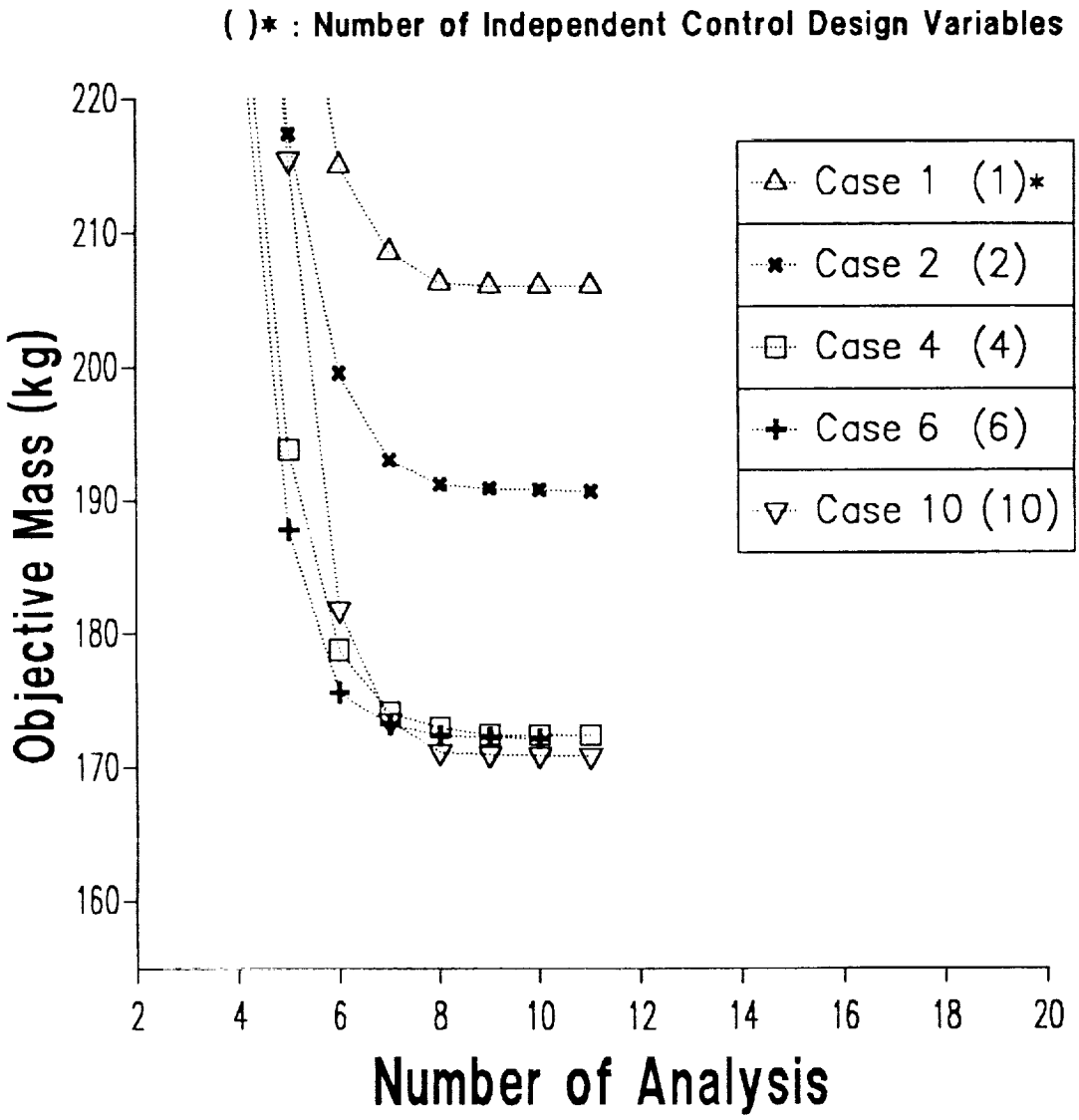

Figure 16: Iteration History for Example 4 - Antenna Structure, Cases 1-10, Control Design Variable Linking (II)

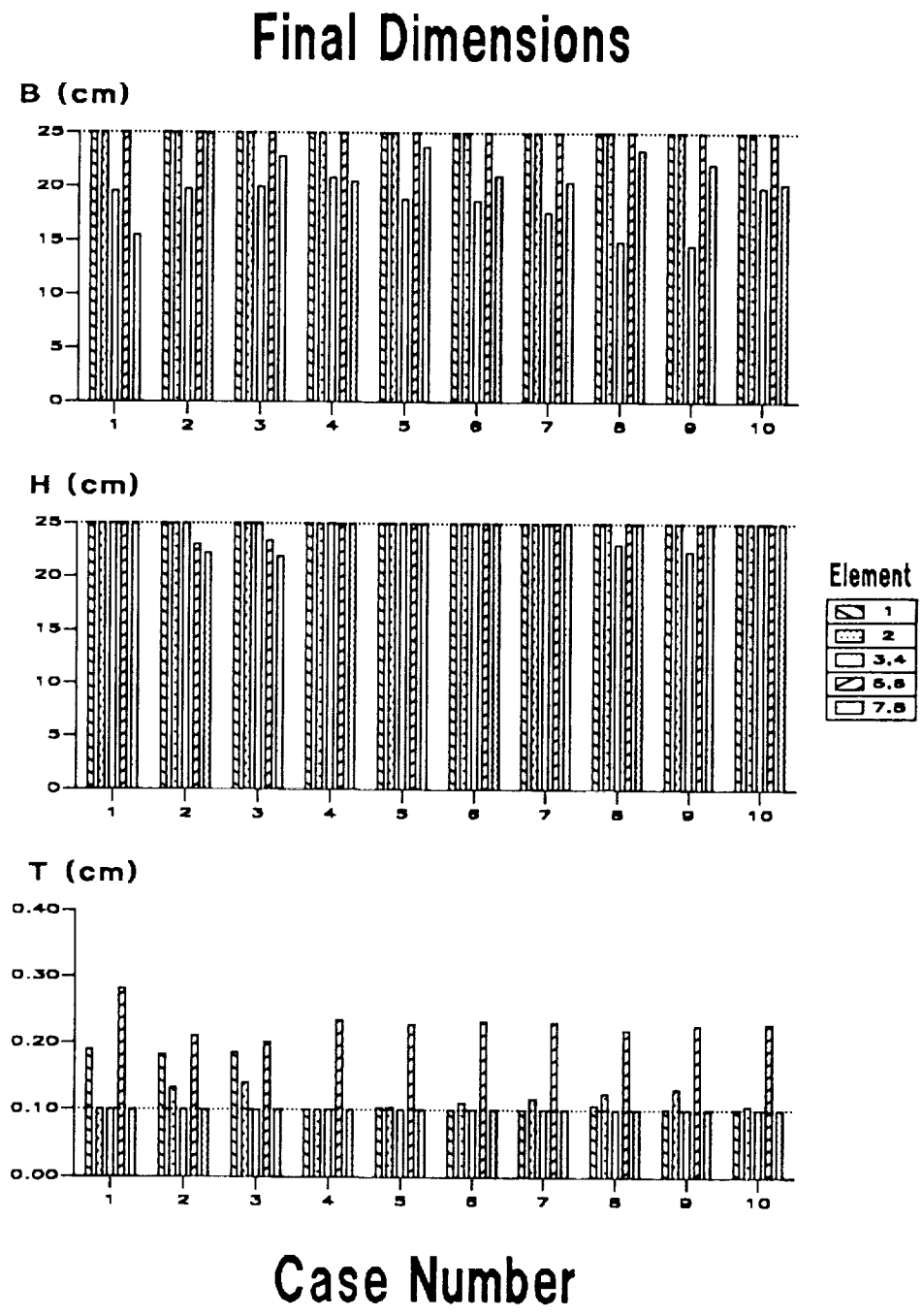

Figure 17: Final Structural Dimensions for Example 4 - Antenna Structure, Cases 1-10, Control Design Variable Linking (II)

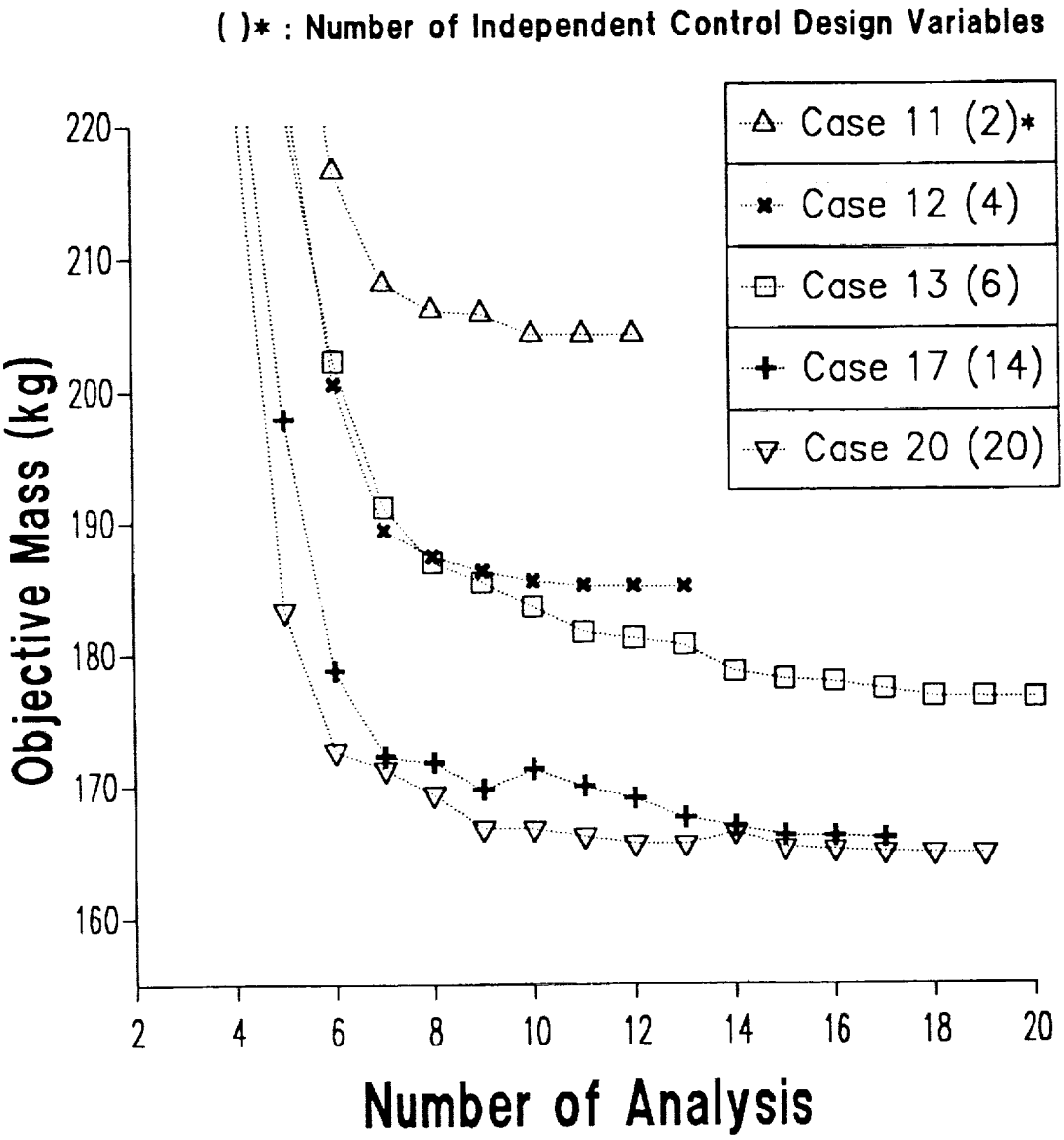

Figure 18: Iteration History for Example 4 - Antenna Structure, Cases 10-20, Control Design Variable Linking (II)

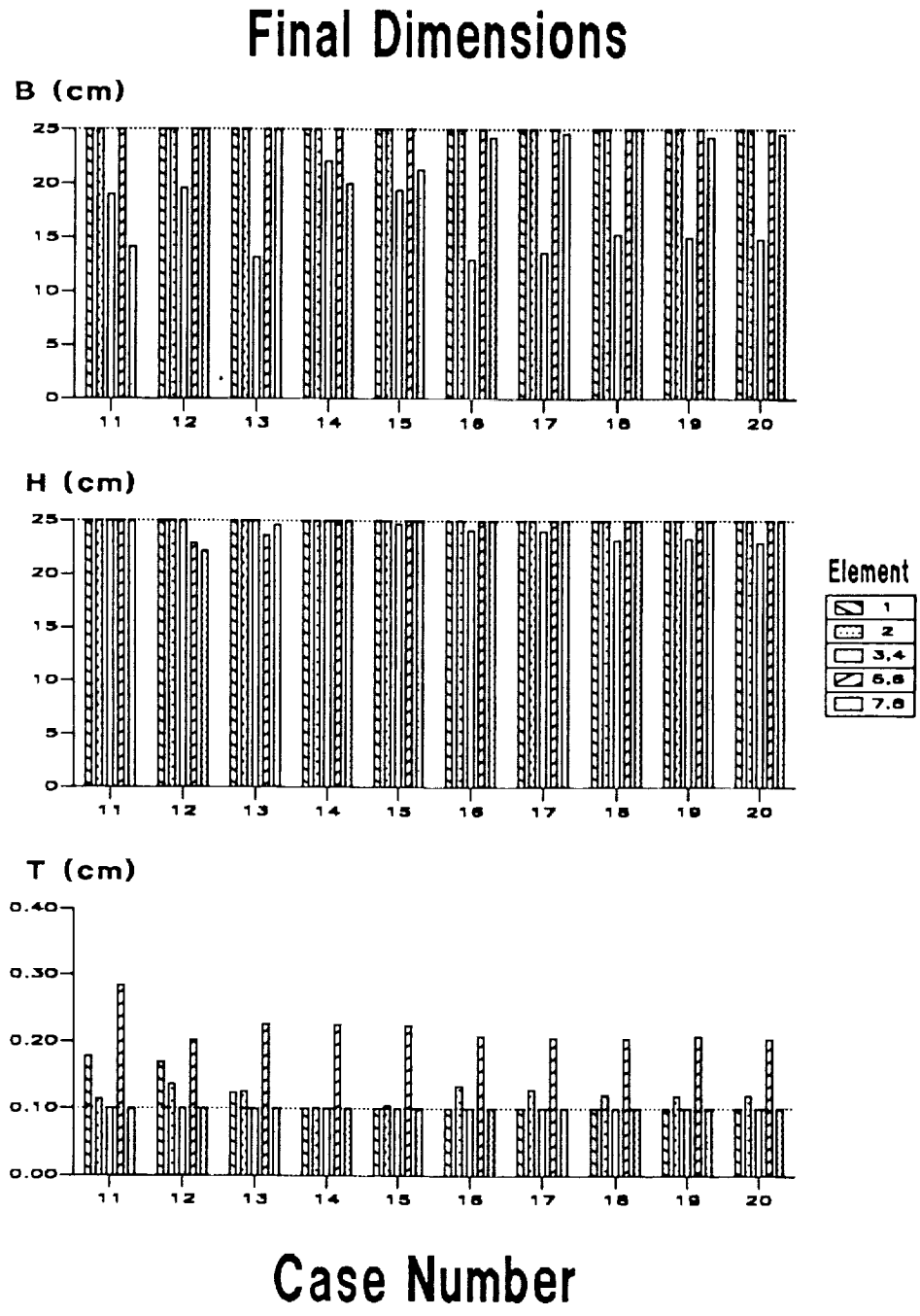

Figure 19: Final Structural Dimensions for Example 4 - Antenna Structure, Cases 10-20, Control Design Variable Linking (II)

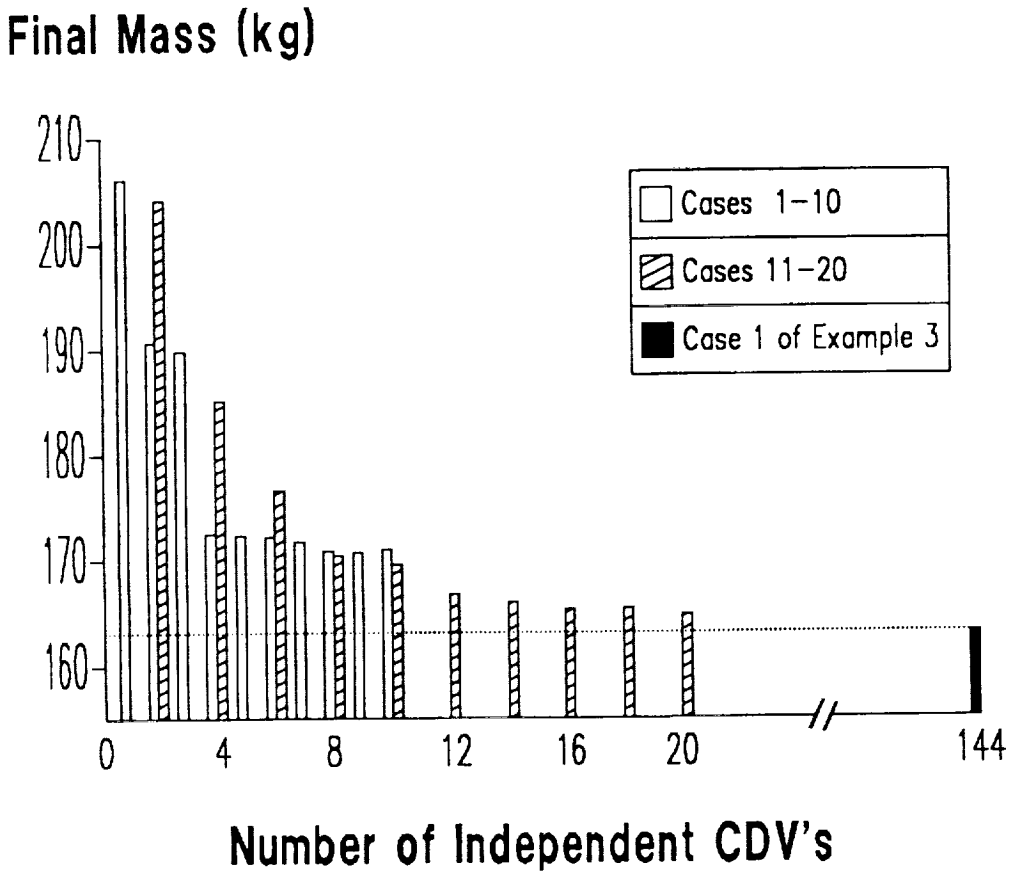

Figure 20: Number of Independent CDV vs. Final Mass - Example 4, Antenna Structure, Control Design Variable Linking (II)

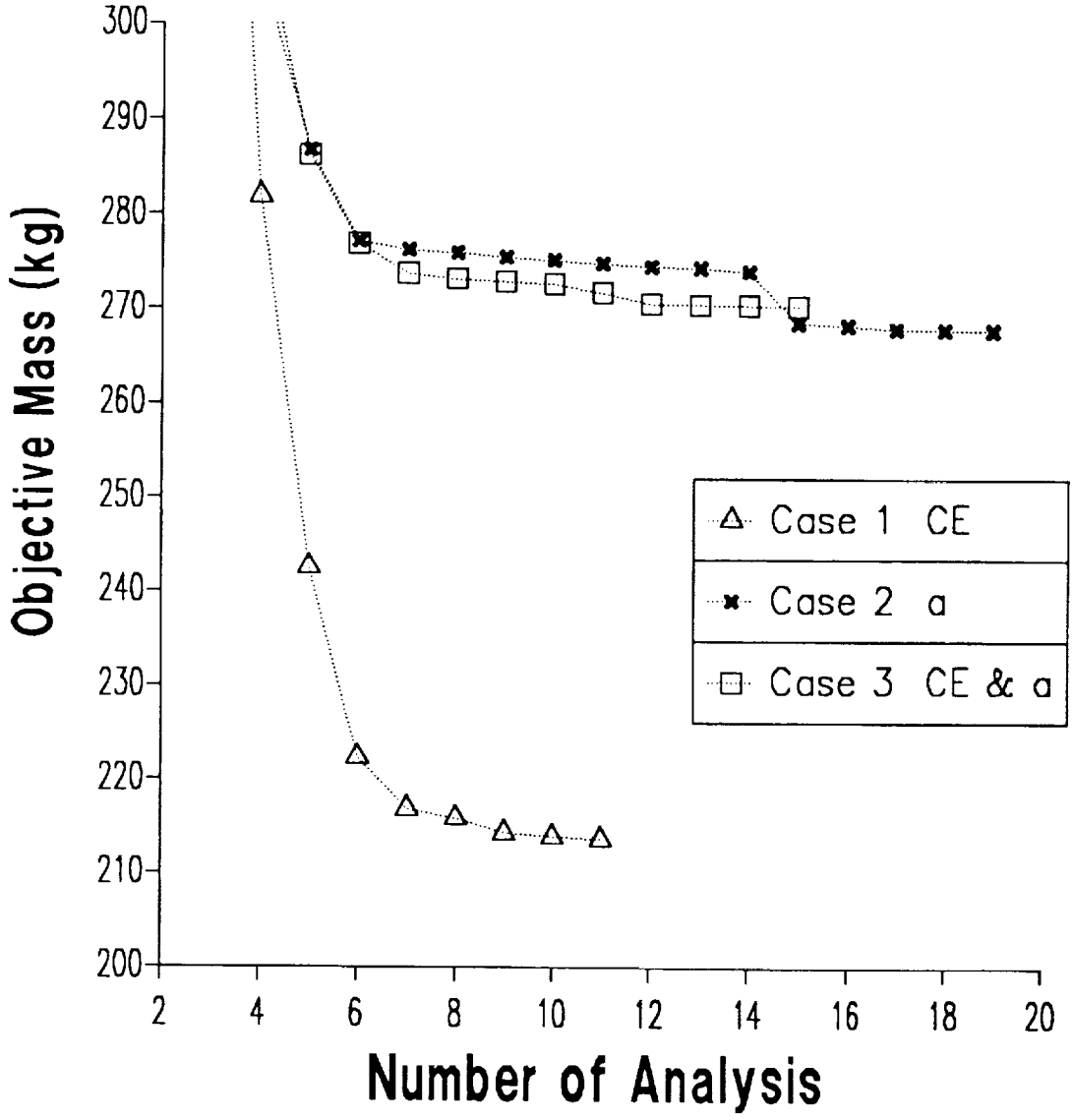

Figure 21: Iteration History for Example 5 - Antenna Structure, Additional Constraints

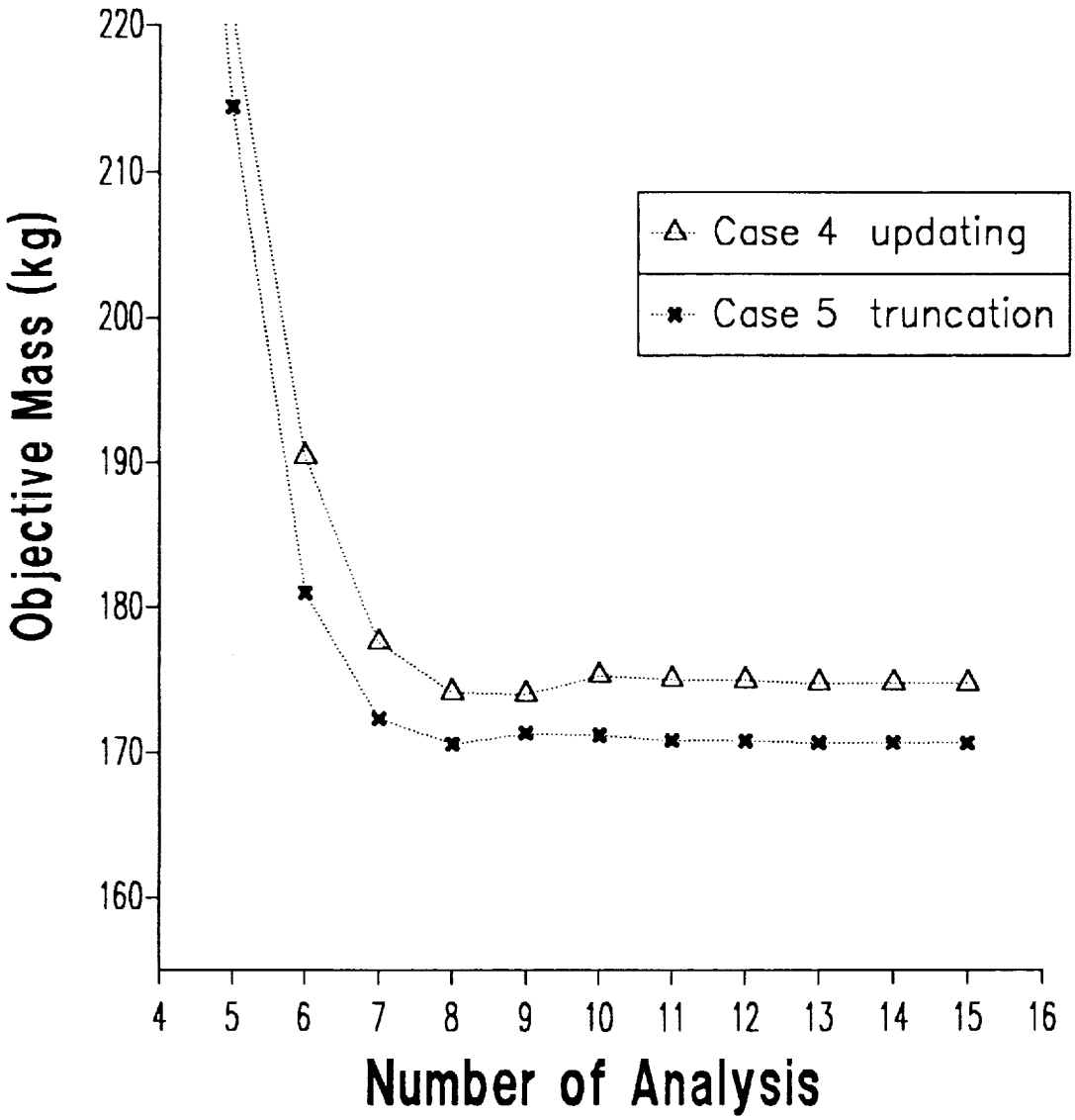

Figure 22: Iteration History for Example 5 - Antenna Structure, Updating and Truncation of Gain Matrices

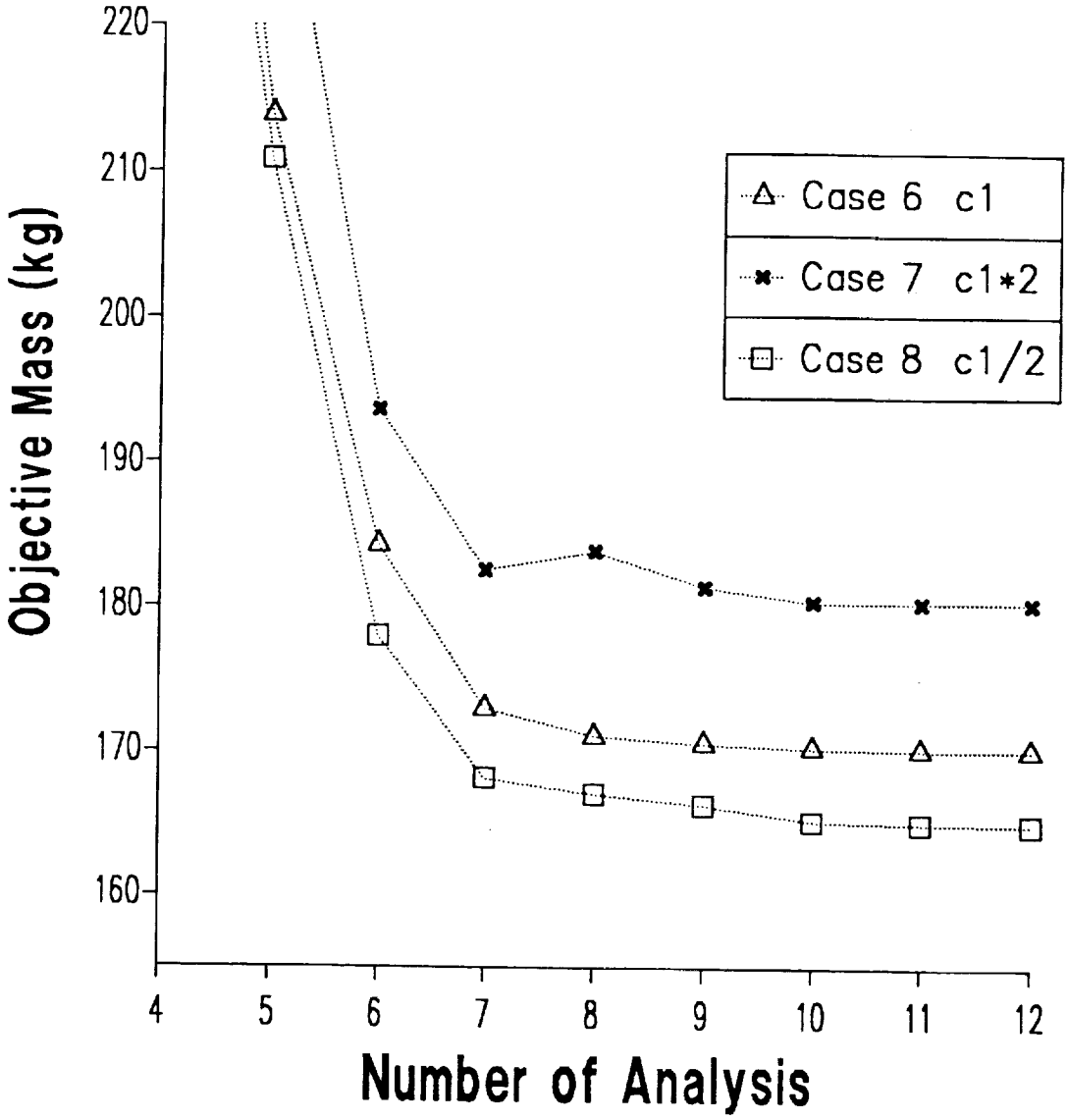

Figure 23: Iteration History for Example 5 - Antenna Structure, Variable Mass Design Elements

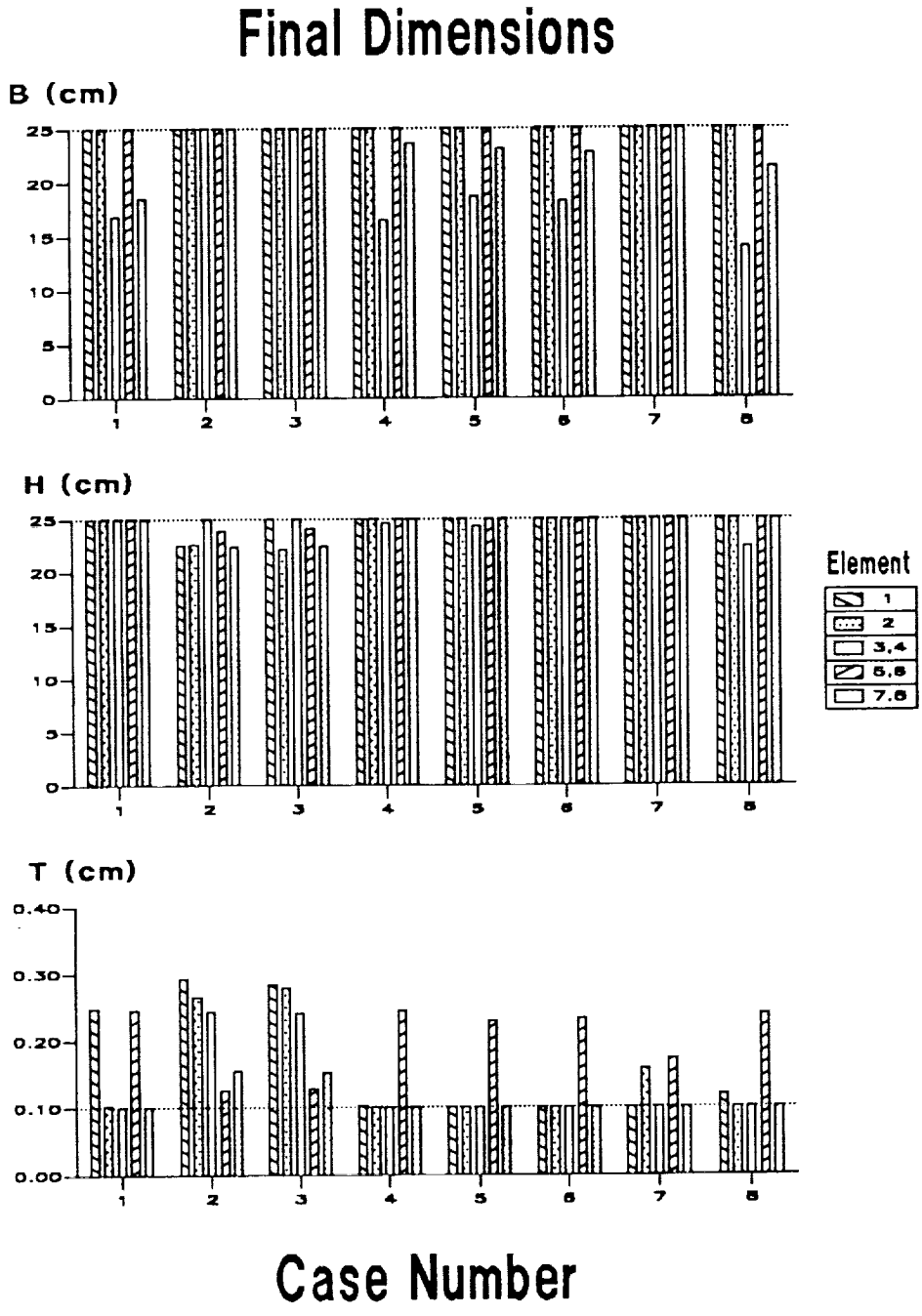

Figure 24: Final Structural Dimensions for Example 5 - Antenna Structure, Additional Constraints and/or Special Features

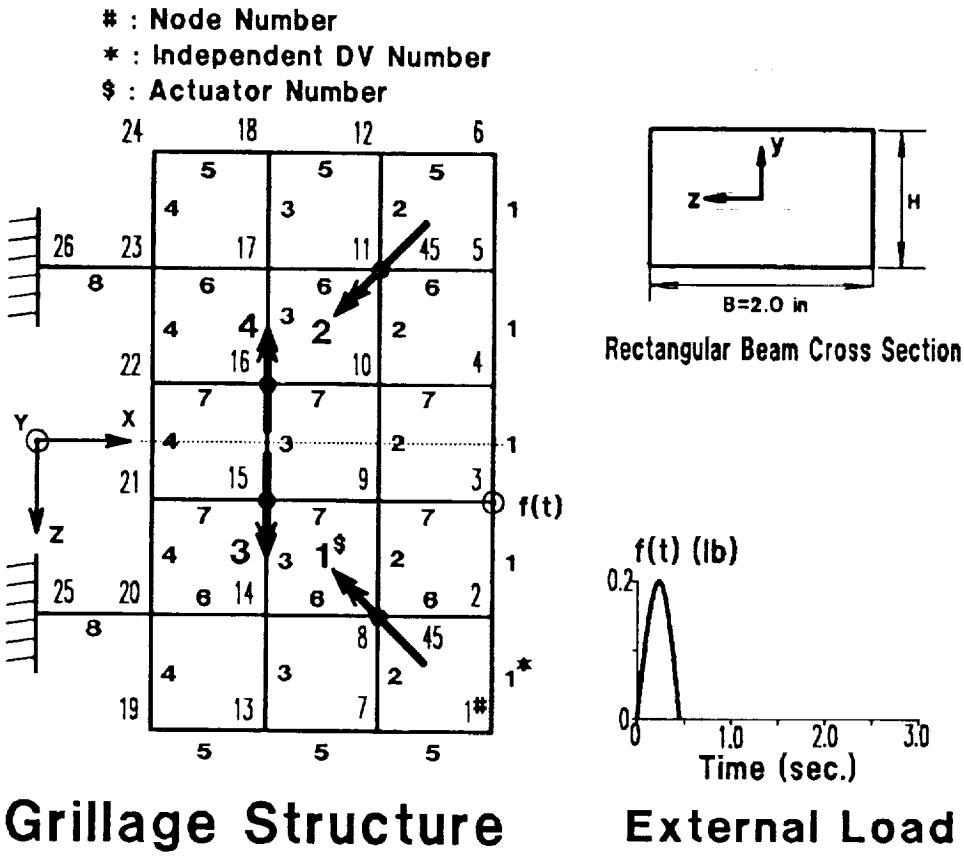

Figure 25: Example 6 - Grillage Structure

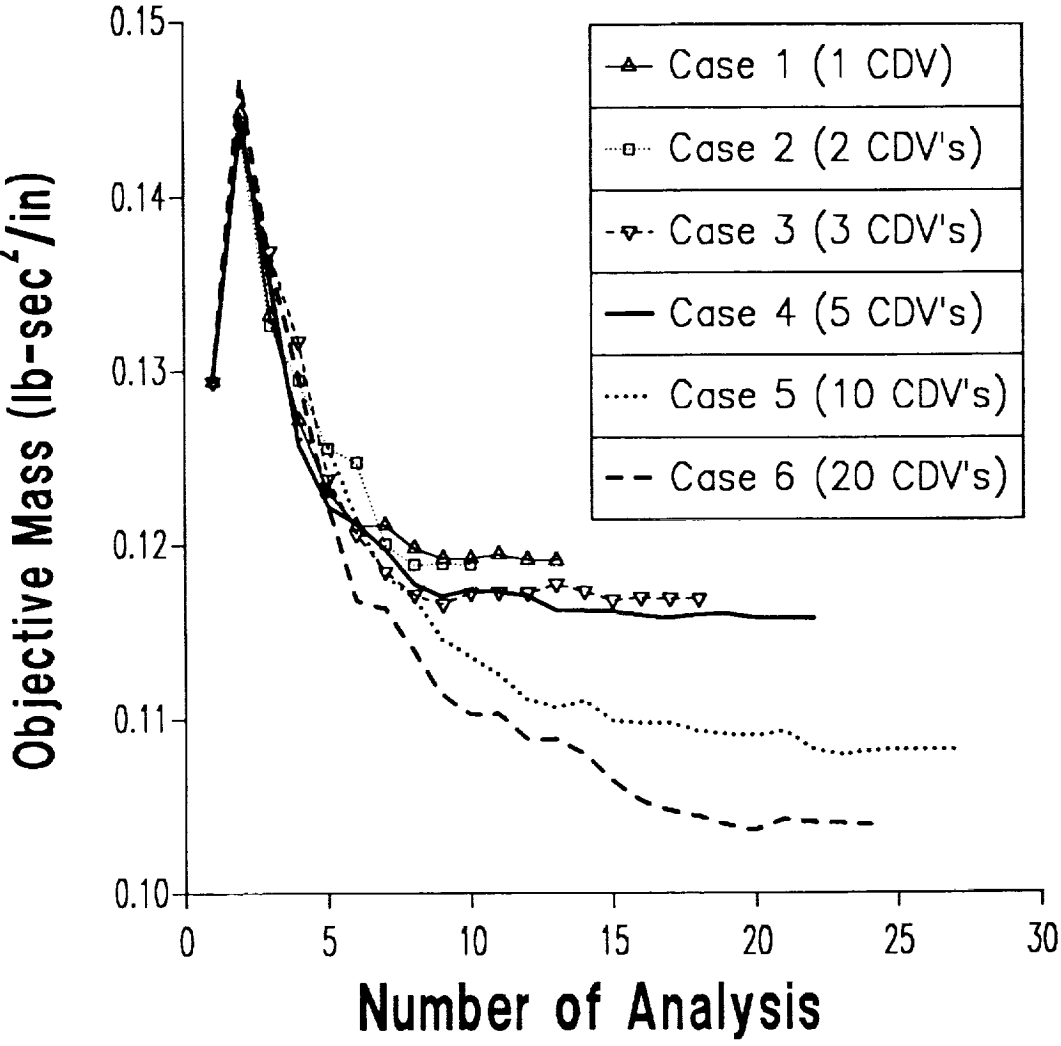

Figure 26: Iteration History for Example 6 - Grillage Structure, Cases 1-6, Control Design Variable Linking (II)

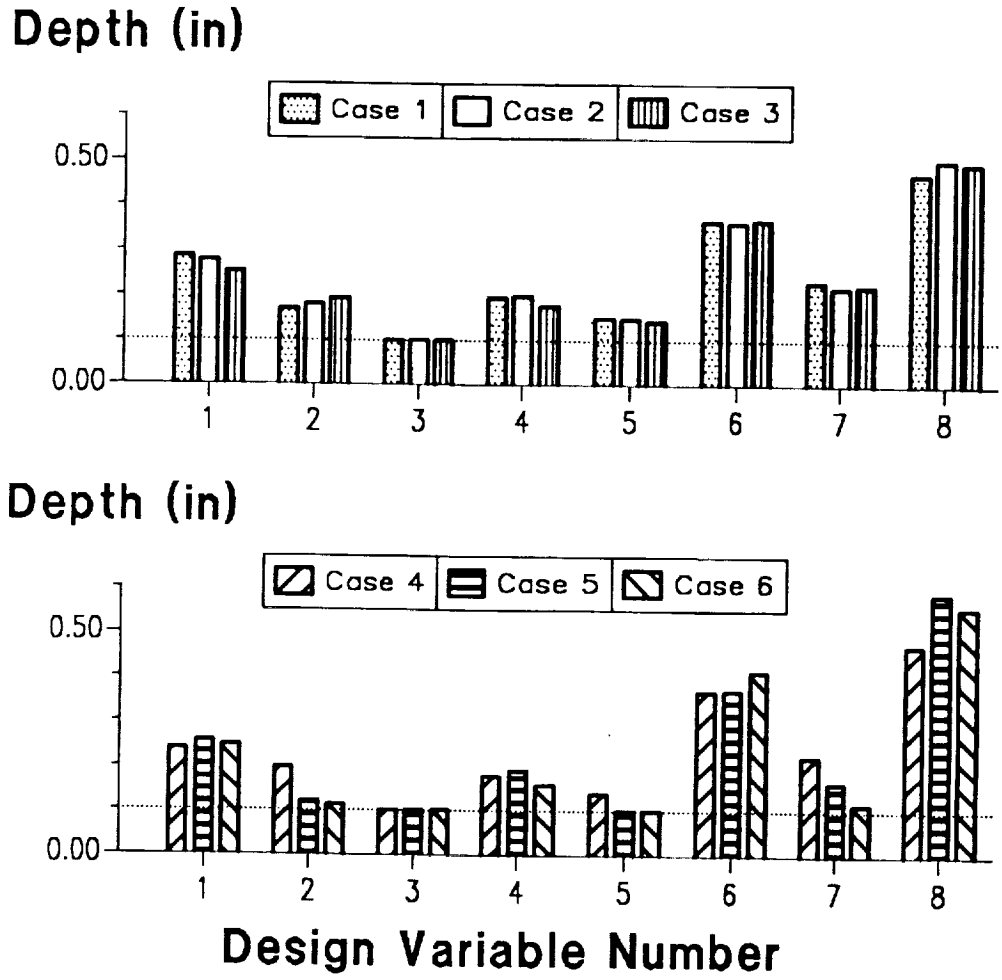

Figure 27: Final Structural Dimensions for Example 6 - Grillage Structure, Cases 1-6, Control Design Variable Linking (II)

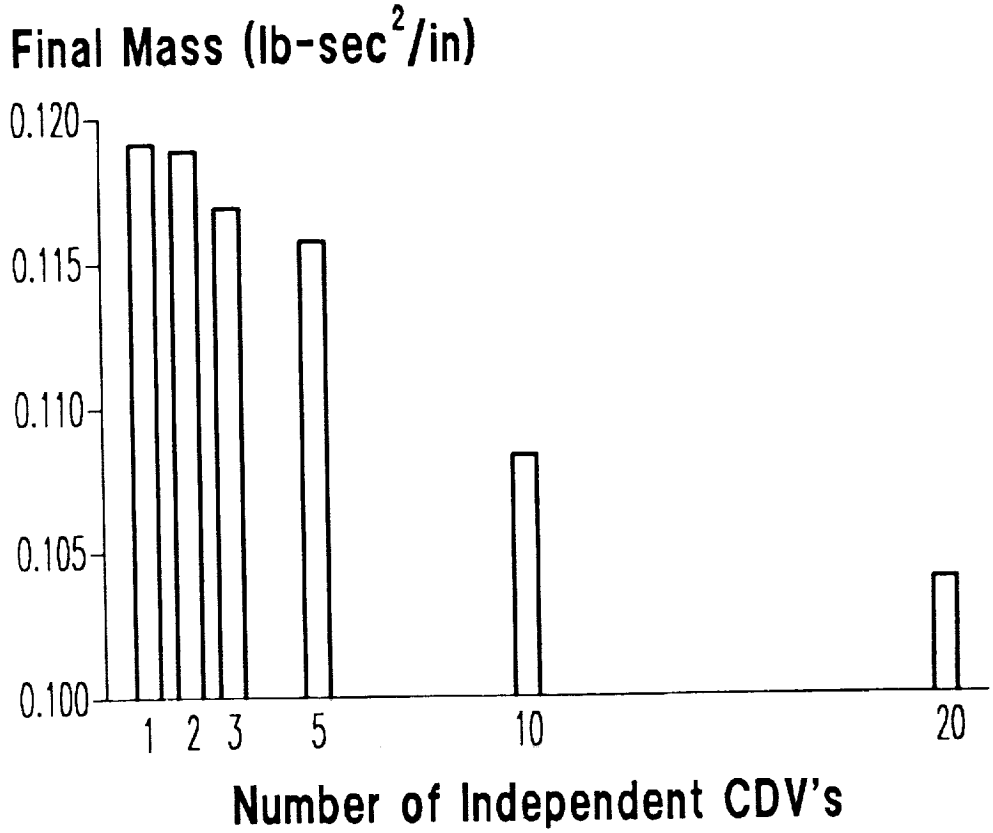

Figure 28: Number of Independent CDV vs. Final Mass - Example 6, Grillage Structure, Cases 1-6, Control Design Variable Linking (II)

REPORT DOCUMENTATION PAGE

Form Approved
OMB No 0704-0188

1. AGENCY USE ONLY (Leave blank)	2. REPORT DATE	3. REPORT TYPE AND DATES COVERED
	February 1993	Contractor Report

4. TITLE AND SUBTITLE
Control Design Variable Linking for Optimization of Structural/Control Systems

5. FUNDING NUMBERS
G NSG-1490

WU 505-63-10-02

6. AUTHOR(S)
Ik Min Jin and Lucien A. Schmit

7. PERFORMING ORGANIZATION NAME(S) AND ADDRESS(ES)
University of California, Los Angeles
School of Engineering & Applied Science
Los Angeles, CA 90024

8. PERFORMING ORGANIZATION REPORT NUMBER

9. SPONSORING / MONITORING AGENCY NAME(S) AND ADDRESS(ES)
National Aeronautics and Space Administration
Langley Research Center
Hampton, VA 23681-0001

10. SPONSORING / MONITORING AGENCY REPORT NUMBER
NASA CR-4493

11. SUPPLEMENTARY NOTES
Langley Technical Monitor: Jaroslaw Sobieski

12a. DISTRIBUTION / AVAILABILITY STATEMENT
Unclassified - Unlimited

Subject Category 05

12b. DISTRIBUTION CODE

13. ABSTRACT (Maximum 200 words)

A method is presented to integrate the design space of structural/control system optimization problems in the case of linear state feedback control. Conventional structural sizing variables and elements of the feedback gain matrix are both treated as strictly independent design variables in optimization by extending design variable linking concepts to the control gains. Several approximation concepts including new control design variable linking schemes are used to formulate the integrated structural/control optimization problem as a sequence of explicit nonlinear mathematical programming problems. Examples which involve a variety of behavior constraints, including constraints on dynamic stability, damped frequencies, control effort, peak transient displacement, acceleration and control force limits, are effectively solved by using the method presented.

14. SUBJECT TERMS	15. NUMBER OF PAGES
Structural/control systems; control design	184
	16. PRICE CODE: A09

17. SECURITY CLASSIFICATION OF REPORT	18. SECURITY CLASSIFICATION OF THIS PAGE	19. SECURITY CLASSIFICATION OF ABSTRACT	20. LIMITATION OF ABSTRACT
Unclassified	Unclassified	Unclassified	